IDENTIFYING MECHANISMS OF INSULIN PRODUCTION AND SECRETION IN SMALL AND LARGE RAT ISLETS

By

Han-Hung Huang

Submitted to the graduate degree program in
Rehabilitation Science
and the Graduate Faculty of the University of Kansas
in partial fulfillment of the requirements for the degree of
Doctor of Philosophy.

_____
Chairperson: Lisa A. Stehno-Bittel, PT, Ph.D.

_____
Irina V. Smirnova, MS, Ph.D.

_____
WenFang Wang, Ph.D.

_____
Patricia M. Kluding, PT, Ph.D.

_____
Paige C. Geiger, Ph.D.

Date Defended: August 31st, 2011

The Dissertation Committee for Han-Hung Huang

certifies that this is the approved version of the following dissertation:

IDENTIFYING MECHANISMS OF INSULIN PRODUCTION AND SECRETION

IN SMALL AND LARGE RAT ISLETS

_____

Chairperson: Lisa A. Stehno-Bittel, PT, Ph.D.

Date approved: August 31st, 2011

ABSTRACT

The existence of islet subpopulations according to size difference has been described since 1869 when Dr. Paul Langerhans first discovered the islets in the pancreas. Unfortunately, little is known about the functional differences between islet subpopulations until recently. Small islets have been shown to secret more insulin than large islets per volume (islet equivalent; IE) and led to better transplantation outcome both in rodents and in humans. Insulin is produced and released from the β cells in islets through a cascading pathway from insulin gene transcription to proinsulin biosynthesis to insulin secretion. The central hypothesis of this dissertation is that small and large islets have different characteristics in insulin production and secretion that lead to different transplantation outcomes. More than ten thousands small (diameter ≤ 100μm) and large (diameter ≥ 200μm) islets from healthy rats were investigated. First, the same percentage of β cells was identified in small and large islets, but small islets had higher density both in vitro and in situ. Next, a new regression model was established to better estimate the islet volume by cell number based on size (diameter), since an overestimation was seen when using conventional IE measurement to normalize islet volume. By applying this new normalization method, a superior glucose-stimulated proinsulin biosynthesis was identified in large islets. However, when normalized to cell number, insulin secretion was not different between small and large islets, unlike the results in literature when normalized to IE. While small and large islets showed no difference in total protein content per cell, large islets showed higher protein levels of prosinulin, NeuroD/Beta2 and MafA with a lower PDX-1 level under basal conditions suggesting that the different characteristics between small and large islets in the insulin production pathway may not correspond to measured insulin secretion. All the findings will not only elucidate new intricacies concerning islet biology research, but also will have significant implications to current islet transplantation research to optimize the success for curing type 1 diabetes.

TABLE OF CONTENTS

LIST OF FIGURES

LIST OF TABLES

Chapter 1

Introduction

Solid understanding of the insulin-producing islet of Langerhans (islets) is a necessary base to optimize the success of curing diabetes. In the pancreas, islets vary in sizes. However, the roles of islet subpopulations remain unclear in current islet biology. The long-term goal of our research is to better understand islet biology to improve therapeutic strategies that can be applied to cure diabetes. Therefore, the objective of this dissertation was to characterize the differences between small and large islets in vitro and in situ, and to investigate the mechanisms of insulin production and secretion in these two populations by using an improved islet volume normalization method to compare the results.

1.1. Islets of Langerhans

The human pancreas is both an exocrine and endocrine organ with an elongated shape. The head of the gland is closely attached to the distal two-thirds of the duodenum. The body of the pancreas is overlaid by the posterior wall of the stomach and the tail region ends near the splenic hilus. The main two functions of the pancreas are digestion and glucose homeostasis. The exocrine cells, which constitute approximately 98% of total mass of adult pancreas, release a mixture of digestive enzymes and bicarbonate into the duodenum to help with food digestion. The endocrine cells constitute 1~2% of total mass of pancreas that release several hormones into the portal vein. Cluster of endocrine cells form the islets of Langerhans, or islets, which were discovered by a German pathological anatomist Dr. Paul Langerhans (1847-1888) in 1869 (Bloomfield, 1958).

In the pancreas, the islets lie scattered throughout the exocrine tissue in between the acini and ductal structures without a recognizable pattern. The distribution of islets varies widely from individual to individual. In the fetuses, islets contact duct closely. In neonates and adults, islets are more separated from the ducts. In adults, about 50% of the islets remain close to the duct (Watanabe, Yaegashi, Koizumi, Toyota, & Takahashi, 1999). In addition, the number of islets

seems to increase toward the tail region of the pancreas (K. Saito, Iwama, & Takahashi, 1978; Wittingen & Frey, 1974).

The islet is surrounded by a thin collagen capsule and glial sheet that separate islet cells from the exocrine tissue (Goldstein & Davis, 1968; Hughes et al., 2006; P. H. Smith, 1975). In the islet, besides the endocrine cells, small amount to connective tissue are present with blood vessels. The islet is pervaded by a dense capillaries network, which has a density five times higher than the exocrine capillary network (Ballian & Brunicardi, 2007; Zanone, Favaro, & Camussi, 2008). The capillary network plays a critical role for glucose homeostasis not only because of the high oxygen consumption of endocrine cells, but also because of the timely response to the changes in blood glucose levels that is required by endocrine cells to secrete hormones into the circulation. In addition, there are some other non-epithelial elements inside the islets such as macrophages (de Koning et al., 1998) and nerve fibers. Islets have sympathetic, parasympathetic and sensory innervations. The nerve fibers usually accompany the vascular system that release acetylcholine or noradrenaline to regulate insulin secretion. Insulin secretion, the most well-known function of the islet, is activated by the parasympathetic system but inhibited by the sympathetic system (Ahren, 1999).

Islets contain at least five different types of endocrine cells: Beta (β) or B cell, Alpha (α) or A cell, Delta (δ) or D cell, PP or F cell, and Epsilon cell. The β cell produces insulin, which lowers the blood glucose levels. The α cell produces glucagon, which plays role in hyperglycemic action. The δ cell produces somatostatin, an inhibitor of insulin and glucagon release. The PP cell produces pancreatic polypeptide, a regulator of pancreatic secreting activities including exocrine and endocrine. The epsilon cell produces ghrelin, which is thought to be important in growth hormone release, metabolic regulation and energy balance (Islam, 2010). Among all types of endocrine cells, the insulin-producing β cells are the majority

(65%~80%) in the islet (el-Naggar, Elayat, Ardawi, & Tahir, 1993). In this dissertation, the mechanisms of insulin production and secretion in the β cells will be focused.

1.2. Mechanisms of Insulin Production and Secretion

Insulin is produced through a cascading process in the β cell. First of all, the insulin gene is transcribed from DNA to preproinsulin mRNA through gene transcription. After transcription, the preproinsulin mRNA is translated into preproinsulin protein which exists the cell shortly. Then, the preproinsulin is processed into proinsulin, after the signal peptide is removed, and stored into granules. The proinsulin will be cleaved by specific enzymes (see below) into c-peptide and insulin. Finally, the mature insulin will be released from the cell by exocytosis to the blood stream (Figure 1).

Glucose stimulates β cells to produce insulin and regulates several aspects of insulin-producing process mentioned above. The elevation in blood glucose concentrations is the primary signal for insulin production which enhances insulin gene transcription, insulin protein synthesis and insulin release through the complex network of intracellular signaling pathways (Figure 1).

1.2.1. Insulin Gene Transcription

1.2.1.1. Preproinsulin mRNA

Preproinsulin mRNA is the product of insulin gene transcription that makes up 10~15% of the total mRNA in the β cell (Goodge & Hutton, 2000). Under basal conditions with a low plasma glucose concentration (<3 mM), large quantities of preproinsulin mRNA are present due to basal insulin gene transcription. However, at higher glucose concentrations, insulin transcription increases and more preproinsulin mRNA is produced. Efrat et al. suggested that high glucose (16.7 mM) stimulates insulin gene transcription about 3-fold after 10 minutes, and the transcriptional activity is maximal at 30 minutes, but markedly decreased thereafter (Efrat, Surana, & Fleischer, 1991).

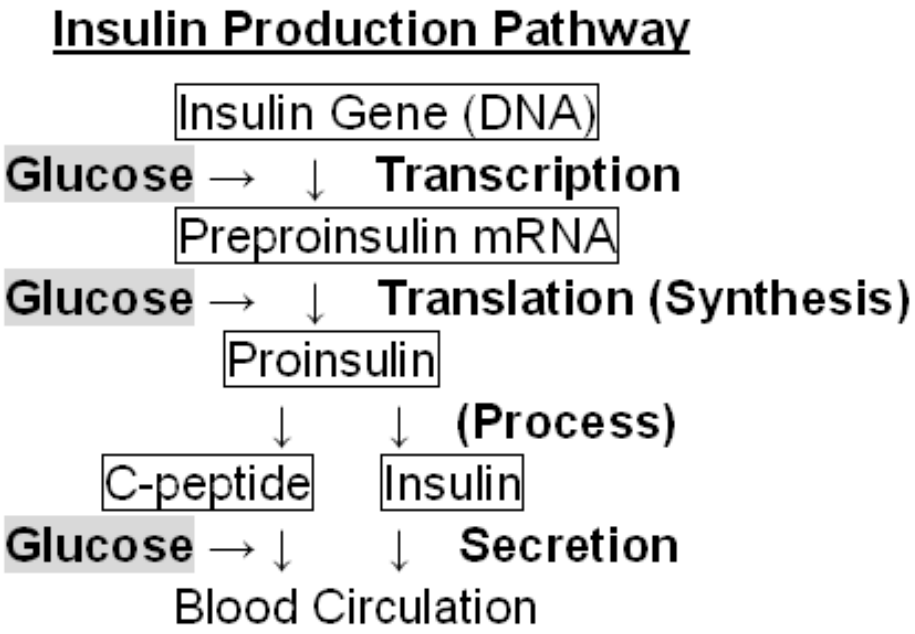

Figure 1. Insulin production pathway. Glucose is the primary signal for insulin production that enhances insulin gene transcription, insulin protein synthesis and insulin secretion through the complex network of intracellular signaling pathways.

In addition, it is reported that incubating insulinoma cells and the isolated pancreatic islets in high glucose (16.7 mM) for only 15 minutes, results in a 2~5 fold elevation in preproinsulin mRNA levels within 60~90 minutes. The authors also observed that the glucose stimulatory effect is most obvious 30 minutes after the glucose exposure, but declines thereafter (Leibiger et al., 1998). Taken together, it is likely that the production of preproinsulin mRNA is affected by high glucose concentration within minutes.

1.2.1.2. Glucose-responsive insulin gene transcription factors

The transcription of insulin gene to preproinsulin mRNA is regulated by the interaction between the insulin promoter and the transcription factors. The human insulin gene is located on chromosome 11p15.5 in the β cell nucleus (Harper, Ullrich, & Saunders, 1981). The insulin promoter is a specific sequence of DNA nucleotides located near the transcription initiation site of the insulin gene that determines which one of the two strands of the double helix DNA will be transcribed. On the other hand, the transcription factors are the proteins that perform as gene switches at the promoter region to activate or repress the gene expression.

Increased glucose levels activate upstream signals that are responsible for the activation of the transcription factors involved in insulin gene transcription. Three critical glucose-responsive transcription factors will be investigated in chapter 4, which are the homeodomain protein pancreas duodenum homeobox-1 (PDX-1), Beta-cell E-box trans-activator 2 (Beta2), and the basic region leucine zipper MafA (Figure 2).

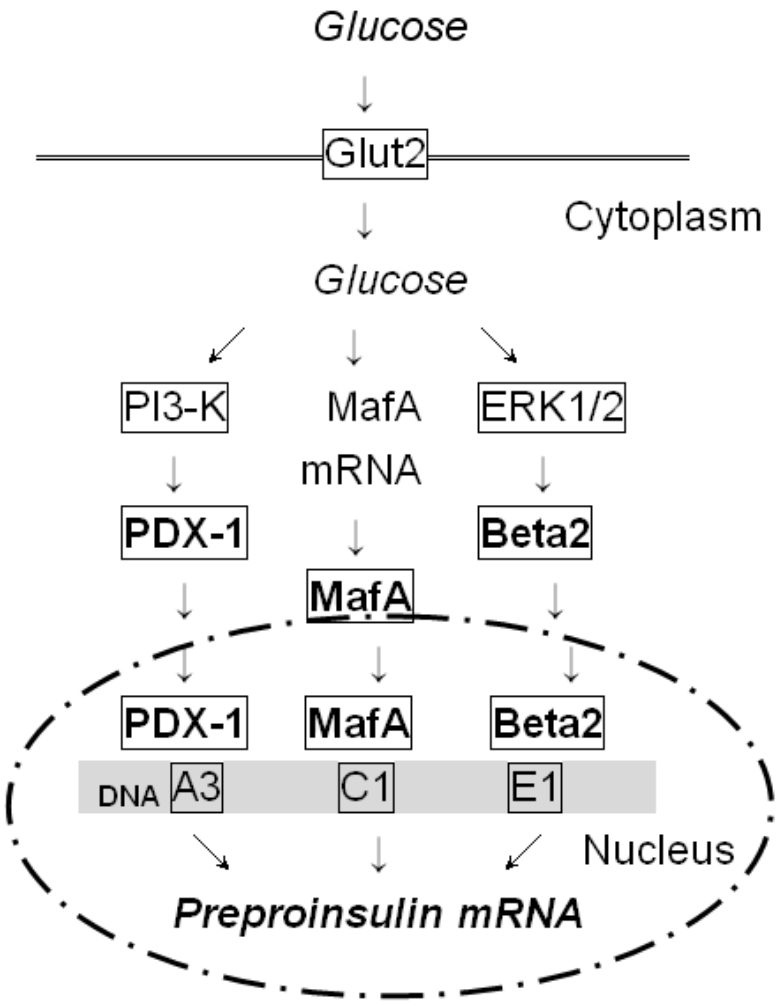

Figure 2. Summary of glucose control of insulin gene transcription. Glucose enters β cell via the glucose transporter 2 (Glut2) located on the plasma membrane and activates factors involved in insulin gene transcription through three main pathways. Pathway on the left: Glucose stimulates PDX-1 translocation from the cytoplasm to the nucleus and increases binding activity of PDX-1 to the insulin promoter (A3) through the pathway involving phosphatidylinosito 3-kinase (PI3-K) activation. Pathway in the center: Glucose affects MafA gene expression at the mRNA level and activates binding activity of MafA to the insulin promoter (C1). Pathway on the right: Glucose also stimulates the binding activity of Beta2/NeuroD to the insulin promoter (E1) in β cells, which is dependent upon the phosphorylation of extracellular signal-regulated kinase (ERK) 1/2.

1.2.1.2.1. PDX-1

PDX-1 is essential for pancreas formation, β cell differentiation, and maintenance of mature β cell function. Mice lacking PDX-1, homozygotes (-/-), fail to develop a pancreas, known as pancreas agenesis (Jonsson, Carlsson, Edlund, & Edlund, 1994; Offield et al., 1996). A single nucleotide deletion in the human PDX-1 gene was reported in one patient with pancreas agenesis (Stoffers, Zinkin, Stanojevic, Clarke, & Habener, 1997). It has been suggested that PDX-1 may have the potency to drive beta-cell-like differentiation in non-beta-cells in adult murine liver (Imai et al., 2005) and intestinal epithelial cells (Yoshida et al., 2002). In addition, PDX-1 heterozygous (+/-) mutant mice have impaired islet insulin-producing function and develop diabetes with age (Ahlgren, Jonsson, Jonsson, Simu, & Edlund, 1998; Dutta, Bonner-Weir, Montminy, & Wright, 1998). A strong family history of maturity-onset diabetes of the young or MODY is associated with heterozygosity for a point mutation in the human PDX-1 gene (Stoffers, Ferrer, Clarke, & Habener, 1997). Taken together, these data clearly suggested that PDX-1 plays a crucial role in pancreas formation, β cell differentiation, and maintenance of mature β cell function.

The PDX-1 also plays an important role in linking glucose metabolism to the regulation of insulin gene transcription (Macfarlane et al., 2000). Increased glucose concentration enhances the potential of the PDX-1 activation domain and the binding of PDX-1 to the insulin gene promoter, a region upstream of the insulin gene termed A3 box, to activate the insulin gene transcription (MacFarlane, Read, Gilligan, Bujalska, & Docherty, 1994). Glucose also stimulates insulin gene promoter activity involving translocation of PDX-1. In MIN6, a cultured β cell line, increasing glucose levels stimulates the shift in PDX-1 from the nuclear periphery and membrane region to the nucleoplasm and increases the activity of insulin promoter and insulin gene transcription (Rafiq, da Silva Xavier, Hooper, & Rutter, 2000; Rafiq, Kennedy, & Rutter,

1998). In addition, it is suggested that glucose activates PDX-1 function and stimulates insulin gene promoter activity via intracellular singling pathways. Glucose entry into the β cell is accomplished via the glucose transporter 2 (Glut2) located on the plasma membrane. After entering the β cell through Glut2, glucose activates the phosphorylation of phosphatidylinositol 3-kinase (PI3-K) to activate PDX-1 function (Elrick & Docherty, 2001; Rafiq et al., 2000). These data suggested that glucose stimulates PDX-1 translocation and increases PDX-1 DNA binding activity through the pathway involving PI3-K activation (Figure 2).

1.2.1.2.2. NeuroD/Beta2

Beta-cell E-box trans-activator 2 (Beta2) belongs to the basic helix-loop-helix (bHLH) proteins, also known as NeuroD (Neurogenic Differentiation Factor). The expression pattern of NeuroD/Beta2 suggests a role in endocrine pancreas development. Abnormal pancreatic islet morphogenesis is found in Beta2-deficient mice (Naya et al., 1997). Mice homozygous for the NeuroD/Beta2 gene deletion develop diabetes and die 3~5 days after birth due in part to inadequate insulin gene expression (Naya et al., 1997). In addition, the mutation in NeuroD/Beta2 leads to the development of type 2 diabetes in humans due to deficit or inactive binding of NeuroD/Beta2 transcription factor to a insulin promoter (Malecki et al., 1999).

NeuroD/Beta2 is an important transcriptional activator in pancreatic β cells for glucose-stimulated insulin gene transcription. NeuroD/Beta2 binds to the E1 box of the insulin gene promoter to transcribe the insulin gene (Naya, Stellrecht, & Tsai, 1995). Glucose stimulates the binding activity of NeuroD/Beta2 to the insulin promoter (E1 box) in β cell. This reaction is dependent upon extracellular signal-regulated kinase (ERK) 1/2 which regulates the gene transcription (Khoo et al., 2003). Glucose activates β cell ERK1/2 phosphorylation, and phosphorylated ERK1/2 further enhance Beta2 and E47 (a ubiquitous bHLH protein) heterodimerization and binding to E-box sites (Lawrence, McGlynn, Park, & Cobb, 2005)

(Figure 2). Taken together, these results suggested that NeuroD/Beta2 plays an important role in pancreas development as well as in regulating insulin gene transcription.

1.2.1.2.3. MafA

MafA belongs to the Maf (v-maf musculoaponeurotic fibrosarcoma oncogene homolog (avian)) family of transcription factors. It is a principal factor required for the pancreatic β cell formation and function. MafA is expressed specifically in the β cells of islets (Olbrot, Rud, Moss, & Sharma, 2002), and its expression is the first detected at the beginning of the β cell development (Matsuoka et al., 2004). MafA-deficient (-/-) mice displayed age-dependent pancreatic islet abnormalities, and diminished expression of PDX-1, NeuroD/Beta2, and Glut2 (Zhang et al., 2005). In addition, MafA is suggested as a master regulator of genes implicated in insulin biosynthesis and secretion (Wang, Brun, Kataoka, Sharma, & Wollheim, 2007). These results strengthen the crucial role of MafA for β cell formation and function.

MafA functions as a glucose-regulated transcriptional activator that binds to the C1 site of insulin promoter for insulin gene expression (Figure 2). In MafA-deficient (-/-) mice, glucose-stimulated insulin secretion is severely impaired (Zhang et al., 2005). The mechanism by which MafA is activated by glucose is different from PDX-1 and NeuroD/Beta2. Glucose induces post-translational modification of PDX-1 and NeuroD/Beta2, but glucose activates MafA through increasing MafA gene transcription. The expression of MafA mRNA and protein in MIN6 β cell line is dependent on glucose concentration, which is correlated with preproinsulin mRNA level. MafA protein is detected in the nucleus of MIN6 β cells when stimulated by glucose (Kataoka et al., 2002). Incubating isolated rat islets in 16.7mM glucose for 24 hours increases MafA mRNA level. Also, MafA protein expression is undetectable under basal conditions (2.8mM glucose), but readily detected at a high concentration of glucose (16.7mM)

(Hagman, Hays, Parazzoli, & Poitout, 2005). Therefore, these data suggest that glucose activates MafA expression to enhance insulin gene transcription.

1.2.2. Insulin Protein Biosynthesis

After transcription, the preproinsulin mRNA moves from the nucleus into the cytoplasm for the insulin biosynthesis through a cascading process as followed. First, the mRNA binds to the free ribosome, a cell organelle that contains the enzymes and rRNAs (ribosomal RNA) required for the translation, to assemble polypeptide chain (protein) (Figure 3A). The first sequence of synthesized peptide, known as signal sequence or signal peptide, on the surface of ribosome then acts as a recognition signal to direct the ribosome to bind to the granular endoplasmic reticulum (ER) to continue the protein assembly (Figure 3B). The growing preproinsulin polypeptide is fed through a protein complex in the granular ER membrane into the lumen of the reticulum. After completion of polypeptide synthesis, the completed preproinsulin protein is released from the ribosome (Figure 3C). Within the lumen of the granular ER, the "pre-portion" of the preproinsulin (such as the signal peptide) is removed enzymatically forming the proinsulin. Following the modification, portions of the ER membrane develop vesicles that contain the newly synthesized proinsulin protein (Figure 3D). These proinsulin vesicles are transported to the Golgi apparatus and fuse with the Golgi membranes (Figure 3E). The Golgi apparatus is a cell organelle that concentrates, modifies and sorts the proteins arriving from the ER. In the Golgi apparatus of β cells, the proinsulin proteins are packaged into immature granules that bud off the surface of the Golgi membrane (Figure 3E) and are further converted to insulin and C-peptide (Figure 3F) by the processing enzymes (Orci et al., 1987). Proprotein convertase 1(PC1), proprotein convertase 2 (PC2) and carboxypeptidase E (CPE) are the enzymes that are involved in proinsulin cleavage resulting in insulin and c-peptide production in the β cell (Figure

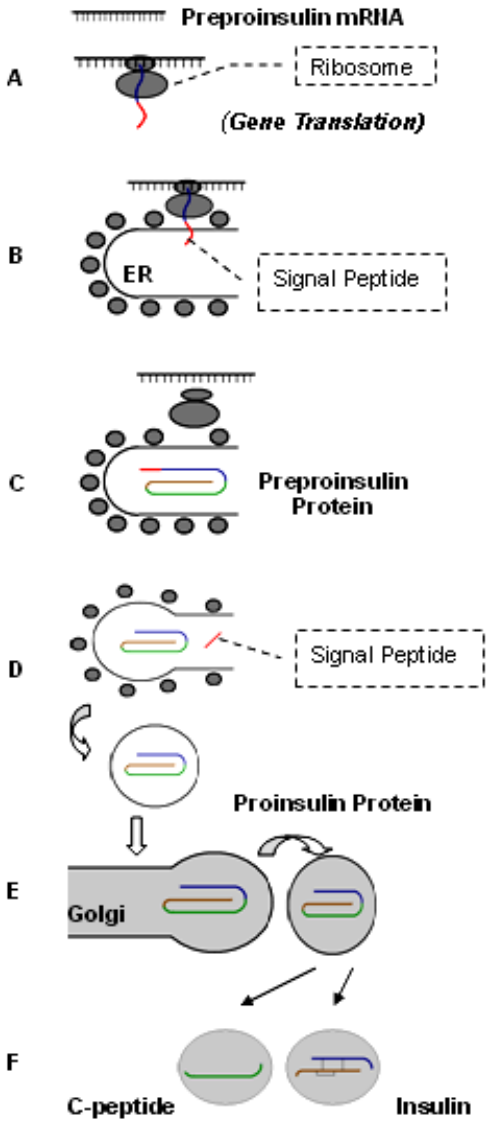

Figure 3. The process of insulin protein biosynthesis. First, the preproinsulin mRNA binds to the free ribosome, to assemble polypeptide chain. The first sequence of synthesized peptide acts as a recognition signal to direct the ribosome to bind to the granular endoplasmic reticulum (ER) to continue the protein assembly. The growing preproinsulin polypeptide is fed through a protein complex in the granular ER membrane into the lumen of the reticulum. After protein assembly, the completed preproinsulin protein is released from the ribosome. Within the lumen of the granular ER, the "pre-portion" of the preproinsulin is removed enzymatically forming the proinsulin. Following the modification, portions of the ER membrane develop vesicles that contain the newly synthesized proinsulin protein. These proinsulin vesicles are transported to the Golgi apparatus and fuse with the Golgi membranes. In the Golgi apparatus of β cells, the proinsulin proteins are packaged into immature granules that bud off the surface of the Golgi membrane and are further converted to insulin and C-peptide by the processing enzymes. The granules then become mature intracellular granules in which the insulin crystals are composed.

3F). The granules then become mature intracellular granules in which the insulin crystals are composed. Since the preproinsulin's life time in the ER is very short, its level is quite difficult to detect. Proinsulin, however, is more stable and is easier to detect than the preproinsulin. Therefore, proinsulin is usually referred to as the product of preproinsulin mRNA translation, even though the preproinsulin is the actual translation product in the whole process of insulin biosynthesis. For simplicity, in this thesis, we will refer to the preproinsulin mRNA translation product as proinsulin.

Glucose is the most physiologically relevant factor that regulates the insulin protein biosynthesis at the translational level. Glucose stimulates the recruitment of preproinsulin mRNA from an inert cytosolic pool to the rough ER, the site of preproinsulin synthesis (Itoh & Okamoto, 1980; Welsh, Scherberg, Gilmore, & Steiner, 1986). After one hour of incubation at high glucose (16.7 mM), proinsulin level in the rat islets increases up to 6-fold (Wicksteed, Alarcon, Briaud, Lingohr, & Rhodes, 2003) and even more than 15-fold shown by another study (Guest, Rhodes, & Hutton, 1989). In addition, proinsulin synthesis is dose-dependent under glucose stimulation. In purified pancreatic β cells, proinsulin synthesis increased 25-fold when glucose was increased from 1 to 10 mM for one hour (Schuit, In't Veld, & Pipeleers, 1988). These results further strengthen the role of glucose in insulin protein biosynthesis.

1.2.3. Insulin Granules Secretion

1.2.3.1. Directing insulin granules to the plasma membrane

After synthesis, the mature insulin granules (or vesicles) in the cytoplasm are secreted into the extracellular space. In order to release insulin, the insulin granules (or vesicles) must be translocated from the cytoplasm to the plasma membrane where they fuse with the membrane. SNARE (soluble *N*-ethylmaleimide-sensitive factor attachment protein receptor) is an important group of proteins that direct the insulin granules to the plasma membrane. The linking of

target-SNARE (t-SNARE) plasma membrane proteins, syntaxin and synaptosomal-associated protein 25 (SNAP-25), with the vesicle-SNARE (v-SNARE) protein, vesicle-associated protein 2 (VAMP-2) or synaptobrevin-2, is critical for docking insulin granules with the plasma membrane and the L-type voltage dependent Ca^{2+}-channel (L-VDCC) on the membrane. After fusing with the plasma membrane, insulin granules are released in response to the products of glucose metabolism.

1.2.3.2. Glucose-induced insulin release

The mechanism for how glucose triggers insulin release has been well established. ATP-sensitive K^+ (K_{ATP}) channel-dependent pathway is one of the glucose-induced insulin release pathways that trigger insulin release (Figure 4). Intracellular glucose is metabolized to generate adenosine triphosphate (ATP), a nucleotide that plays a role as the source of energy for intracellular energy transfer. The K_{ATP} channel on the cell membrane will be closed by an increase in ATP that depolarizes the membrane and enhances membrane excitability. The membrane depolarization then opens the L-type voltage dependent Ca^{2+} -channels (L-VDCC) in pancreatic β cell, and increases the influx of calcium. The elevated intracellular Ca^{2+} concentration causes exocytosis of the insulin granules located close to the plasma membrane and the Ca^{2+}-channels (Bratanova-Tochkova et al., 2002). After granules have undergone exocytosis, the empty vesicle membrane is rapidly dissociated from the plasma membrane and recaptured by endocytosis, a process with opposite function as exocytosis, for the recycling purpose (Sudhof, 1995). In addition, glucose stimulates the discharges of the docked insulin granule and dissociates the docking proteins SNARE complex between the vesicle and plasma membrane (Daniel, Noda, Straub, & Sharp, 1999). Taken together, glucose plays a crucial role in insulin secretion through K_{ATP} channel-dependent pathway.

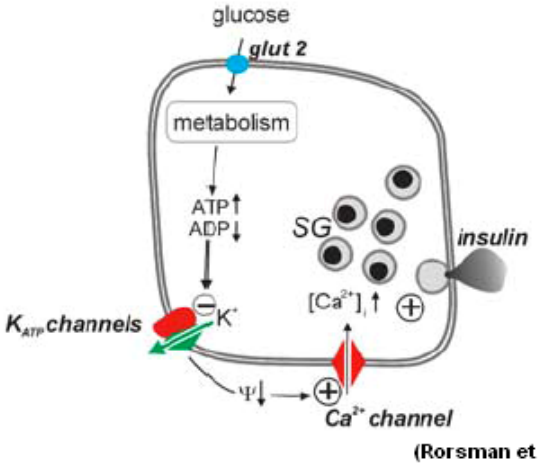

Figure 4. Glucose-induced insulin release through the ATP-sensitive K^+ (K_{ATP}) channel-dependent pathway. Intracellular glucose is metabolized to generate ATP. The K_{ATP} channel on the cell membrane is closed by an increase in ATP that depolarizes the membrane and enhances membrane excitability. The membrane depolarization then opens the L-type voltage dependent Ca^{2+} -channels (L-VDCC) in pancreatic β cell, and increases the influx of calcium. Elevated intracellular Ca^{2+} concentration causes exocytosis of the insulin granules located close to the plasma membrane and the Ca^{2+}-channels. (SG: Secretory Granules)

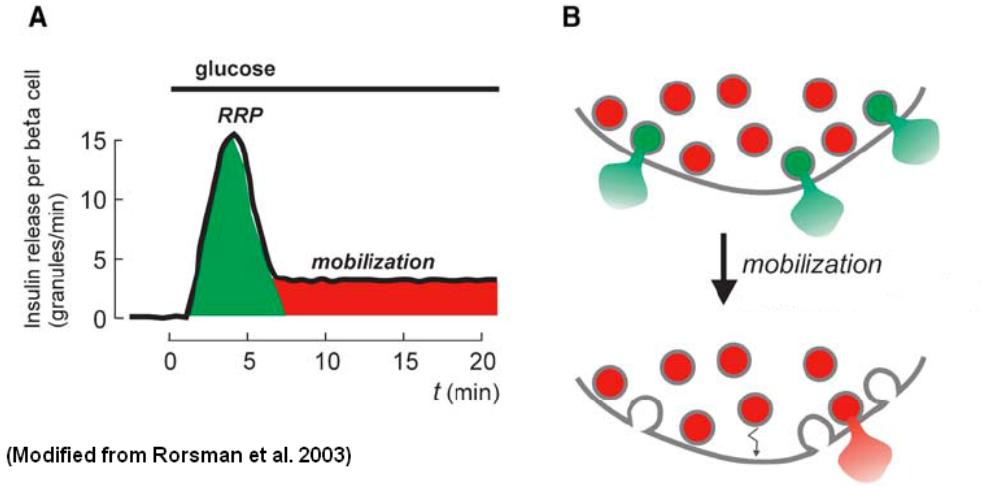

Figure 5. Granule pools and biphasic insulin secretion. (A) Schematic of glucose-induced insulin secretion. (B) β cell contains two pools of secretory granules. A limited pool of granules (<5%) are immediately available for release, the readily releasable pool (RRP) of granules (green). Most granules (>95%) initially belong to a reserve pool (red) and must undergo a series of preparatory reactions in order to gain release competence (mobilization). The release of RRP granules accounts for first-phase secretion and its end marks the depletion of this pool. The subsequent supply of new granules for release by mobilization accounts for second-phase insulin secretion.

1.2.3.3. Biphasic insulin secretion

Insulin secretion in response to increased glucose concentrations exhibits a biphasic pattern consisting of a rapidly initiated and transient first phase (lasting 5~10 minutes) followed by slowly developing and sustained second phase (Figure 5). This characteristic biphasic pattern has been identified more than 30 years ago (Curry, Bennett, & Grodsky, 1968). It is observed both in vitro (islets) and in vivo (including human) (Cerasi, 1975; Lacy, Walker, & Fink, 1972; Luzi & DeFronzo, 1989).

Only a small fraction of the β cell insulin content is released in response to a single glucose stimulus. In the first phase, less than 5% of the insulin granules in the β cell are available in the readily releasable pool for membrane fusion, and the granule secretion rate has been reported to amount to 0.14% of the total insulin content in the β cell per minute. However, more than 95% of insulin granules belong to a reserve pool. In the second phase, the granule secretion rate is only 0.05% of the total insulin content per minute (Rorsman & Renstrom, 2003). Given that every β cell contains about 13,000 granules (Dean, 1973), these release rates correspond to approximately 18 and 7 granules per minute per beta cell in the first and second phases, respectively. In addition, the first phase insulin release from the readily releasable pool is regulated by glucose stimulation through the K_{ATP} channel-dependent pathway, with increasing Ca^{2+} causing insulin granule release or exocytosis. While the readily releasable pool is associated with the first phase of glucose-induced insulin release, glucose also plays a role in the second phase of glucose-induced insulin release that involves the mobilization and priming process of insulin granules from reserve pools to the readily releasable pool to gain the competence for the sustained second phase release (Bratanova-Tochkova et al., 2002).

1.3. Small and large islets

1.3.1. Size-frequency distribution

The existence of islet subpopulations according to size difference has been recognized since the Dr. Paul Langerhans discovered the islets in the pancreas in 1869 (Bloomfield, 1958). Islets vary in size and range from a very small cell cluster with only a few cells to large aggregates of many thousands of cells. The size and volume of islets is associated with significant morphological difference distinguishing islet subpopulations in mammalian pancreas.

The size distribution of islets was continuous from 20μm to more than 400μm in diameter and skewed with only one peak in the distribution curve (Figure 6). In 1959, it was reported that smaller islets are more numerous in human pancreas (Hellman, 1959a). In 1986, a Japanese group investigated the radial size and number of human islets by a thin serial pancreas section technique combined with immunostaining insulin and glucagon. They suggested that the majority of islets were the small islets, but the small islets accounted for only a very small percentage of the total islet volume in the pancreas (Kaihoh, Masuda, Sasano, & Takahashi, 1986). In addition, with advances in the methods of islet isolation and digital image analysis, researchers were able to confirm these findings (Buchwald et al., 2009; Friberg et al., 2011; Girman, Berkova, Dobolilova, & Saudek, 2008). For example, by dividing islets population into two groups by size which are small (diameter below 125μm) and large (diameter above 150μm), the amount of small islets in the pancreas is near 3-fold greater than large islets. However, in terms of the proportion of the total volume, large islets account for approximately 73% of total islet volume and small islets comprise the remaining 27% (MacGregor et al., 2006). In addition, more small islets were identified in the upper duodenal region of pancreas, while more large islets were seen in the splenic region (A. A. Elayat, M. M. el-Naggar, & M. Tahir, 1995).

1.3.2. Size-related insulin secretion and transplantation outcome

Islet size is a major determinant in islet insulin secretion. While one small islet produces less insulin than one large islet (T. Aizawa et al., 2001), in terms of islet tissue volume, however, the small islets have been shown superior in insulin secretion as compared to the large islets per volume (Fujita et al., 2011; Hayek & Woodside, 1979; H.-H. Huang, L. Novikova, S. Williams, I. Smirnova, & L. Stehno-Bittel, 2011; Lehmann et al., 2007; MacGregor et al., 2006; Su et al., 2010; Williams et al., 2010). In 2006, our group published a paper describing that the small rat islets (diameter <125μm) are superior to large islets (diameter >150μm) in insulin secretion per volume when using the islet equivalent (IE) to normalize. After separating small islets from large islets through sedimentation, we identified that the small islets released three times and four times respectively more insulin under basal conditions (3mM) and high concentration (30mM) than did large islets (MacGregor et al., 2006). Subsequent experiments found similar results in mouse and human islets (Lehmann et al., 2007; Su et al., 2010). Small human islets produce almost twice the amount of insulin compared to same IE of large islets in the basal state (2.8mM glucose) and during high simulation (20mM) glucose perifusion experiments (Lehmann et al., 2007). In addition, transplanting small rat islets into type 1 diabetic animal model surprisingly led to better blood glucose control 60 days after transplantation in comparison to the same volume of large islets (Figure 7)(MacGregor et al., 2006). In human, the type 1 diabetic patients who received relatively higher amount of small islets were shown having better transplantation outcome (Lehmann et al., 2007). Taken together, **our central hypothesis is that small and large islets may have different mechanisms in insulin production and secretion**.

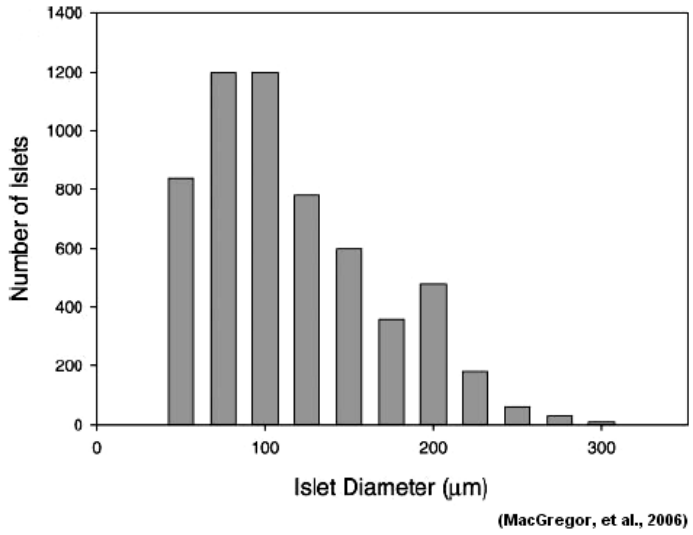

Figure 6. Size and number dispersion of isolated rat islets. The figure illustrates a typical rat islet dispersion on the basis of islet size. The distribution curve skewed with only one peak in the small islet (75~100µm). (MacGregor, R.R., et al., 2006)

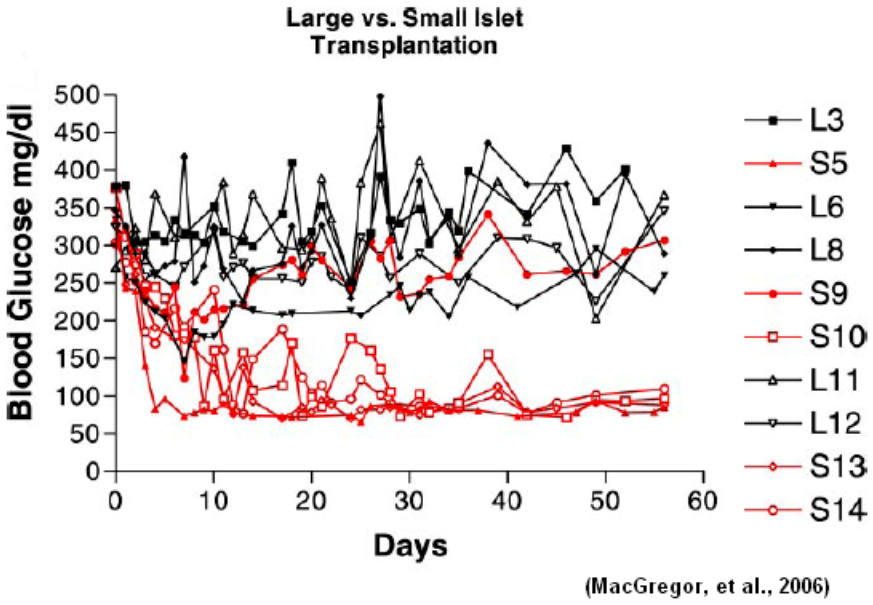

Figure 7. 60 days follow-up for small and large islet transplantation in rat model of type 1 diabetes. When small islets were transplanted (red lines), glucose levels of rats were normal in all but 1 animal after transplantation. Transplants using large islets (black lines) were all unsuccessful. (MacGregor, R.R., et al., 2006)

1.4. Research question

The long-term goal of our research is to better understand islet biology to improve islet transplantation strategies. Since the small islet secretes more insulin per volume (IE) of tissue than the large islet, we believe there must be some characteristics different in the insulin producing capacity between small and large islets. However, the differences in the mechanisms of insulin production between small and large islet subpopulations are unclear. Therefore, the objective of this dissertation was to investigate the mechanisms of insulin production and secretion in small and large rat islets.

In chapter 2, "Low insulin content of large islet population is present in situ and in isolated islets", we determined whether the differences of insulin producing capacity in isolated small and large islets are solely a result of the ability to withstand the isolation procedure, or whether these characteristic differences between islet subpopulations exit inherently in the pancreas (in situ).

In Chapter 3, "Total cell number- a superior model for volume quantification of isolated islets", we created and tested a new method to more accurately quantify the amount of islet tissue being used in the experiments, and found that the IE normalization method actually affected some of our initial results.

In Chapter 4, "The insulin biosynthesis pathway in small and large islets does not correspond to insulin secretion", by applying the more accurate normalization method described in Chapter 3, we compared the mechanisms of insulin production and secretion in early response to glucose stimulation in small and large islets at cellular levels.

In Chapter 5, we summarized all the findings from chapters 2 through chapter 4. We also discussed the implications of this dissertation to the islet biology and transplantation fields. In addition, the future directions were suggested in this chapter.

Chapter 2

Low Insulin Content of Large Islet Population is Present *in Situ* and in Isolated Islet

2.1. Abstract

The existence of morphologically distinct populations of islets in the pancreas was described over 60 years ago. Unfortunately, little attention has been paid to possible functional differences between islet subpopulations until recently. We demonstrated that one population, the small islets, were superior to large islets in a number of functional aspects. However, that work did not determine whether these differences were inherent, or whether they arose because of the challenge of isolation procedures. Nor, were there data to explain the differences in insulin secretion. We utilized immunohistochemistry, immunofluorescence, ELISA, and transmission electron microscopy to compare the unique characteristics found in isolated rat islet populations in situ and after isolation. Insulin secretion of small isolated islets was significantly higher compared to large islets, which correlated with higher insulin content/area in small islets (in situ), a higher density of insulin secretory granules, and greater insulin content/volume in isolated islets. Specifically, the core β-cells of the large islets contained less insulin/cell with a lower insulin granule density than peripheral β-cells. When insulin secretion was normalized for total insulin content, large and small islets released the same percentage of total insulin. Small islets had a higher density of cells/area than large islets in vitro and in situ. The data provide a possible explanation for the inferior insulin secretion from large islets as they have a lower total cell density and the β-cells of the core contain less insulin/cell.

2.2. Introduction

Morphometrical analysis, first reported in 1947, showed differences in size distribution, number and volume of islets from several species (T Aizawa et al., 2001; Bonnevie-Nielsen & Skovgaard, 1984; A. Elayat, M. el-Naggar, & M. Tahir, 1995; Furuzawa, Ohmori, & Watanabe, 1992; Haist & Pugh, 1947; Jörns, Barklage, & Grube, 1988; White, Hughes, Contractor, & London, 1999) including human (Aguayo-Mazzucator, Sanchez-Soto, Godinez-Puig, Gutie'rrez-Ospina, & Hiriart, 2006; Baetens, Malaisse, Perrelet, & Orci, 1979; Bosco et al., 2010; Cabrera et al., 2006; K Saito, Takahashi, Yaginuma, & Iwama, 1978). In spite of morphological analysis showing distinct populations of islets, most researchers and clinicians still consider all islets to be functionally equivalent.

It is surprising that many of the details about the function of islets are still unknown (Cabrera et al., 2006; Tasaka, Matsumoto, Inoue, & Hirata, 1989). In 2001 an important paper examined the functional differences between islets that related to their size (T Aizawa et al., 2001). The authors showed a variety of functionally different islet characteristics, including the fact that 60% of the islets responded to glucose challenge with a dose-dependent insulin release, versus 32% of islets that had an all-or-none response. Other structural variations based on islet size were published recently (Bosco et al., 2010).

Our laboratory reported that isolated small islets from rats were superior to large islets in function and in transplantation outcomes, especially when measuring insulin secretion (MacGregor et al., 2006). Subsequent experiments by other laboratories confirmed similar results in human and mouse islets (Lehmann et al., 2007; Su et al., 2010). To further characterize these differences, we determined that large islets contained a significant diffusion barrier that hampered viability of the islets in culture (Williams et al., 2010). Surprisingly, elimination of the diffusion barrier in large rat islets did not restore insulin secretion to the same rate as intact small

islets, suggesting that there were inherent cellular differences between large and small islets (Williams et al., 2010) that might explain the inferior insulin secretion by the cells within the large islets.

The behavior of islets in culture has important implications for islet transplantation. Yet a more important question lingers, are these differences in islet function solely a result of the ability of islets of different sizes to withstand the isolation procedure, or do these functional differences exist *in vivo*? The experiments described in this paper begin to elucidate the morphological and functional differences in rat islet subpopulations, and to determine whether these differences exist prior to isolation.

2.3. Methods

Rat islet isolation

Twenty-six adult, male Sprague Dawley rats (ages 7-10 weeks) were housed on a 12 hours light/dark cycle with free access to standard laboratory chow and water. All animals received care in compliance with the Principles of Laboratory Animal Care formulated by the National Society for Medical Research and the Guide for the Care and Use of Laboratory Animals published by the US National Institutes of Health (NIH Publication No. 85-23, revised 1996).

Islet isolation methods followed our published procedures described in detail.(MacGregor et al., 2006; Williams et al., 2010; S. Williams et al., 2009). Briefly, rats were anesthetized by intraperitoneal injection of a mixture of ketamine and xylazine. After the peritoneal cavity was exposed, the pancreatic main duct to the intestine was clamped and the pancreas cannulated *in situ* via the common bile duct. The pancreas was distended with collagenase and removed. Islets were gently tumbled, washed, and passed through a sterile 30 mesh stainless steel screen and centrifuged. The pellet was mixed with Histopaque, centrifuged, and the islets floating on the gradient were collected and sedimented. Islets were passed through a sterile 40μm mesh cell strainer with Hank's Buffered Salt Solution (HBSS). After this cleaning process, islets were placed into CMRL 1066 medium containing 2 mM glutamine, 10% fetal bovine serum (FBS) and 1% antibiotic/ antimycotic solution and put into a 37ºC culture chamber containing 5% CO_2.

Prior to experiments, the islet culture media was changed to L15 containing 10% FBS and 5mM HEPES, and islets were transferred into 37ºC culture chamber without CO_2. Isolated islets were separated by size manually or by using the COPAS biosorter (Williams et al., 2010). The diameter of every islet was recorded for calculating total islets volume using light microscopy. Islet Equivalents (IE) were calculated by taking duplicate samples of each batch of islets (comprising < 2% of the islet fraction). Individual islets were counted and their diameters

measured. For irregularly shaped islets, two to four diameter measurements were taken at different locations on the islet and averaged. Islet volumes were calculated and converted to IE for the sample and the entire islet fraction.

Cell dispersion

For single cell assays, intact isolated islets from 8 rats were exposed to calcium-magnesium free HBSS 14.8 mM HEPES with papain (5 U/ml final concentration) using our published protocol (S. Williams et al., 2009). After incubation on a rotator at 37°C for 30 min, the islets were pipetted, dispersing them into single cells. The cells were transferred to CMRL 1066 as the final culture medium. When necessary, islets or dispersed β-cells were identified with dithizone labeling following published procedures (Mythili, Patra, & Gunasekaran, 2003; S. Williams et al., 2009).

Tissue preparation for immunostaining

Seven rats were anesthetized and transcardially perfused with 80-100 ml of physiological saline, followed by 250 ml of a fixative solution containing 4% paraformaldehyde in 0.1 M phosphate buffered saline (PBS, pH 7.4) within 9 min of extermination. The pancreas was removed and dissected into three parts (head, middle and tail). Only the tail section was used for the analysis in this study.

Pancreatic samples and isolated islets were fixed in 10% normal buffered formalin in PBS, pH 7.4 for three days at 4°C. Paraffin embedded tissue sections were cut (7-10 μm thickness), mounted on Superfrost/Plus microscope slides (Fisher Scientific, # 12-550-15) and dried at 40°C overnight and stored at 4°C until processing. The paraffin embedded sections were deparaffinized/rehydrated in xylene followed by ethanol and PBS serial rehydration. Antigen

retrieval was completed in 0.01M citrate buffer, pH 6.2, with 0.002M EDTA for 30 min using a steamer. Slides were permeabilized in 1.0 % Triton X-100 in 0.1 M PBS for 30 min.

Immunofluorescence staining

Sections from 3 rats (> 75 islets) were blocked in 10% normal donkey serum (NDS), 1.0% bovine serum albumin (BSA), and 0.03% Triton X-100 diluted in 0.1 M PBS for 30 min. Incubation with the primary antibody mix was performed at 4°C overnight in a wet chamber followed by incubation with the mix of fluorophore conjugated secondary antibodies at room temperature for 2 hr in a wet chamber protected from light. Both primary and secondary antibodies were diluted in 1% NDS, 1% BSA, and 0.03% Triton X-100. Slides were mounted with anti-fading agents. In some cases, 4',6-diamidino-2-phenylindole (DAPI, 0.5 µg/ml Molecular Probes, # D1306) staining was performed to reveal the nuclei for 5 min at room temperature after the secondary antibody exposure.

Primary antibodies used were the following: anti-insulin (1:100, Abcam, # ab7842; 1:100, Santa Cruz Biotechnology, # sc-9168),), anti-glucagon (1:200, Abcam, # ab10988), and anti-somatostatin (1:200, Abcam, # ab53165). Corresponding secondary antibodies were conjugated with Cy2 (1:200, Jackson ImmunoResearch Laboratories Inc., # 706-225-148), Alexa 647 (1:400, Molecular Probes, # A31573), Alexa 555 (1:400, Molecular Probes, # A31570), or DyLight 488 (1:400, Jackson ImmunoResearch Laboratories Inc., # 706-485-148).

Images were obtained on an Olympus Fluoview 300 confocal microscope or using a Nikon C1Si or a C1Plus confocal microscope. Images were acquired using 10X - 100X objectives (depending on the experiment), and analyzed using FlouView or Ps Adobe Photoshop CZ4 software.

Immunohistochemistry

Insulin immunohistochemistry (IHC) was completed on pancreatic sections from four rats using anti-insulin (1:100, Santa Cruz Biotechnology, Inc**.,** # sc-9168) and Vectastain Elite ABC kit (Vector Laboratories, #PK-6101) in combination with 3,3'-diaminobenzidine Peroxidase Substrate kit (Vector Laboratories, # SK-4100) as per manufacturer instructions. On occasions, 3-amino-9-ethyl-carbazole (AEC) was used. After staining, slides were dehydrated in xylene and placed on coverslips in Permount mounting medium (Fisher Scientific, #S15-100). The specificity of insulin immunoreactivity was confirmed by omitting the primary antibodies from some sections. Images were collected on a Nikon Eclipse 80i microscope and analyzed with Ps Adobe Photoshop CZ4 extended software, by determining the average pixel value of staining per cell or per islet. Background staining was subtracted from each value.

Cell composition

To determine the cell composition, the relative proportion of immuno-labeled endocrine (α, β, and δ) cells in pancreatic sections from 3 rats or preparations of single dispersed cells [200 islets from 6 rats dissociated into single cells with 6 aliquots of single cells from each group (small or large)] were evaluated by counting the number of individual types of cell and dividing by the total sum of endocrine cells per islet. In addition, DAPI was used to count the total cell number in the preparation.

Islet perifusion

Small and large islets (1400 islets) from six rats were preincubated for 90 minutes in RPMI 1640 medium containing 10% FBS and 3mM glucose at a 37°C with 5% CO_2. After preincubation, the islets were incubated in the glucose perifusion system individually with a constant flow rate (500µl/min) at 37°C for 90 minutes including: 30 minutes of basal condition

(3mM glucose) following by 30 minutes of high glucose concentration (20mM) and 30 minutes of basal condition (3mM glucose). During the perifusion, samples of medium with released insulin were collected from the output fraction every 3 minutes starting with the last 10 minutes of the first low glucose exposure. Samples were frozen at -80°C. At the end of the perifusion, the islets were harvested and frozen at -80°C. The total protein in the islets was extracted by acid ethanol (0.18M HCl in 95% ethanol). The released insulin and the total intracellular insulin amounts of large and small islets were determined by the ELISA (ALPCO, Salem, NH) as we have published previously (MacGregor et al., 2006; Williams et al., 2010; S. Williams et al., 2009).

Transmission electron microscopy

Islets from 5 rats were treated with 10 nM AuNP-DNA-Cy for 24 hours, washed twice with PBS, and then transferred to fresh media containing no AuNPs for an additional 72 hours. Islets were pelleted and immersed in 2% paraformaldehyde/2.5% glutaraldehyde in 0.1M sodium cacodylate buffer (SCB). The islets were then rinsed with 0.1M SCB and placed in secondary fixative containing 2% osmium tetraoxide in 0.1M SCB. Next, islets were rinsed with distilled water and stained with 3% uranyl acetate. The fixed islet samples were rinsed with distilled water before undergoing a graded ethanol dehydration series. Propylene oxide was used as a transitional solvent and tissues were embedded in Embed 812 resin. Samples were placed in a 60°C oven to cure. The blocks were sectioned at the islet equatorial region using a Leica UCT ultramicrotome (80nm thin) and then mounted on grids for imaging. Images were captured from random sections using a J.E.O.L. JEM-1400 electron microscope. Insulin granules (halo-containing granules) were counted per μm^2 in β-cells from small islets (105 cells from 46 islets) and in the periphery (outer 3 layers) or core of large islets (155 cells from 60 islets) using standard procedures (Pisania, Weir et al., 2010; Stefan, Meda, Neufeld, & Orci, 1987). Total cell

density was analyzed by counting cells within a 25X25 μm region of interest in the core of each islet using published protocols at 3,800X magnification (Obermuller et al., 2010). This method tends to overestimate the absolute cells/area, but the objective of the calculations was to compare one population of islets to another, rather than obtain an absolute value, and the approach was applied uniformly to islets of both populations. Our published protocol was utilized to determine mitochondrial quality from final magnifications of 10,800X (Y. M. Searls, I. V. Smirnova, B. R. Fegley, & L. Stehno-Bittel, 2004).

Statistics

Over 2225 islets from 26 rats were analyzed for this study. The experimental design included comparing large and small islets from healthy animals, thus each animal provided islets for both groups. The exact number of islets/experiment is shown in the methods section. Two-Way ANOVA with Fisher Least Significant Difference (LSD) test or a Kruskal-Wallis ANOVA on Ranks was used to compare multiple groups. For the single cell assays (immunostaining and TEM experiments) nested ANOVA was used. All figures and tables include means ± SE. P value < 0.05, was considered statistically significant.

2.3. Results

Insulin secretion

Perifusion experiments illustrated that under basal conditions, and at each time point of the biphasic response, the small islets released more insulin per volume (islet equivalent; IE) than large islets. Figure 8 shows the results of the enzyme linked immunosorbent assay (ELISA) from approximately 1,400 islets from 6 rats. While similar results have been published previously with human islets (Lehmann et al., 2007), the rationale given for the difference in insulin secretion between large and small islets has been attributed to core cell death in the large isolated islets (MacGregor et al., 2006). Our previous publication indicated that such an explanation was insufficient to account for the dramatic differences in insulin secretion from large islets (Williams et al., 2010). Thus, we designed a series of experiments to determine whether there existed inherent differences in large and small islets prior to isolation that could account for the different insulin secretion rates.

Islet cell composition

The first hypothesis to be tested was that small islets contained a higher percentage of β-cells than large islets and this accounted for the higher insulin secretion. Using immunofluorescently-stained serial sections of the pancreas, the islet cell composition was analyzed (Figure 9A & B). In order to critically classify the islet as large or small, serial sections of 10 μm were obtained and only sections with the greatest islet diameter were analyzed. Approximately 60% of the endocrine cells were composed of β-cells in large and small islets *in situ* (

Table **1**).

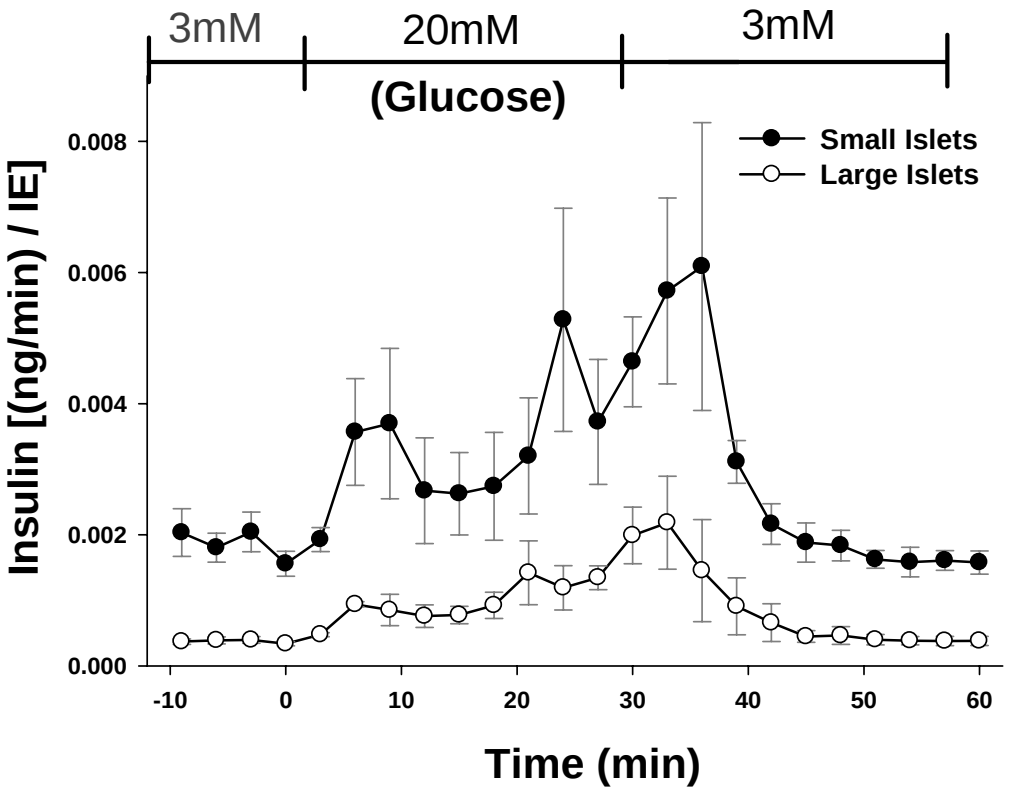

Figure 8. Small isolated islets secrete more insulin per volume. Isolated islets were separated into large and small populations and exposed to low and high glucose (indicated at top of graph). At each time point more insulin was released by the small islets than the large ($p < 0.001$).

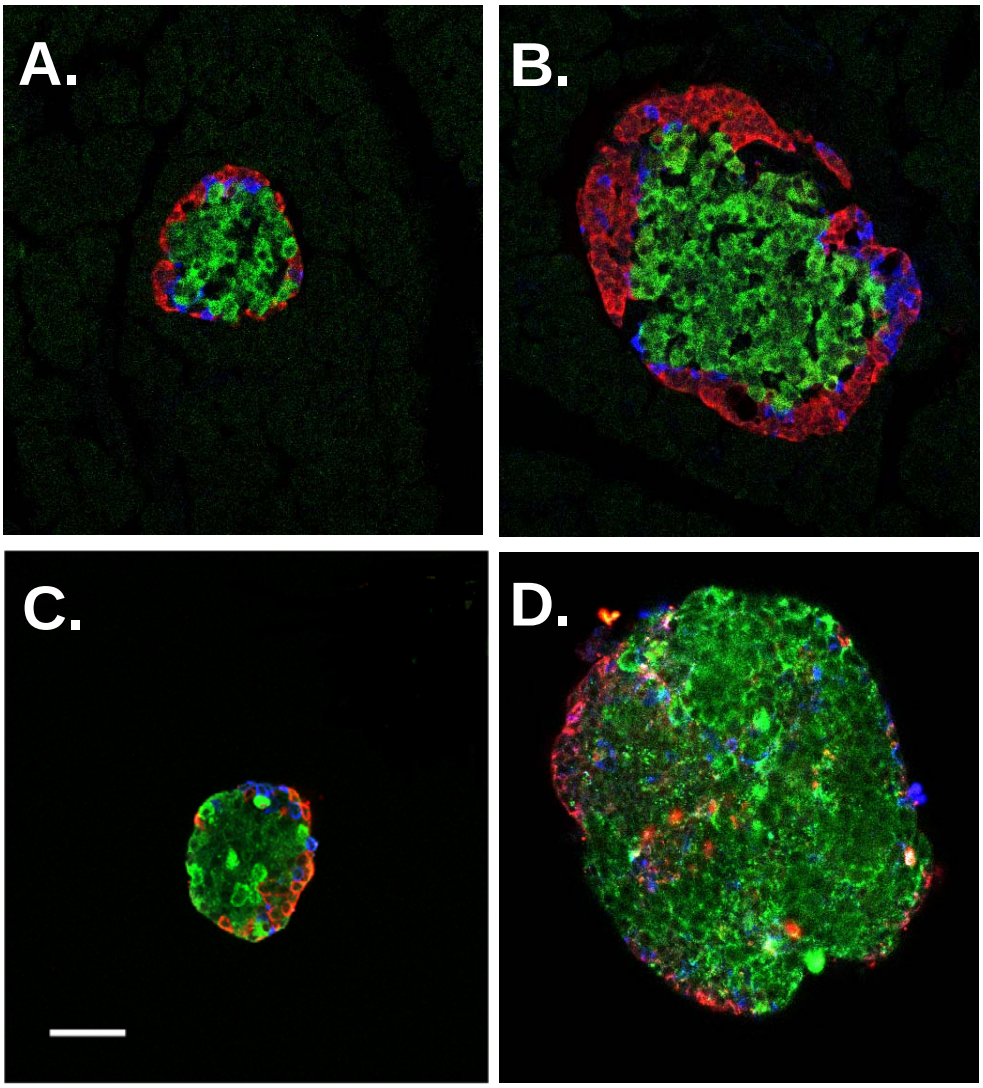

Figure 9. Cellular composition does not differ with islet population. Islets were immuno-fluorescently labeled for β-cells (insulin = green), α-cells (glucagon = red), and δ-cells (somatostatin = blue). Small (A) and large (B) islets labeled within pancreatic sections (*in situ*) show same general cell composition. Small (C) and large (D) islets after isolation also have the same general composition. Loss of peripheral α-and δ-cells was noted in the isolated islets (C & D) compared to *in situ* (A & B). (Scale bar = 50μm for all images)

Table 1. Cell composition in small and large islets in situ and in vitro.

	Small Islets (% of endocrine cells)			Large Islets (% of endocrine cells)		
	β-cells	**α-cells**	**δ-cells**	**β-cells**	**α-cells**	**δ-cells**
In situ	59	25	16	61	29	10 *
***In vitro* (intact)**	69	19	12	65	24 *	11
***In vitro*(dissociated)**	74	17	9	70	24 *	6

The proportion of β-, α-, and δ-cells in small and large islets were compared in isolate intact islets (*in vitro*, intact), isolated islets dissociated into single cells (in *vitro*, dissociated), and in pancreatic sections (*in situ*). (* indicates a statistically significant difference for the individual cell type between large and small islets; $p < 0.05$)

Table 2. The density of cells in small and large islets

Islet Diameter (µm)	Cells per islet (mean ± SE)	Cells/IE
Small (50µm)	**83 ± 22**	**2235**
Large (200µm)	**2071 ± 75**	**874 ** **

The number of cells dissociated from small or large islets were counted and calculated as cells/volume (IE). Small islets contain significantly more cells per volume than large islets. (**$p < 0.001$).

The cellular make-up of the large and small islets was analyzed after isolation (Figure 9C & D). Again, 65-69% of the stained cells were β-cells (

Table **1**). The isolated large islets had a higher proportion of α-cells than isolated small islets, but the difference was minor and did not appear to be enough to alter the total insulin secreted from this population of islets (Table 1). Unlike humans, the rat islet architecture is organized with α- and δ̃-cells localized to the periphery, while β-cells were predominately found in the center of the islet. In the large islets, three to four layers of α- or δ-cells were located at the periphery *in situ* (Figure 9A & B). There was a clear loss of the peripheral α- and δ-cells after isolation (Figure 9C & D). This loss of peripheral cells was likely due to the isolation process, in agreement with the results of others (el-Naggar et al., 1993; Morini et al., 2006).

One limitation with the analysis of serial sections is that it is possible to miss or over-count certain cell types, because of the 2-D properties of the preparation. To overcome this limitation, we repeated the experiments using islets from the two populations dissociated into single cells and labeled for cell types. The results show that there was no significant difference in the proportions of β-cells to other endocrine cells between small and large islets (

Table **1**). Finally, we co-stained isolated islets with insulin antibodies (to identity β-cells) and DAPI (to stain nuclei, providing a total cell count). There was no significant difference in the proportion of β-cells to total islet cells between small (47%) and large (50%) islets. Thus, the first hypothesis of a greater proportion of β-cells in small islets compared to large islets proved to be false.

Islet cell density

While the proportion of α-, β- and δ-cells within islets from the two populations was not different, we hypothesized that the total cell density might be greater in small islets, leading to a

higher total number of β-cells per small islet volume. Immunofluorescence of islets in pancreatic sections and after isolation showed that small islets consistently had a higher endocrine (α-, β- and δ-cells) cell density that was significantly greater than large islets (Figure 10A). Isolated small and large islets viewed with transmission electron microscopy (TEM) illustrated a higher total cell density in small islets compared to large (Figure 10B).

As described above, the inherent limitations when counting cells within a 2-D image required that we verify the results with a third method. Thus, we isolated 293 islets with diameters of either 50 or 200 μm. The islets were dispersed into single cells, and the number of cells/islet counted. Using this method, the total cell count per volume was recorded. The density of cells was calculated as the total number of cells/volume (IE) of the original islets (Table 2). Again, the results demonstrate that the total number of cells/volume of islets was greater in the small than large islets. In summary, immunofluorescence (*in situ* and *in vitro*), calculations from TEM micrographs (in vitro), and the counting of dispersed cells all agreed that the small islets had a higher cell density.

Insulin Content

With a greater total cell density in the small islets, we hypothesized that the insulin content stored within individual β-cells could be greater in cells from small islets compared to large islets. To test this hypothesis, we utilized three approaches; the density of insulin granules from isolated islets was calculated from TEM, the total insulin content of isolated islets was determined by ELISA, and the *in situ* insulin content per islet and per cell was calculated with immunohistochemistry.

The mean insulin granule density (granules/area) was calculated from β-cells within large islets and small islets. Figure 11 illustrates the differences in granule density between small (A) and large (B) islets. There was a statistically significant increase in the average density of insulin

granules in the small islets compared to large islets (Figure 11C). Our granule counts are consistent with published figures using the same methods (Yorde & Kalkhoff, 1986).

Further confirmation was obtained by analyzing the total intracellular insulin content of isolated islets. Again, more total insulin per volume (IE) was measured in small islets compared to the large islets under both basal conditions (low glucose) and following a 30 min *in vitro* high glucose exposure (Figure 11D). To test insulin content *in situ*, pancreatic sections were stained for insulin and the intensity of the immunohistochemistry stain/islet was quantified. Once more, the insulin content was greater in the small islets (Figure 11E). Thus, using three independent approaches from both *in situ* and *in vitro* preparations, evidence supported the hypothesis that small islets contain more insulin per volume or area than large islets.

Interestingly, normalization of the glucose-stimulated insulin release as a percentage of the total insulin content of the islets demonstrated that large and small islets actually secreted the same percentage of their total insulin content over time (Figure 11F). The difference in absolute insulin secretion levels was not likely due to secretory mechanisms, but rather in the increased insulin stored within the β-cells of the small islets.

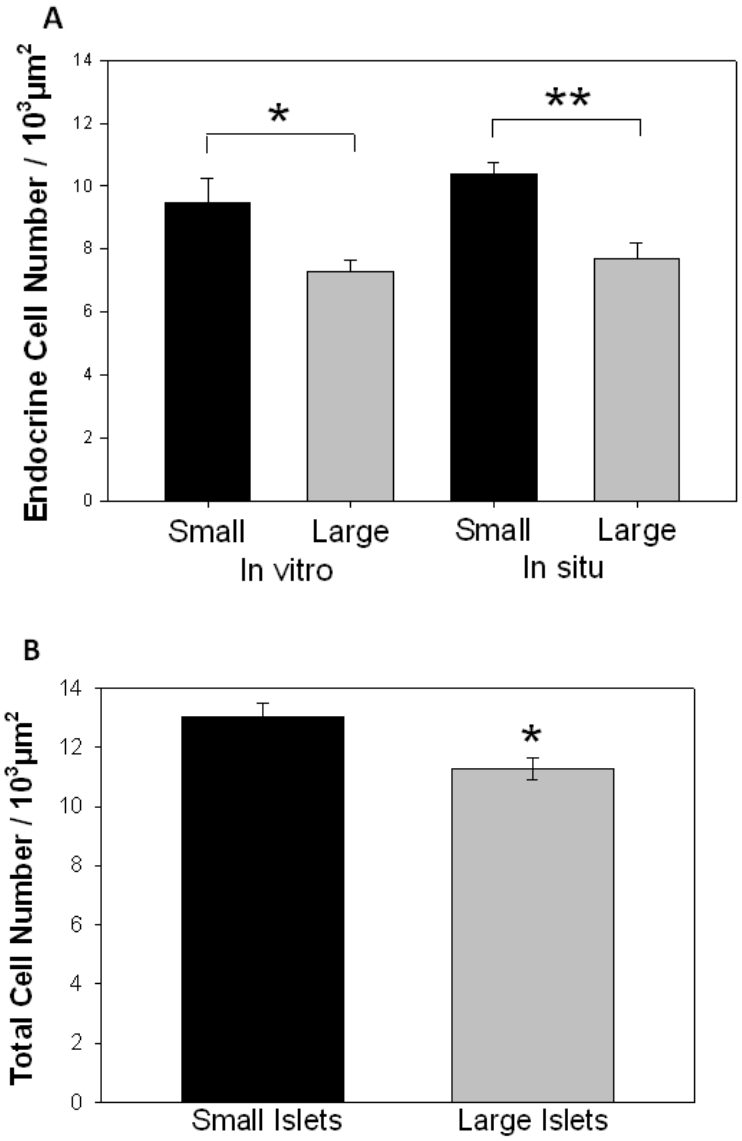

Figure 10. Cell density higher in small islets. (A) The density of α-, β-, and δ-cells within small and large islets were calculated as cells/area from immunofluorescent images of pancreatic sections (*in situ*) and from isolated islets (*in vitro*). (B) The total cellular density was measured from TEM micrographs of isolated islets. (* $p < 0.05$) and (** $p < 0.01$)

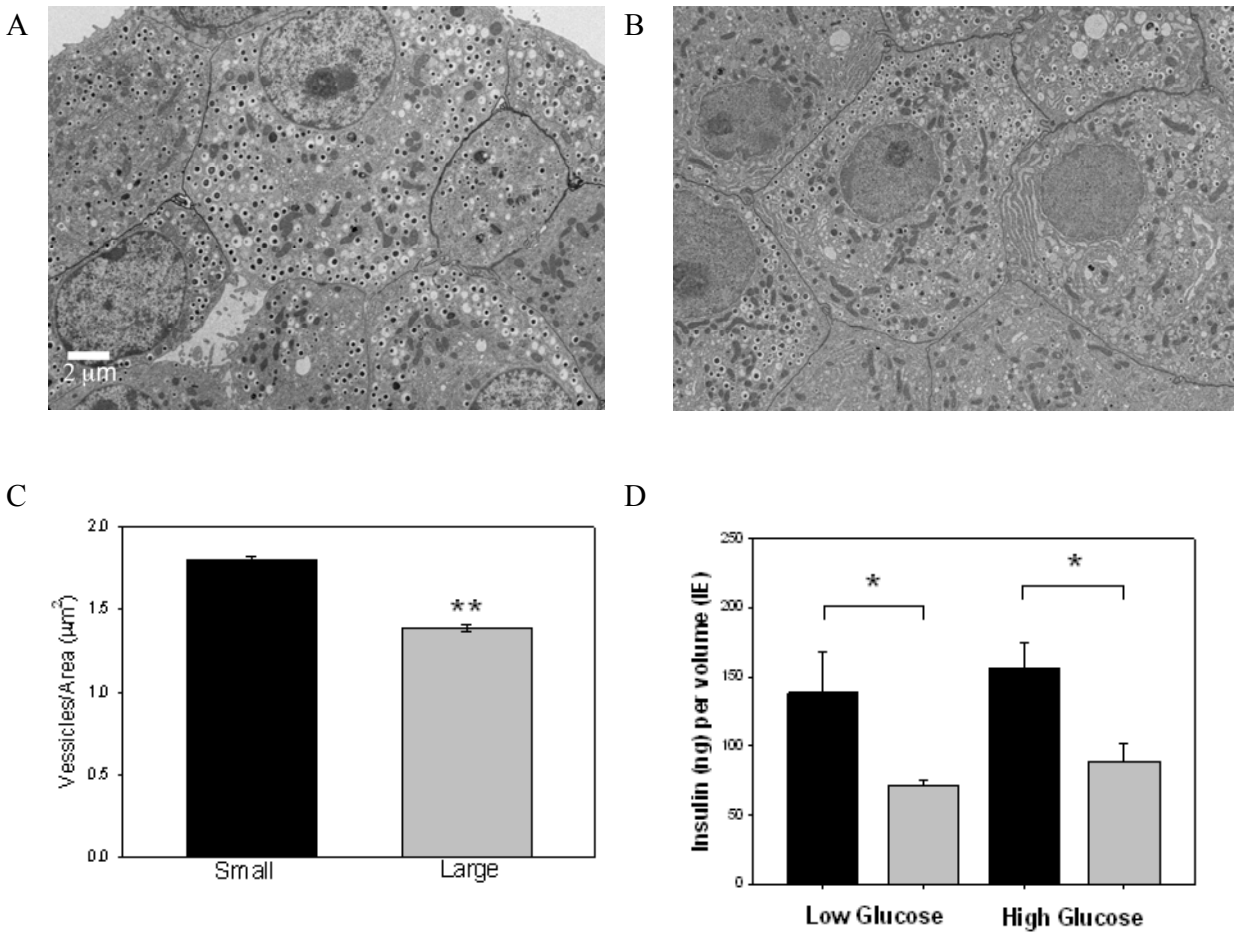

Figure 11. Small islets have greater insulin content than large islets. (A) Typical TEM micrograph showing β-cells from small islet with densely packed insulin granules. (B) Typical β-cells from large islet with fewer insulin granules. Scale bar = 2 µm for images A and B. (C) β-cells from isolated small islets have a greater density of insulin granules than β-cells from large islets ($p < 0.001$). (D) Total insulin content from small (black bars) and large (gray bars) isolated islets (measured by ELISA) showed that small islets, in low or high glucose, contained more insulin per volume ($p < 0.05$).

E

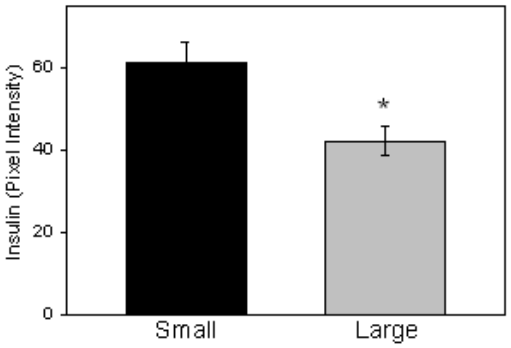

F

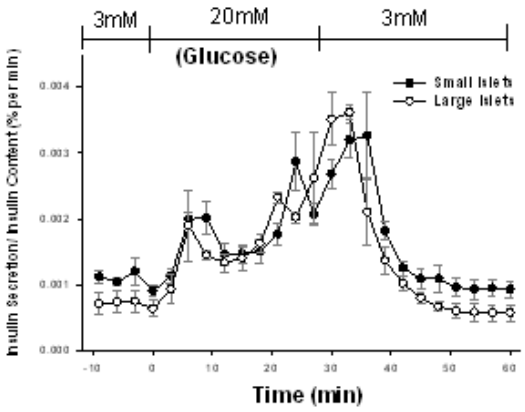

Figure 11(cont.). Small islets have greater insulin content than large islets. (E) Insulin labeling intensity of islets *in situ* also demonstrated higher values for β-cells from the small islets compared to large islets ($p < 0.05$). (F) After normalizing insulin secretion to total insulin content/islet, there was no statistical difference in the level or timing of the first or second phase insulin secretion amount between large and small islets.

Insulin Location

Immunohistochemistry demonstrated a stark difference in the intensity of insulin staining depending on the location of the β-cell in the islet. We analyzed the intensity of the insulin immunostaining per cell within the islets. In small islets all β-cells contained approximately the same level of insulin staining (Figure 12A). In large islets, insulin-containing β-cells located at the periphery of the islets contained approximately the same level of insulin per cell as those within the small islets (Figure 12B). However, β-cells located within the core of the large islets contained significantly less insulin per area (Figure 12B & C). This observation was extremely reproducible with 100% of the examined large islets illustrating the insulin-prominent outer layer of cells. Due to the inherent variation in staining intensity, comparisons were made within preparations. Figure 12C shows the results from one animal, but is representative of three independent replications. Because these findings had not been reported previously, we undertook a series of experiments to confirm the results. We stained serial sections of the pancreas for insulin using a 3-amino-9-ethyl-carbazole or a 3,3'-diaminobenzidine chromogen substrate to visualize staining. Both resulted in less insulin staining in the core cells of the large islets. Subsequently, we repeated the experiments using three different insulin antibody dilutions (1:50, 1:100, and 1:200) to be sure that the lighter insulin staining in the core was not an artifact of the procedures. With all three dilutions, the results were the same; the insulin staining of the core cells within the large islets was less compared to the periphery and compared to the cells of small islets. The same characteristic, low insulin-containing β̃-cells in the core of large islets, was noted in isolated islets in culture. In large islets, insulin-secreting β̃-cells located at the periphery of the islets contained more insulin than the cells located within the central core (results not shown).

TEM analysis of the insulin-containing vesicles in β-cells from the core of the large isolated islets compared to the periphery supported the immunohistochemistry results. Figure 13A & B illustrate typical sections from the core (A), and periphery (B) of a large islet. The density of secretory granules was calculated by counting the number of granules/defined area and the results are shown in Figure 13C. There were statistically more secretory granules in the β-cells of the peripheral cells when compared to the core cells of the large islets. Thus, the differences in intracellular insulin content between large and small islets appears to be at least partially due to a lower amount of insulin in the β-cells within the core of the large islets.

Characteristics of core β-cells in situ

Because most explanations concerning the functional differences between large and small islets focus on the core cell death found in isolated large islets, and we identified inferior insulin content in large islets *in situ*, we examined the general characteristics of the core β-cells within the large islets using TEM. Using previously published methods to quantify the quality of mitochondria with electron micrographs (Y. Searls, I. Smirnova, B. Fegley, & L. Stehno-Bittel, 2004), we determined that 92% of the mitochondria from β-cells of large islets were completely intact (grade 1) with the remaining 8% scored as grade 2 (< 50% disruption of inner mitochondrial membrane). No mitochondria from β-cells within large or small islets contained compromised mitochondria (grade 3-5). There was no difference in the mitochondrial scores for the cells from large or small islets. Thus, cell damage during tissue processing could not explain the poor insulin staining in the core of the large islets.

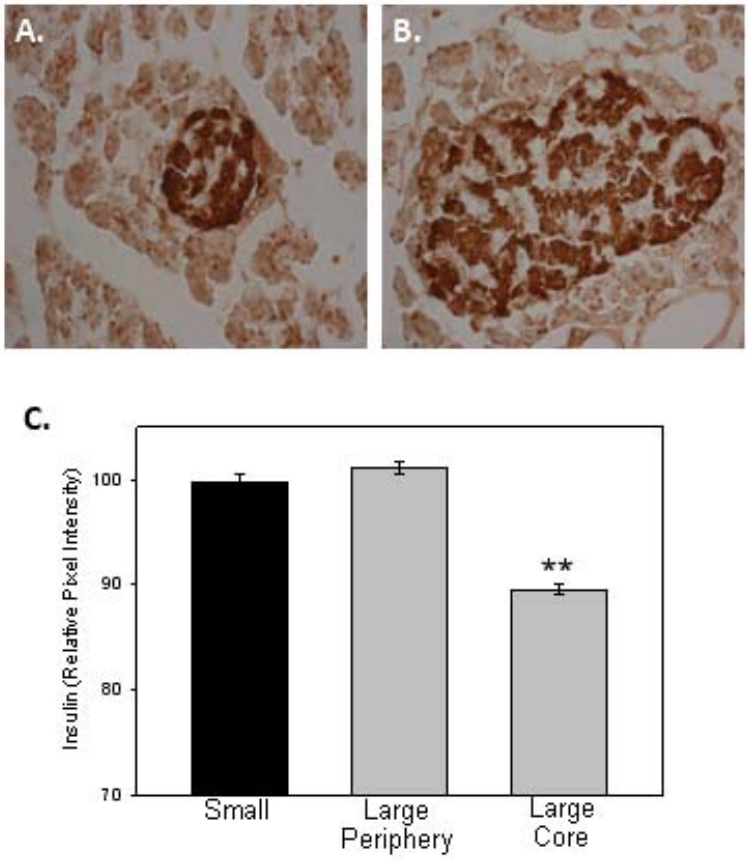

Figure 12. Core β-cells of large islets have less insulin than peripheral β-cells *in situ*. (A) Typical small islet showing dark insulin staining (brown) throughout the islet. (B) Typical large islet contains lighter insulin-stained β-cells at the core of the islet. (C) Analysis of single cells illustrates that the core β-cells of the large islets contain less insulin/cell. (** $p < 0.001$)

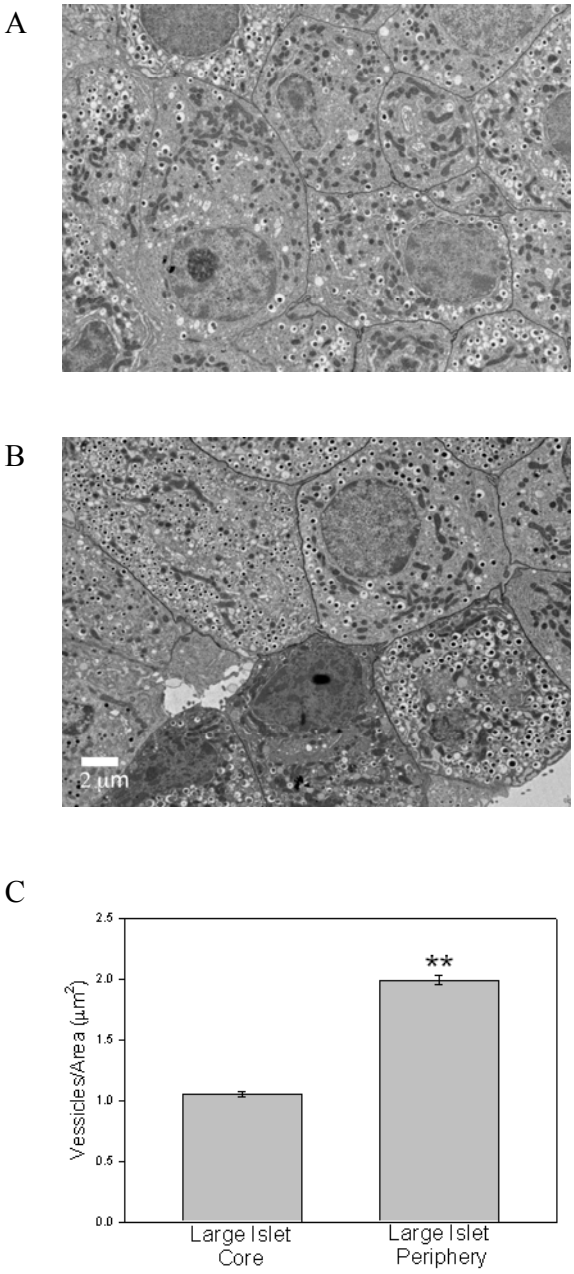

Figure 13. Core β-cells of large islets have less insulin than peripheral β-cells *in vitro*. (A) Typical β-cells from core of large islet with few insulin granules/area. (B) Typical β-cells from periphery of large islet with a higher density of insulin granules. (Scale bar = 2 µm for both images) (C) Analysis of cells from core and periphery of large islets showed statistically greater insulin granules/area in the peripheral region. (** $p < 0.001$)

2.4. Discussion

In 1979 Baeten et al. described different islet architecture associated with islets located in regions of exocrine tissue that drained into different ducts (Baetens et al., 1979).They concluded that their research contradicted the widely-held belief that all islets have similar composition. Since that time, numerous labs have extended the description of morphological differences in islet populations to quantifiable functional outcomes. The functional differences previously described between isolated large and small islets have been impressive. For example, stimulation by high glucose (20 mM), caused a release of insulin that is 6 times higher in the small compared to large islets (MacGregor et al., 2006; Williams et al., 2010). Such results have been verified in human and mouse islets (Lehmann et al., 2007; Su et al., 2010). Other differences between the populations that we have identified suggest that isolated small islets have: 1) greater oxygen uptake, 2) better survival in culture, and 3) superior diffusion properties (MacGregor et al., 2006). However, all of these characteristics could be due to the manner in which the two populations tolerate the isolation procedures, and thus could have no relevance to the *in vivo* condition.

With the work described here, we have shown that small islets have a greater cell density *in vitro* and *in situ*, and a greater insulin content *in vitro* and *in situ.* These results suggest that at least some of the functional and morphological differences noted between the large and small islets *in vitro*, are present *in vivo*. Further, the results supply the first mechanistic explanation for the differences in insulin secretion between the populations, other than large islets are more susceptible to core cell death. The concept that core cell death of large islets is responsible for all functional differences between large and small islets is no longer valid, as methods that improve the diffusion barrier of large islets reversed core cell death, but did not reverse the poor insulin secretion phenotype of the large islets (Williams et al., 2010).

We tested several hypotheses to determine how small islets secreted more insulin per volume. First, we questioned whether small islets contained a greater percentage of β-cells compared to large islets, thus making them more efficient insulin-secretors. However, our results showed that there was no difference in the cellular composition between large and small islets *in vitro* or *in situ*. Therefore, a greater percentage of insulin-producing β-cells cannot explain the superior insulin secretion in small islets. Next, we hypothesized that each β-cell within the islet was more efficient at releasing insulin. For the first time, we showed that cells of small islets contained more total insulin than cells from large islets. Thus, the two populations of islets actually secrete the same percentage of their total insulin, but cells from large islets store far less insulin to be released. More specifically, the β-cells found in the core of the large islets have a lower insulin content compared to the peripheral cells or the β-cells found in small islets. Functional differences in the core and peripheral β-cells has been described previously *in vivo* and *in vitro* with core β-cells containing fewer insulin granules after stimulation (Salomon & Meda, 1986; Stefan et al., 1987).

The two most important findings were that the total number of cells per islet area was greater in small islets and the average β-cell contained more insulin than cells from large islets. Although the small islets account for a vast majority of the total number of islets, they make up only a very small percentage of the total islet volume. From this observation, many labs have concluded that large islets are responsible for the bulk of the pancreatic endocrine function (Hellman, 1959b; Kaihoh et al., 1986). This concept has been prevalent in the literature, with little functional data to support it. The finding that, on average, the cells of small islets contain more insulin than cells from large islets, and the *in vitro* data showing that small islets secrete significantly more insulin/volume than large islets, argues for an important role for small islets in glucose regulation *in vivo*.

It is interesting to consider the role of different islet populations during the onset and progression of type 1 and type 2 diabetes. In a rat model of type 2 diabetes (fa/fa) exposure of islets to high glucose was more detrimental to the β-cells of the large islets than cells from small islets (C. B. Chan & Surette, 1999; Chang, 2002). These studies showed that large islets released less insulin per cell than smaller ones from the same obese animals, and significantly less than the islets from the lean animals(C. B. Chan et al., 1998). Additionally there were fewer insulin-secreting cells within the large islets of the obese rats. The authors concluded that it was the large islets that were predominantly affected in the obese diabetic rat and that the small islets maintained normal insulin secretion during the time when the large islets had become non-functional.(C. Chan, Saleh, Purje, & MacPhail, 2002). In studies of people with type 2 diabetes, researchers noted a shift in cellular composition, with an increase in α-cells and a decline in β-cells that was particularly noticeable in the large islets (Yoon et al., 2003).

The results presented here demonstrate that many of the characteristics associated with islets of different sizes after islet isolation, were consistent when examined *in situ* in rats. Unique characteristics, inherent within the pancreatic tissue of rats, included a higher density of cells in the small islets with greater insulin content. Different islet populations may have important distinctions, many of which are yet to be characterized, but which may be necessary for a healthy endocrine pancreas.

Chapter 3

Total Cell Number- A Superior Model for Volume Quantification of Isolated Islets

3.1. Abstract

Islet equivalent (IE), the standard estimate of isolated islet volume, is based on the assumption that all islets are spherical. Yet, certain populations of islets are ellipsoidal, creating errors in volume quantification. Here, we developed and tested a new easy-to-use method to quantify islet volume with greater accuracy. Isolated rat islets were dissociated into single cells and the total cell number per islet were determined by using a computer-assisted cytometry. Based on cell number per islet, we created a regression model to convert islet diameter to cell number with a high R-squared value and a good validity and reliability. An inverse correlation between the cell number per IE and islet size was identified. Overall, IE measurement overestimated the tissue volume in islets with diameter above 150μm suggesting that the larger the islet, the greater the error in IE values. To compare results obtained using IE or our new method, we compared Glut2 protein levels determined by immunoblotting and proinsulin content via ELISA between small (diameter ≤ 100μm) and large (diameter ≥ 200μm) islets normalized by standard IE counts or our new cell number method. When normalized by IE, large islets showed significantly lower Glut2 level and proinsulin content. However, when normalized by cell number, large and small islets had no different Glut2 levels, but large islets contained more proinsulin. In conclusion, normalizing islet volume by IE overestimated the tissue volume in large islets, which may lead to some erroneous results. Normalizing by cell number is a more accurate method to quantify tissue amount used in islet transplantation and research.

3.2. Introduction

Islets of Langerhans are spherical-like clusters of endocrine cells that have a large range of sizes from 20µm to more than 400µm in diameter both in rodent (MacGregor et al., 2006) and humans (Buchwald et al., 2009; Ricordi, Socci et al., 1990). An accurate and consistent method to quantify the amount of tissue being used in experiments is of crucial relevance for islet research and transplantation. Early experimental results were incomparable between laboratories until the islet equivalent (IE) was suggested by Ricordi et.al. in 1990 at the Second Congress of the International Pancreas and Islet Transplantation Association (Ricordi, Gray et al., 1990). One IE corresponds to the tissue volume of a perfectly spherical islet with a diameter of 150µm. In the standard measurement procedure, a sample islet preparation is stained with dithizone (diphenylthiocarbazone) to discriminate islet from exocrine tissue. Under light microscopy with an ocular micrometer, a single diameter of islet is directly measured manually by the operator. Next, islets are categorized according to their diameters within 50-µm increments and the number of islets in each category is multiplied by a related conversion factor that convert the islet number and diameter to IE (Ricordi, 1991; Ricordi, Gray et al., 1990).

Currently, IE is the most common measurement used both in the clinic and in the laboratory. At transplantation sites, IE is a rapid measurement for quantifying the dosage of the transplanted material. The IE is used to estimate the yield of islets isolated from the donor, and the IE per kilogram of body weight is the unit commonly used to report the graft amount transplanted to the patient (Balamurugan et al., 2010; Bellin et al., 2011; D'Aleo et al., 2010; Kaddis, Danobeitia, Niland, Stiller, & Fernandez, 2010; Kessler, Bakopoulou et al., 2010; Kessler, Greget et al., 2010; Lehmann et al., 2007; Matsumoto et al., 2010; Niclauss et al., 2011; O'Gorman et al., 2010; Ris et al., 2011; T. Saito et al., 2010; Shapiro et al., 2000; Shimoda et al., 2010a, 2010b; Sutton et al., 2010; Takita et al., 2011). In the laboratory, IE is commonly applied

to normalize the amount of islets between preparations for functional assays such as insulin secretion (Fujita et al., 2011; H. H. Huang, L. Novikova, S. J. Williams, I. V. Smirnova, & L. Stehno-Bittel, 2011; Lehmann et al., 2007; MacGregor et al., 2006; Williams et al., 2010).

Recently, the accuracy, repeatability and intermediate precision of standard IE measurement procedure were tested in a multi-center study (Kissler et al., 2010). However, the results were very disappointing. For example, more than 50% of centers overestimated the IE count on the same (photographic) samples compared to the expert standard. The intra-technician coefficients of variation (CVs) from one repeat count in the 35 technicians participating, which were calculated to assess the repeatability, ranged from 0 to a maximum of 42.5% and approximately 30% of technicians had a CV% over 10%. In addition, the inter-technician CVs within each center were used to assess the intermediate precision, and the average inter-technician CV% was around 15%. Overall, these results indicated that the validity and reliability of IE measurement were unsatisfying.

In fact, the accuracy of IE measurement has been challenged for years (Buchwald et al., 2009; Fetterhoff, Wile, Coffing, Cavanagh, & Wright, 1994; Kissler et al., 2010; Niclauss et al., 2008; Pisania, Papas et al., 2010; Pisania, Weir et al., 2010; van der Burg, Scheringa, Basir, & Bouwman, 1997), because the IE calculations are based on the assumption that all islets are spherical; an assumption that has already been suggested to be incorrect (Cummings et al., 2008; Girman et al., 2008; Lehmann et al., 1998; Niclauss et al., 2008; Perez-Armendariz, Atwater, & Rojas, 1985; Pisania, Papas et al., 2010; Ricordi, Socci et al., 1990). In reality, most islets are disk-shaped oblate ellipsoid or irregular shapes, especially in culture. A measurement of the three largest dimensions in mutually perpendicular directions of the isolated islets has been reported. In a perfect sphere, the three major radii a, b and c would equate to a = b = c.

However, the average measured ratios of b/a is 0.82 and c/a is 0.6 suggesting that islets are more like ellipsoids (Avgoustiniatos, 2002).

Several digital image analysis methods were proposed to replace manual estimation to improve quality assurance of islet product for transplantation (Friberg et al., 2011; Girman et al., 2008; Girman, Kriz, Friedmansky, & Saudek, 2003; Kissler et al., 2010; Lehmann et al., 1998; Lembert et al., 2003; Niclauss et al., 2008; Stegemann, O'Neil, Nicholson, & Mullon, 1998; Stegemann, O'Neil, Nicholson, Mullon, & Solomon, 1997). By photographing islets digitally, the area and diameter of each islet were measured by computer and the islet volume (IE) was calculated accordingly. In addition, Buchwald, et al. recently proposed a refinement of current IE measurement to improve the accuracy (Buchwald et al., 2009). However, most of these efforts were still based on the assumption that islet is a sphere. Therefore, we suggested either one-dimensional (longitudinal axis) or two-dimensional (area) approach of IE measurement used currently is oversimplified, leading to an inaccuracy when estimating the actual tissue amount of a three-dimensional islet.

In the present study, we developed and tested a new method for estimating islet volume based on cell number counts. We completed validity and reliability studies on our new method and showed that it is a fast, more accurate and reliable method of estimating islet volume. These efforts are relevant to improving the accuracy of measure of transplanted tissue volume, and assuring that erroneous results are not reported in the literature.

3.3. Methods

Rat islet isolation, separation and IE measurement

Adult male and female Sprague Dawley rats (200~350g BW) were housed on a 12 hours light/dark cycle with free access to standard laboratory chow and water. All animals received care in compliance with the Principles of Laboratory Animal Care formulated by the National Society for Medical Research and the Guide for the Care and Use of Laboratory Animals published by the US National Institutes of Health (NIH Publication No. 85-23, revised 1996).

Islet isolation methods followed our published procedures described in detail (H.-H. Huang et al., 2011; MacGregor et al., 2006; Williams et al., 2010; S. Williams et al., 2009). Briefly, rats were anesthetized by intraperitoneal injection of a mixture of ketamine and xylazine. After the peritoneal cavity was exposed, the pancreatic main duct to the intestine was clamped and the pancreas cannulated *in situ* via the common bile duct. The pancreas was distended with collagenase and removed. Islets were gently tumbled, washed, and passed through a sterile 30 mesh stainless steel screen and centrifuged. The pellet was mixed with Histopaque, centrifuged, and the islets floating on the gradient were collected and sedimented. Islets were passed through a sterile 40μm mesh cell strainer with HBSS. After this cleaning process, islets were placed into CMRL1066 medium containing 2 mM glutamine, 10% fetal bovine serum (FBS) and 1% antibiotic/ antimycotic solution or DMEM/F12 medium (17 mM glucose) containing 10% FBS, 20 ng/ml epidermal growth factor (EGF) and 1% antibiotic/ antimycotic solution and put into a 37ºC culture chamber containing 5% CO_2. For manual separation of islets, the islet culture media was changed to L15 containing 10% FBS and 5mM HEPES, and islets were transferred into 37ºC culture chamber without CO_2. Islets were manually separated by size based on the criteria that small: diameter $\leq$ 100μm; large: diameter $\geq$ 200μm. After measuring the IE, the selected islets were frozen by liquid nitrogen and preserved in -80 ºC until being used.

The IE measurements for each preparation followed our previously published procedures (H. H. Huang et al., 2011; MacGregor et al., 2006; Williams et al., 2010). Briefly, the diameter of each islet was recorded manually using light microscopy with an ocular micrometer at 40X total magnification. For irregularly shaped islets, two to four diameter measurements were taken at different locations on the islet and averaged. The volume of each islet was calculated based on the diameter and converted to IE individually, where one IE is equal to 1.77×10^6 μm^3 (the volume of a spherical islet with 150μm diameter) (Buchwald et al., 2009; Fujita et al., 2011; Niclauss et al., 2008; Stegemann et al., 1998; van der Burg et al., 1997).

Islet dissociation and cell number estimation

For single cell assays, isolated islets were picked manually and individually distributed into a well of a 96-well black plate with clear bottom (Corning® No.3603) in medium containing calcium-magnesium free HBSS. After recording the diameter of each islet as described above, the islets were dissociated into single cells using our published protocol (H.-H. Huang et al., 2011; S. Williams et al., 2009). Briefly, after adding concentrated papain into each well with a final concentration of 5 U/ml, islets were incubated at 37°C for 20 min. Following that, the islets were dispersed into single cells by repeated pipetting and the dissociated cells in the wells were spun down in the plate with 300 rpm for 1 min at room temperature. The cell number in each well was analyzed using Celigo™ adherent cell cytometer with following procedure. Every well containing single cells was photographed digitally and the cells were counted using the Celigo software (1.3). Cells were counted from at least 340 islets from both male and female rats with two different ages (two month-old or six month-old). In addition, all islets were cultured in either CMRL1066 or DMEM/F12 medium overnight before being used.

To test the reliability of the cell count, manual counts using a hemocytometer were performed. Islets were grouped manually into size categories based on diameters. The number of

islets in each group was recorded before dissociating the islets into single cells based on our published protocol. A 10 µl sample of dispersed cells was loaded into a hemocytometer for cell counting. Six repetitions were performed in each sample set.

Total protein yield

Islets within groups were homogenized using a $26G^{1}/_{2}$ syringe with extraction buffer containing 10mM TRIS HCl pH7.4, 150mM NaCl, 1mM EDTA, 20mM Na Molybolate, 50mM Na Fluoride, 0.2mM Na-Orthovanidate (pH 10), 1% Triton X-100, and 0.2mM PMSF. The extracts were centrifuged for 15 minutes with 15,600 rcf at 4°C. Measurement of protein concentrations in supernatants was performed using Micro BCA Protein Assay Kit (Pierce, Rockford, IL, U.S.A., #23235).

Total DNA yield

In the total protein per DNA study, the small or large islets were further aliquoted evenly into two parts for protein and DNA content measurement respectively. Islets within groups were lysed with lysis buffer containing 10mM TRIS HCl pH7.5, 150mM NaCl, 5mM EDTA (pH8.0), 0.5% SDS, and 50µg/ml proteinase K, and vortexed until the cell pellet was dispersed. After incubation overnight at 55°C, the sample was spun at 12,000 rpm for 10 minutes at room temperature. The supernatant was collected and equal volume of isopropanol was added into each sample. After letting the sample to sit for 5 minutes, another centrifugation (12,000 rpm for 10 minutes at RT) was performed. The supernatant was discarded, and TE buffer was added to dissolve the DNA with a 1 hour incubation at 55°C. The DNA concentrations were measured using Quant-iT™ PicoGreen® dsDNA Assay Kit (Invitrogen, Carlsbad, CA, U.S.A., #P11496).

Western Blot

Hand-picked small and large islets were washed individually in phosphate-buffered saline (PBS) twice. After removing the supernatant, the islets were homogenized as described previously. Samples from large and small islets extracts were prepared for electrophoresis by heating at 95 ^{o}C for 3 min in SDS gel-loading buffer (0.125M Tris, pH6.8, 5% glycerol, 2.5% mercaptoethanol, 2% SDS, and 0,001% bromophenol blue). Proteins were separated on a 4-15% Tris-HCl Ready Gels (Bio-Rad Laboratories, Hercules, CA, U.S.A., #161-1158) with 0.025 M Tris, 0.192 M Glycine, 0.1% SDS running buffer. Equal amounts of total protein (10 µg) were loaded in each lane. Molecular weight markers See Blue Plus2 Pre-Stained Standard (Invitrogen, Carlsbad, CA, U.S.A., #LC5925) was used to determine the size of the antigen. After electrophoresis, the proteins were transferred from the gel to Bio Trace PVDF membranes 0.45 µm (Pall Life Sciences, East Hills, NY, U.S.A., #P/N 66547) using 0.012 M Tris, 0.096 M Glycine transfer buffer. Blots was blocked with 5% nonfat dry milk diluted in 0.1M PBS 0.1% Tween (PBST) for 1 hour. Primary and secondary antibodies were diluted in the 5% nonfat dry milk in PBST. All incubations were performed at room temperature. Blots was probed with primary antibodies against Glut2 (Santa Cruz Biotechnology Inc., Santa Cruz, CA, U.S.A., #sc-9917), for 1 hour at room temperature. After washing in 0.1M PBS 0.1% Tween (10 minutes for 3 times), blots were incubated for 30 minutes with secondary antibody horseradish peroxidase-conjugated goat anti-rabbit IgG (Santa Cruz Biotechnology Inc., Santa Cruz, CA, U.S.A., #sc-2004) or goat anti-mouse IgG (Santa Cruz Biotechnology Inc., Santa Cruz, CA, U.S.A., #sc-2005). After washing in 0.1M PBS 0.1% Tween (10 minutes for 3 times), bound antibodies were detected using SuperSignal® West Pico Chemiluminescent Substrate (Thermo Fisher Scientific Inc., Rockford, IL, U.S.A., # 34080). For a protein loading control, the membrane was reprobed with mouse anti-GAPDH (Sigma-Aldrich®, St. Louis, MO, U.S.A., #G8795), for 1 hour at room temperature.

Proinsulin content

Islet static incubation assays were followed by our published procedures (H.-H. Huang et al., 2011; MacGregor et al., 2006; Williams et al., 2010). Isolated islets were placed in 24-well plate with a minimum of 5 large or 15 small islets per well. All wells were preincubated for 2.5 hours in RPMI 1640 containing 10% fetal bovine serum and 3 mM glucose in a 37°C containing 5% CO_2. After preincubation, media was removed and fresh media was added. After a 30 minutes static incubation at 37°C and 5% CO_2, the islets were harvested and frozen at -80°C. The total protein in the islets was extracted by sonication in acid ethanol (0.18M HCl in 95% ethanol) and incubated overnight at 4°C. The total intracellular proinsulin amounts were determined by the ELISA (ALPCO, Salem, NH).

Statistics

The exact number of islets or replicates is shown in each figure legend. Results were expressed as mean of each group or cell population ± SEM, and were compared using the Student's *t* test. The Pearson product-moment correlation was used to test the correlation between two cell counting techniques. Significant differences were defined as $p < 0.05$.

3.4. Results

Cell number per islet

The dissociated islet cells were counted using computer-assisted cytometry. The total cell number per islet from different sizes of islets is summarized in Table 3. No significant differences were seen between animals' gender, ages or the mediums used for islet culturing. Based on the measured cell numbers, a third-order polynominal regression trend line was the best fit with the equation:

$$y = -0.0001x^3 + 0.0912x^2 - 6.2162x + 182.1125$$

where y equals the total cell number and x equals the islet diameter (μm). The R-squared value was 0.8, indicating the regression trend line fit the data very well.

Next, we compared the our measured cell number per islet with the conventional IE measurement by Ricordi et al. (Ricordi, Gray et al., 1990) and the refined IE measurement by Buchwald et al (Buchwald et al., 2009) using 1560 cells per IE as a norm, which was published recently by Pisania, et al (Pisania, Weir et al., 2010). The results were plotted in Figure 14A. Compared to the our actual cell counts, as the islet size increased, the difference between the actual and theoretical cell counts (using Ricordi's algorithm with Pisania's cell number per IE) was more prominent, which indicated that using currently published methods to estimate islet volume may overestimate the actual tissue volume per islet, especially in large islets. Even though Buchwald's refined algorithm introduced a downward correction, the adjustment was marginal and a significant overestimation still existed (Figure 14A). In addition, we plotted another theoretical curve based on our actual cell count (934 cells) in a 150μm-diameter islet and assuming that islets are perfect sphere and all cell size are equivalent. As shown in Figure 14B,

Table 3. Cell number per islet estimated by computer-assisted cytometer

Islet diameter (μm)	Number of islets evaluated*	Cell number per islet
50	25	92 ± 11
75	48	188 ± 15
100	40	322 ± 24
125	36	642 ± 48
150	33	943 ± 60
175	46	1308 ± 68
200	42	1674 ± 91
225	31	2099 ± 94
250	21	2731 ± 137
275	7	2831 ± 216
300	5	3586 ± 689
325	9	4003 ± 506

Data are presented in mean ± SEM. * The islets were harvested from 8 animals.

A

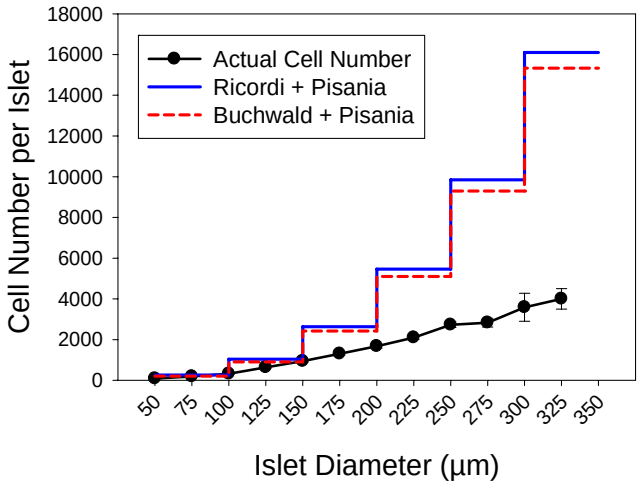

B

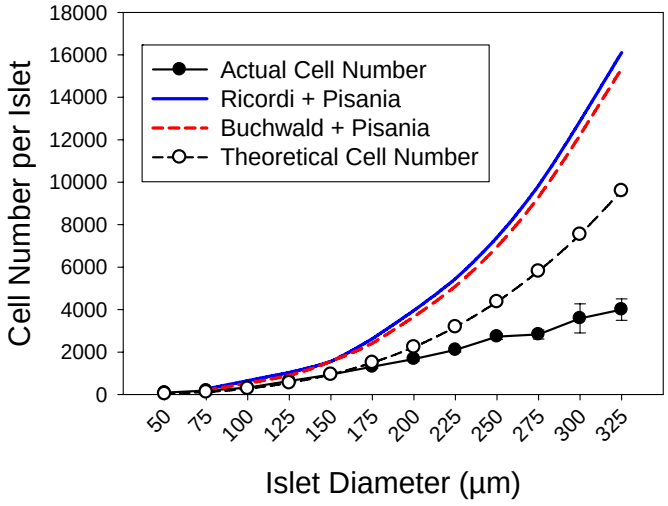

Figure 14. IE measurements overestimated the actual tissue volume in large islets.
(A) Relation curve between islet size and actual cell number per islet (black dots) were plotted in the black solid line. Two theoretical curves were plotted using the Ricordi's conventional IE measurement with different categories of sizes in a 50-µm increments (blue step plot) (Ricordi, Gray et al., 1990) and using Buchwald's refined IE measurement (red step plot) (Buchwald et al., 2009), based on 1560 cells per IE (volume of islet with 150µm diameter) as suggested by Pisania, et al (Pisania, Weir et al., 2010). (B) The two theoretical steps curves (blue and red) were slightly modified into curves based on the average islet diameter in each category of size and the theoretical estimated cell number (based on 1560 cells per IE). Additionally, another theoretical curve (black dash line with white dots) was plotted based on the actual cell number of a 150µm islet (934 cells) with the assumptions that islets are perfect sphere and all cell sizes are equivalent.

this theoretical spherical curve was overall lower than both IE measurement curves, which have been slightly modified from Figure 14A (based on the average islet size in each category and theoretical cell number per islet). However, this theoretical spherical curve was also different to the curve of actual cell count especially in large islets. This result may implicate that the assumption of spherical 150μm-diameter islet was not appropriate.

Cell number per IE

To further demonstrate the errors within the current IE calculations, we plotted the cell number within islets divided by the islet's IE (Figure 15). If the IE calculations accurately reflected the true volume of the islet, then this graph should have resulted in a flat line. Rather it shows that as the size of the islet increased the IE calculation overestimated the true volume.

Validity

Total DNA content per IE and per cell

Small and large islets were separated manually and IE was estimated as described in the methods. The total cell numbers in both small and large islets were estimated by using the equation above. IE normalization resulted in the conclusion that small islets have significantly higher DNA content per IE compared to large islets ($p < 0.001$). However, the total DNA content, when calculated per cell, showed no difference ($p = 0.43$) in small and large islets (Table 4). The averaged total DNA content per cell was approximately 6.05 ± 0.69 pg, which is in agreement with other reports (Lernmark, 1974; Pipeleers et al., 1985; Pisania, Papas et al., 2010).

Total protein content per IE and per cell

Normalization to IE resulted in the conclusion that small islets contained a significantly higher total protein amount than large islets ($p < 0.05$). However, when using the equation to

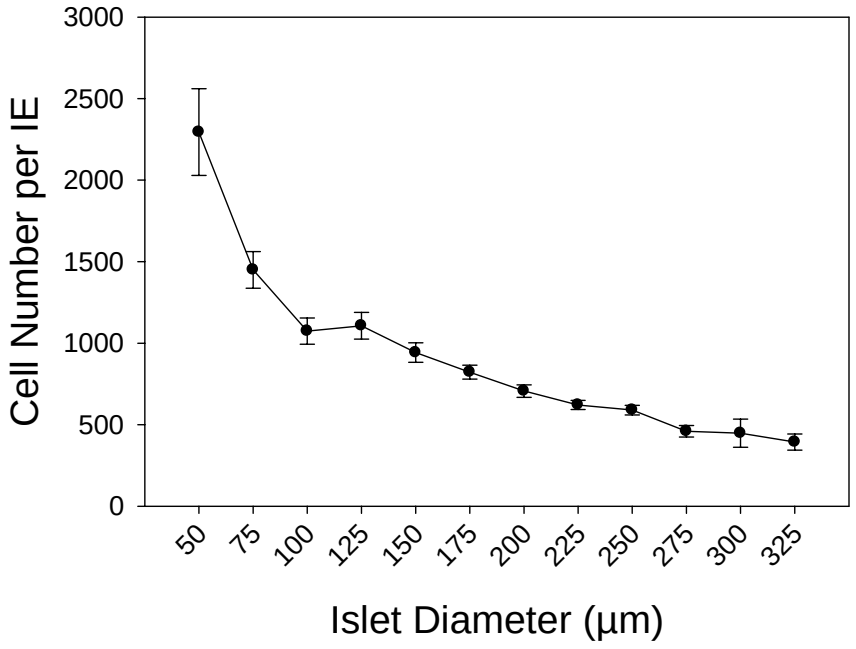

Figure 15. Cell number per IE. There was a negative correlation between islet size and cell number per IE.

estimate total cell number, there was no significant difference ($p = 0.35$) in protein content per cell between small and large islets (Table 5). In addition, total protein content per DNA content was calculated, since DNA content is commonly used for cell number normalization. No differences ($p = 0.40$) were seen in total protein per DNA between small and large islets (Table 6), which further supported the finding that small and large islets had no difference in total protein per cell.

Inter-method reliability

Islets were manually separated into five categories based on diameters of 50, 100, 150, 200, and 250 μm. Figure 16 provides an example of the uniform separation that was achieved for each size category. After dissociation, the cell number per islet in each category was evaluated by using hemocytometer. The results showed a high correlation ($r = 0.99$) with the cell count by using the computer-assisted cytometer indicating a good inter-method reliability (Figure 17).

Glut2 protein levels

As an example of how IE measurements can alter the conclusions one draws from an experiment, Glut2 and proinsulin levels were measured from small and large islets and the data were normalized using the traditional IE (Ricordi, 1991; Ricordi, Gray et al., 1990) and our cell number method.

To determine the Glut2 protein levels, 10 μg of protein from small and large islets were used for Western Blot. The representative results were shown in Figure 18A. When the blot densitometry was normalized to the levels of the internal control, GAPDH, there was no significant difference ($p = 0.69$) in the Glut2 protein levels between small and large islets (Figure 18B). The IE values and total cell number that result in 10 μg of protein in the large and small islets were calculated based on the results shown in Table 7. The IE value per 10 μg of protein

was significantly higher ($p < 0.05$) in small islets, while the total cell number per 10 μg of protein was not significantly different ($p = 0.37$) in small and large islets (Table 7). When the blot densitometry was further normalized by IE, Glut2 levels were significantly higher ($p < 0.05$) in small islets than in large islets (Figure 18C). However, when normalized by total cell number, there was no significant difference of Glut2 protein levels ($p = 0.25$) between the two groups (Figure 18D).

Proinsulin content

Proinsulin content in small and large islets was determined by ELISA. The results also varied based on the normalization methods. When normalized by IE, the proinsulin levels were significantly lower ($p < 0.05$) in the large islets compared to the small islets (Figure 19A). However, when normalized by the total cell number, the results were opposite with significantly higher levels ($p < 0.05$) in the cells of the large islets compared to the small (Figure 19B).

Table 4. Total DNA content per IE and per cell in small and large islets

	Small Islets	Large Islets	*p* value
DNA (pg) / IE	8.19 ± 1.12	3.62 ± 0.70	<0.001
DNA (pg) / Cell	6.17 ± 0.97	5.93 ± 1.00	0.43

Data are presented in mean ± SEM. For small islets, N = 21 experiments from 6 rats. Each experiment contained at least 50 small islets. For large islets, N = 20 experiments from 6 rats. Each experiment contained at least 20 large islets.

Table 5. Total protein content per IE and cell in small and large islets

	Small Islets	Large Islets	*p* value
Protein (μg) / IE	0.82 ± 0.07	0.50 ± 0.08	< 0.05
Protein (ng) / Cell	0.58 ± 0.06	0.69 ± 0.10	0.35

Data are presented in mean ± SEM. For small islets, N = 4 experiments. Each experiment contained at least 450 small islets from 1 rat. For large islets, N = 4 experiments. Each experiment contained at least 50 large islets from 1 rat.

Table 6. Total protein content per DNA in small and large islets

	Small Islets	Large Islets	*p* value
Protein (μg) / DNA (ng)	0.13 ± 0.00	0.12 ± 0.01	0.40

Data are presented in mean ± SEM. N = 4 experiments from 2 rats. Each experiment contained at least 250 small islets or 20 large islets.

Table 7. IE and total cell number in 10μg of protein in small and large islets.

	Small Islets	Large Islets	*p* value
IE / 10μg protein	12.43 ± 1.12	21.84 ± 3.35	< 0.05
Cell / 10μg protein	17855 ± 1698	15379 ± 1910	0.37

Data are presented in mean ± SEM. N = 4 samples. Each sample contained more than 450 small islets or 50 large islets from 1 rat.

Figure 16. The isolated rat islets. The isolated islets with high purity were manually separated with specific size (diameter of 50, 100, 150, 200 and 250 µm).

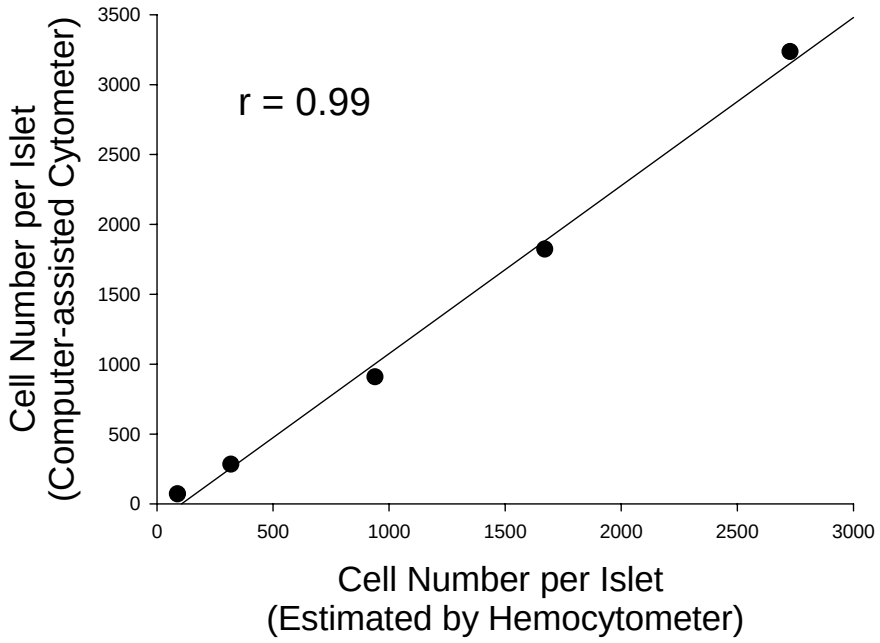

Figure 17. Correlation between cell count using hemocytometer and the computer-assisted cytometer. In the hemocytometer, N = 3 samples in each group with identical size of islets. Each sample contained more than 256 islets in 50 µm, 94 islets in 100 µm, 83 islets in 150 µm, 37 islets in 200 µm or 16 islets in 250 µm from 2 adult male rats. The hemocytometer data were correlated with the data showing in Table 3.

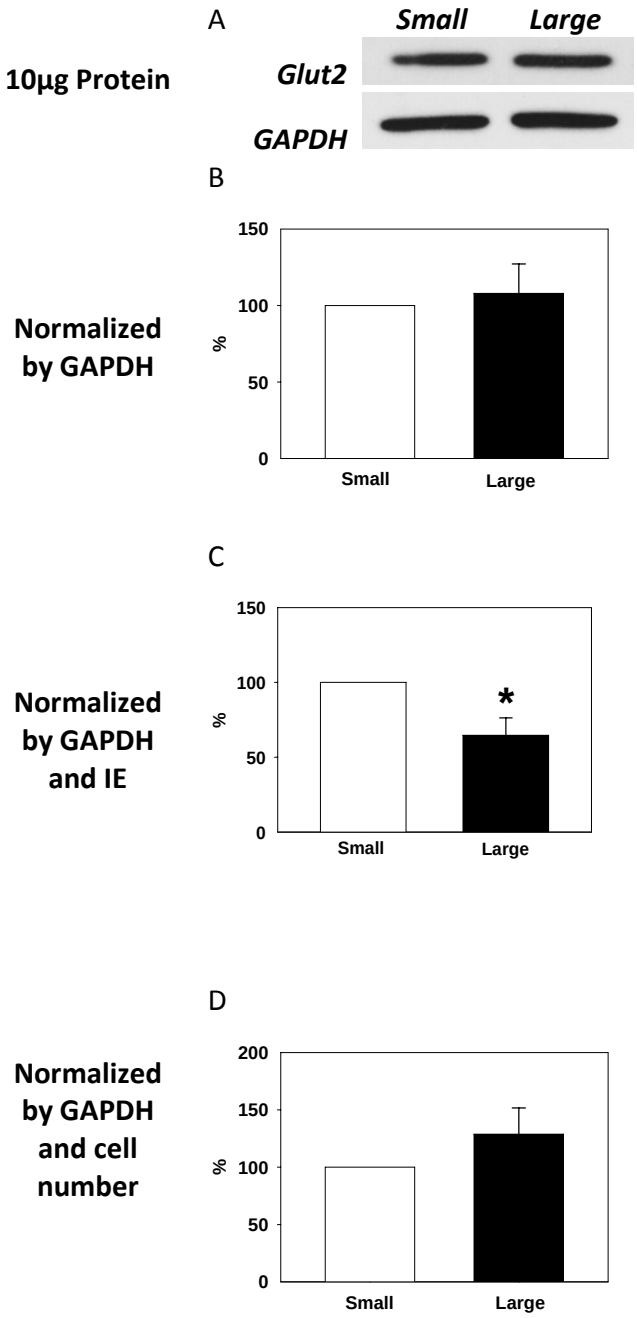

Figure 18. Glut2 protein levels in small and large islets. The representative bands done by Western Blot were shown in (A).The blot densitometry was normalized to internal control GAPDH (B), GAPDH and IE (C), GAPDH and cell number (D) . N = 5 experiments, each experiment contained at least 1,500 small islets or 300 large islets from 6 adult male rats. (*, $p < 0.05$)

A

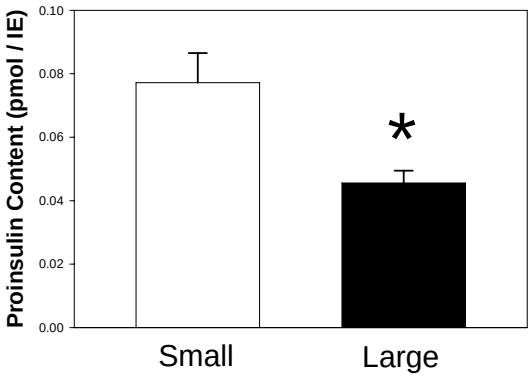

B

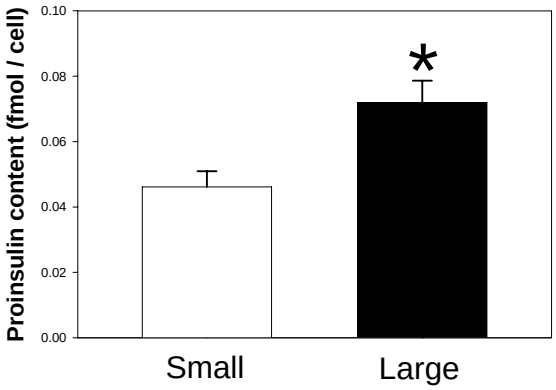

Figure 19. Proinsulin content in small and large islets. When normalized by IE (A), small islets showed a higher proinsulin content. When normalized by cell number (B), the results were opposite showing that large islets had a higher proinsulin content. N = 3 experiments, each experiment contained two replicates with at least 16 small islets or 6 large islets per replicate from 2 adult male rats. (*, $p < 0.05$)

3.5. Discussion

The accuracy of the international-standardized IE measurement has been questioned for years. Several factors which may affect the accuracy have being recognized such as subjective judgment of the examiners, sampling techniques and islet purity. While most research groups were engaged in studying computer-assisted digital image analysis (DIA) to compensate these disadvantages, the accuracy of the algorithm that converting islet size into IE was paid little attention until recently. Buchwald, et al. suggested that the algorithm, first proposed by Ricordi et al., overestimated total IEs by 4~8%. Accordingly, they proposed a modified conversion factors to estimate IE (Buchwald et al., 2009). However, here we showed both conventional IE measurement and the Buchwald's refined measurement overestimated the actual tissue volume especially in large islets. It has been suggested that grouping islets into a 50-μm range in current standard procedure might lead to a overestimation in IE (Buchwald et al., 2009; Niclauss et al., 2008). We suggest that the incorrect assumption that islets are spheres in the current algorithm causes IE measurement inaccuracy, because many research groups, in addition to us, have recognized that shapes of islets are irregular (Cummings et al., 2008; Girman et al., 2008; Lehmann et al., 1998; Niclauss et al., 2008; Perez-Armendariz et al., 1985; Pisania, Papas et al., 2010; Ricordi, Socci et al., 1990).

Since islets are cluster of cells, we proposed to estimate islet tissue volume by total cell number. Recently, Pisania et al. estimated the islet volume by using cell nuclei count. They concluded an overestimation when using IE measurement and suggested the overestimation might be due to the possible space such as intra-islet vessel and intracellular space not accounted for by IE measurements (Pisania, Weir et al., 2010). Compared to Pisania's work, we also base our volume estimations on cell numbers, but our approach does not require an extra step in the experimental process (nuclei isolation and staining).

We developed a regression model to estimate the number of cells per islet over a wide range of islet diameters with a high R-squared value and a good validity and reliability. When comparing the standard IE measurement to our method using cell number, we identified a significant overestimation of tissue volume in large islets by using IE calculations. The inverse correlation between total cell number per IE and islet size can explain this finding, because when normalized total cell number to IE, there were fewer cells per IE in large islets compared to small islets, which might be due to there are more intracellular space and vessels in the large islets as described previously. (Pisania, Weir et al., 2010).

Current islet volume normalizing methods in islet research need to be reconsidered, because completely different results may be obtained depending to the normalization methods. Here, we provide examples of Western Blot to study the Glut2 protein levels and ELISA to report proinsulin content comparing small and large islets. We show contradicting results based solely on the normalization method used. Since total protein content per IE was different in small and large islets, normalizing any protein by IE is not correct. Instead, normalizing by total protein amount used in the experiment (such as an internal control) and/or normalizing by total cell number produces more accurate results.

Our findings may have a tremendous impact on assumptions made about the volume versus size of islets within the rat pancreas. It is frequently reported that large islets (diameter >150μm) comprise 47% of total volume of endocrine tissue from the pancreas, even though they come from a relative small number count (5% of the total number of islets) (Korsgren et al., 2005). Moreover, when considering islets of 100μm in diameter and greater, it is thought that they make up 20% of the total number of islets but nearly 75% of the total islet volume (Korsgren et al., 2005). However, those estimates are based on Hellman's early work that still

considered islets as mainly spherical (Hellman, 1959a). Thus, the actual percentage of volume defined by large islets may be less and needs to be reconsidered.

In clinical transplant settings, the implications are immediate. Large islets are preferentially used for transplantation due to their relatively high assumed tissue volume. However, the volume of large islets has to be assessed more carefully, because recently the high variability in IE measurement due to large islets has been recognized by others (Buchwald et al., 2009). We suggested that if one calculates the typical volume of islets transplanted during the process, and corrects it based on Figure 14A, then the actual volume transplanted will be significantly less. In order to freely distribute the method described here for researchers, we created a spreadsheet that automatically calculates cell number from the measured islet diameter. The spreadsheet is available online for free public downloads.

In conclusion, the assumption of spherical islets used by conventional IE measurement has been shown to be incorrect. IE measurement overestimated the islet volume, potentially affecting the results of islet research and transplantation. We established a new method to estimate islet volume via the total cell number per isolated islet in rats. This model needs to be further established in humans to better estimate the tissue volume used in human islet research and transplantation.

Chapter 4

The insulin biosynthesis pathway in small and large islets does not correspond to insulin secretion

4.1. Abstract

Insulin is produced and released from the β cells of pancreatic islets through a cascading pathway from insulin gene transcription to proinsulin biosynthesis to insulin secretion. The elevation in glucose concentration is the primary signal to activate each step respectively through a complex network of intracellular signaling pathways. Small islets are thought to have more insulin secretion when compared to the same tissue volume of large islets. However, the possible unique mechanisms of glucose-stimulated insulin production and secretion between small and large islets are unidentified. In the present work, we challenged the isolated small and large rat islets with 30 minutes high glucose and compared the responses of insulin gene transcription (including the preproinsulin mRNA and insulin gene transcription factors: NeuroD/ Beta2, MafA and PDX-1), proinsulin and insulin synthesis, and insulin secretion between large and small islets. The results showed that levels of Glut2, the glucose transporter in β cells, were not different between large and small islets. In transcription level, 30 minutes of high glucose did not alter the preproinsulin mRNA (insulin 1 and insulin 2) and the gene expressions of NeuroD/ Beta2 and MafA. Yet, 30 minutes high glucose suppressed the PDX-1 gene expression in protein levels in both small and large islets. In translation level, 30 minutes of high glucose significantly increased the proinsulin levels, and large islets showed a higher proinsulin content per cell under high glucose. However, insulin content per cell was not significantly different between small and large islets under high glucose. Surprisingly, the glucose-stimulation insulin secretion was not significantly different between small and large islets when normalized by cell number, even though higher stimulation index was seen in large islets. Interestingly, when comparing small and large islets under basal conditions by t-test, higher NeuroD/Beta2 and MafA gene expressions in both protein and mRNA levels were seen in the large islets, but with a lower of PDX-1 protein levels, when compared to small islets. In summary, the difference in insulin gene

transcription between small and large islets can not be identified under short period glucose stimulation. In spite of what appears to be upregulation of the proinsulin biosynthesis in large islets, these changes did not correspond to insulin content and insulin secretion levels. Therefore, when comparing large and small islets, there might be disconnections between the insulin biosynthesis pathway and insulin secretion levels.

4.2. Introduction

Insulin, an important hormone for blood glucose hemostaisis in mammals, is produced through a cascading process in the β cells of pancreatic islets. Through gene transcription, the insulin gene is transcribed from DNA to preproinsulin mRNA. Following that, the preproinsulin mRNA is translated into preproinsulin protein, which exists the cell shortly. Then, the preproinsulin is processed into proinsulin and stored into granules. The proinsulin is cleaved by specific enzymes into c-peptide and insulin. Finally, the mature insulin is released from the cell by exocytosis to the blood stream.

The elevation in blood glucose concentrations is the primary signal for insulin production and secretion. By entering into the β cell via the glucose transporter (Glut2) on the plasma membrane, glucose is thought to enhance insulin biosynthesis (including gene transcription and translation) and insulin release through the complex network of intracellular signaling pathways.

At the transcription level, it is suggested that high glucose (16.7 mM) stimulates insulin gene transcription about 3-fold after 10 minutes, and the transcriptional activity is maximal at 30 minutes, but markedly decreased thereafter (Efrat et al., 1991). Leibiger, et al. also reported that incubating the isolated islets in a high glucose (16.7 mM) for only 15 minutes, resulted in a 2 to 5- fold elevation in preproinsulin mRNA levels within 60~90 minutes. The authors also suggested that the glucose stimulatory effect is most obvious 30 minutes after the glucose exposure, but declines thereafter (Leibiger et al., 1998). Therefore, it is likely that the production of preproinsulin mRNA is affected by high glucose concentration within minutes. In addition, increased glucose levels activate upstream signals that are responsible for the activation of the transcription factors involved in insulin gene transcription, which are the homeodomain protein pancreas duodenum homeobox-1 (PDX-1), Beta-cell E-box trans-activator 2 (Beta2 or NeuroD) proteins, and the basic region leucine zipper MafA. Glucose stimulates PDX-1 translocation and

increases PDX-1 DNA binding activity through the pathway involving phosphatidylinosito 3-kinase (PI3-K) activation (Elrick & Docherty, 2001; MacFarlane et al., 1994; Macfarlane et al., 2000; Rafiq et al., 2000; Rafiq et al., 1998). Glucose also stimulates the binding activity of Beta2/NeuroD to the insulin promoter (E1) in β cells, which is dependent upon the phosphorylation of extracellular signal-regulated kinase (ERK) 1/2 (Khoo et al., 2003; Lawrence et al., 2005; Naya et al., 1995). In addition, glucose stimulates MafA expression and activates binding activity of MafA to the insulin promoter (C1) to enhance insulin gene transcription (Hagman et al., 2005; Kataoka et al., 2002; Zhang et al., 2005).

At the translational level, glucose is the most physiologically relevant factor that regulates the proinsulin synthesis. Glucose stimulates the recruitment of preproinsulin mRNA from an inert cytosolic pool to the rough ER, the site of preproinsulin protein synthesis (Itoh & Okamoto, 1980; Welsh et al., 1986). After one hour of incubation at high glucose (16.7 mM), proinsulin protein levels in the rat islets increases up to 6 to 15 fold (Guest et al., 1989; Wicksteed et al., 2003). In addition, proinsulin synthesis is dose-dependent, and has been reported to increase 25-fold when glucose is increased from 1 to 10 mM for one hour (Schuit et al., 1988).

Insulin secretion in response to increased glucose concentrations exhibits a biphasic pattern consisting of a rapidly initiated and transient first phase (lasting 5~10 minutes) followed by a slowly developing and sustained second phase (Cerasi, 1975; Curry et al., 1968; Lacy et al., 1972; Luzi & DeFronzo, 1989). The insulin granule secretion rate has been reported to amount to 0.14% and 0.05% of the total insulin content per minute in the first and second phase respectively (Rorsman & Renstrom, 2003). The first phase insulin release from the readily releasable pool, which contains less than 5% of total insulin granules per β cell, is regulated by glucose stimulation through the ATP-sensitive K^+ (K_{ATP}) channel-dependent pathway, increasing Ca^{2+} causing insulin granule release or exocytosis (Bratanova-Tochkova et al., 2002). In the

second phase, glucose involves the mobilization and priming process of insulin granules from reserve pools, which contains more than 95% of total insulin granules per β cell, to the readily releasable pool to gain the competence for the sustained second phase release (Bratanova-Tochkova et al., 2002).

Small islets have been shown to secret more insulin than large islets when normalized to tissue volume (islet equivalent; IE) (H.-H. Huang et al., 2011; Lehmann et al., 2007; MacGregor et al., 2006; Su et al., 2010; Williams et al., 2010; Yasutaka Fujita, 2011) and led to better transplantation outcome both in rodents (MacGregor et al., 2006; Su et al., 2010) and in human (Lehmann et al., 2007). However, the detailed mechanisms of insulin production and secretion in different sized islets are unclear. Previously, our group suggested that diffusion barrier in isolated large islets may hamper the islet function. Surprisingly, elimination of diffusion barrier in large islets improved the survival, but failed to improve the inferior in vitro insulin secretion to the same rate as intact small islets, indicating that there might be an inherent cellular difference in insulin production or secretion capacity between small and large islets (Williams et al., 2010).

The objective of present work was to determine whether the insulin producing mechanisms are different between the β cells in small and large islets. We investigated the insulin biosynthesis and secretion during the early response to glucose stimulation in small and large isolated rat islets, with the goal of elucidating new intricacies concerning cell biology according to the size differences of islets.

4.3. Methods

Rat islet isolation and separation

Adult male Sprague Dawley rats (200~250g BW) were housed on a 12 hours light/dark cycle with free access to standard laboratory chow and water. All animals received care in compliance with the Principles of Laboratory Animal Care formulated by the National Society for Medical Research and the Guide for the Care and Use of Laboratory Animals published by the US National Institutes of Health (NIH Publication No. 85-23, revised 1996).

Islet isolation methods followed our published procedures described in detail (H.-H. Huang et al., 2011; MacGregor et al., 2006; Williams et al., 2010; S. Williams et al., 2009). Briefly, rats were anesthetized by intraperitoneal injection of a mixture of ketamine and xylazine. After the peritoneal cavity was exposed, the pancreatic main duct to the intestine was clamped and the pancreas cannulated *in situ* via the common bile duct. The pancreas was distended with collagenase and removed. Islets were gently tumbled, washed, and passed through a sterile 30 mesh stainless steel screen and centrifuged. The pellet was mixed with Histopaque, centrifuged, and the islets floating on the gradient were collected and sedimented. Islets were passed through a sterile 40μm mesh cell strainer with HBSS. After this cleaning process, islets were placed into CMRL1066 medium containing 2 mM glutamine, 10% fetal bovine serum (FBS) and 1% antibiotic/ antimycotic solution and put into a 37ºC culture chamber containing 5% CO_2.

For large and small islet separation, the islet culture media was changed to L15 containing 10% FBS and 5mM HEPES, and islets were transferred into 37ºC culture chamber without CO_2. Isolated islets were manually separated by size based on the criteria that small: diameter $\leq$ 100μm; large: diameter $\geq$ 200μm. Finally, the total cell numbers in the selected small or large islets being used in each experiment were estimated based on our model in Chapter 3.

Islet perifusion

Approximately 850 small islets and 120 large islets were used individually in each set of perifusion experiment. First, small and large islets were preincubated for 90 minutes in RPMI 1640 medium containing 10% FBS and 3mM glucose at a 37°C with 5% CO_2. After preincubation, the islets were incubated in the glucose perifusion system individually with a constant flow rate (500 μl/min) at 37°C for 90 minutes including: 30 minutes of basal condition (3mM glucose) following by 30 minutes of high glucose concentration (20mM) and 30 minutes of basal condition (3mM glucose). During the perifusion, samples of medium with released insulin were collected from the output fraction every 3 minutes starting with the last 10 minutes of the first low glucose exposure. Samples were frozen at -80°C. At the end of the perifusion, the islets were harvested and frozen at -80°C. The total insulin content in the islets was extracted by acid ethanol (0.18 M HCl in 95% ethanol). The released insulin and the total islet insulin content were determined by the ELISA kit (ALPCO, Salem, NH, USA) as we have published previously (H.-H. Huang et al., 2011; MacGregor et al., 2006; Williams et al., 2010). The stimulation index was calculated as the ratio of averaged insulin released amount per 100 cells under high glucose over averaged insulin released under low glucose (basal condition) (Clayton, Turner, Swift, James, & Bell, 2001; Coffey, Berman, Willman, & Kenyon, 2009; Robitaille, Dusseault, Henley, Rosenberg, & Halle, 2003).

Islet static incubation

Islet static incubation assays followed our published procedures (H.-H. Huang et al., 2011; MacGregor et al., 2006; Williams et al., 2010). Isolated islets were placed in 24-well plates with a minimum of 5 large or 15 small islets per well. All wells were preincubated for 2.5 hours in RPMI 1640 containing 10% fetal bovine serum and 3 mM glucose in a 37°C containing 5% CO_2. After preincubation, media was removed from each well and discarded. Low (3 mM as basal

condition) or high (16.6 mM) glucose solutions were added, according to the design. After a 30 minutes static incubation at 37°C and 5% CO_2, the islets were harvested and frozen at -80°C. The total protein in the islets was extracted by sonication in acid ethanol (0.18M HCl in 95% ethanol) and incubated overnight at 4°C. The total intracellular proinsulin and insulin amounts in the extracts were determined separately by the ELISA (ALPCO, Salem, NH, USA).

Western Blot

After 30 minutes low or high glucose static incubation, the small and large islets were harvested and washed in phosphate-buffered saline (PBS) twice. After removing the supernatant, the large and small islets were homogenized using a $26G^1/_2$ syringe with extraction buffer containing 10mM TRIS HCl pH7.4, 150mM NaCl, 1mM EDTA, 20mM Na Molybolate, 50mM Na Fluoride, 0.2mM Na-Orthovanidate (pH 10), 1% Triton X-100, and 0.2mM PMSF. The extracts were centrifuged for 15 minutes with 15,600 rcf at 4°C. Measurement of protein concentrations in supernatants was performed using Micro BCA Protein Assay Kit (Pierce, Rockford, IL, U.S.A., #23235). The protein samples from large and small islets extracts were prepared for electrophoresis by heating at 95 ^oC for 3 min in SDS gel-loading buffer (0.125M Tris, pH6.8, 5% glycerol, 2.5% mercaptoethanol, 2% SDS, and 0,001% bromophenol blue). Proteins were separated on a 4-15% Tris-HCl Ready Gels (Bio-Rad Laboratories, Hercules, CA, U.S.A., #161-1158) with 0.025 M Tris, 0.192 M Glycine, 0.1% SDS running buffer. Equal amounts of total protein (10 µg) were loaded in each lane. Molecular weight markers See Blue Plus2 Pre-Stained Standard (Invitrogen, Carlsbad, CA, U.S.A., #LC5925) were used to determine the size of the antigen. After electrophoresis, the proteins were transferred from the gel to Bio Trace PVDF membranes 0.45 µm (Pall Life Sciences, East Hills, NY, U.S.A., #P/N 66547) using 0.012 M Tris, 0.096 M Glycine transfer buffer. Blots were blocked with 5% nonfat dry milk diluted in 0.1M PBS 0.1% Tween (PBST) for 1 hour. Primary antibodies were diluted

in the 5% nonfat dry milk or 5% BSA in PBST according to the manufacturer's directions. Blots were probed with primary antibodies against Glut2 (Santa Cruz Biotechnology Inc., Santa Cruz, CA, U.S.A., #sc-9917), MafA (Santa Cruz Biotechnology Inc., Santa Cruz, CA, U.S.A., #sc-66958), PDX-1 (Cell Signaling Technology Inc. Danvers, MA, U.S.A., #2437), NeuroD (Cell Signaling Technology Inc. Danvers, MA, U.S.A., #4373) and incubated at room temperature for 1 hour or at 4°C overnight according to the manufacturer's directions. After washing in 0.1M PBS 0.1% Tween (10 minutes for 3 times), blots were incubated for 30 minutes with secondary antibody horseradish peroxidase-conjugated goat anti-rabbit IgG (Santa Cruz Biotechnology Inc., Santa Cruz, CA, U.S.A., #sc-2004) or goat anti-mouse IgG (Santa Cruz Biotechnology Inc., Santa Cruz, CA, U.S.A., #sc-2005). After washing in 0.1M PBS 0.1% Tween (10 minutes, 3 times), bound antibodies were detected using SuperSignal® West Pico Chemiluminescent Substrate (Thermo Fisher Scientific Inc., Rockford, IL, U.S.A., # 34080). For a protein loading control, the membrane was reprobed with mouse anti GAPDH (Sigma-Aldrich®, St. Louis, MO, U.S.A., #G8795), for 1 hour at room temperature.

RT-qPCR

Total RNA was isolated from islets using RNeasy Mini kit (Qiagene) according to the manufacturer's instructions and quantified by spectroscopy. An equal quantity of total RNA (500 ng) from each subject was reverse transcribed into cDNA using TaqMan® Reverse Transcription Reagents (Applied Biosystems, Chicago, IL, U.S.A., #N8080234) according to the manufacturer's instructions. For real-time PRC, 150ng cDNA products were mixed in TaqMan® Gene Expression Master Mix (Applied Biosystems, Chicago, IL, U.S.A., #4369106) together with gene specific primers: Insulin 1, Insulin 2, PDX1, MafA, NeourD (Applied Biosystems, Chicago, IL, U.S.A., #4448892) and GAPDH (Applied Biosystems, Chicago, IL, U.S.A., #4331182). Real-time PCR was carried out in an ABI Prism 7000® Sequence Detection System

(Applied Biosystems, Chicago, IL, U.S.A.). The amount of transcript was calculated using the comparative cycle threshold (C_T) method, which determines the amount of target genes against GAPDH as the normalization gene. Normalized C_T values were averaged to produce the mean C_T value for each gene analyzed.

Statistics

The experimental design included comparing islets from healthy animals, thus each animal provided both large and small islets for the comparison studies (low and high glucose). The exact number of islets used in each experiment is shown in each figure legend. Results were expressed as mean of each group or islet population ± SEM. Where appropriate, differences between groups were examined for significance using one- or two-way ANOVA (factors: islet size and glucose concentration) followed by the Fisher's least significant difference (LSD) post hoc test. Unpaired Student's t-test was used for the comparisons between small and large islets under basal conditions. Significant differences were defined as $p < 0.05$.

4.4. Results

Glucose transporter (Glut2)

Glucose entry into the β cell is accomplished via the Glut2 located on the plasma membrane and activates insulin gene transcription, translation, and secretion through a complex network of intracellular signaling pathways described previously. The protein levels of Glut2 were determined by Western Blot. After 30 minutes of high glucose, Glut2 levels did not change significantly. In addition, Glut2 was not significantly different between small and large islets (Figure 20).

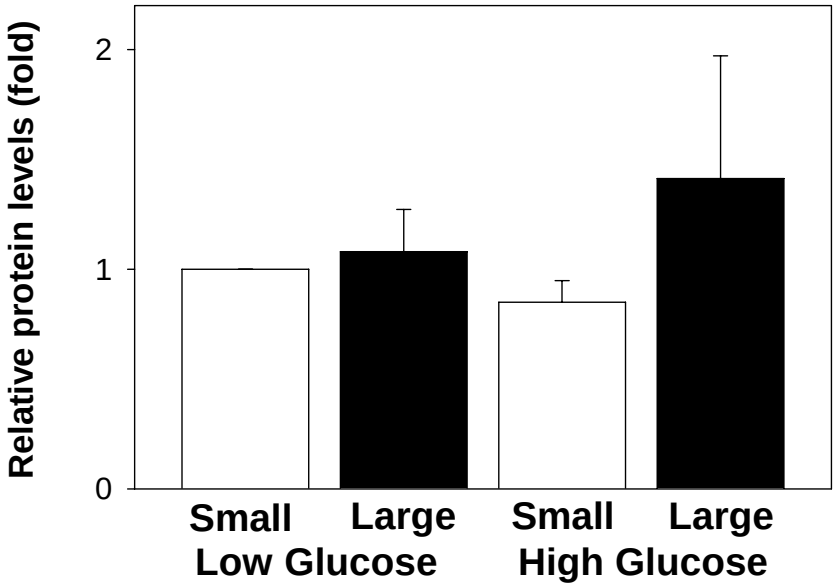

Figure 20. Glucose transporter (Glut2) protein levels. There were no differences in Glut2 levels between small and large islets, under basal conditions (3mM glucose) or after 30 minutes high (16.6mM) glucose stimulation. N = 5 experiments in each group. Each experiment contained at least 3,000 small islets or 600 large islets from 6 rats. The expressions in each group were presented as relative fold difference to small islets under low glucose.

Glucose-stimulated Insulin Gene Transcription

In rat islets, there are two insulin genes, insulin 1 and insulin 2, which are transcribed into two preproinsulin mRNAs, insulin 1 mRNA and insulin 2 mRNA. After 30 minutes of high glucose, the mRNA levels of insulin 1 and insulin 2 in either small or large islets did not increase significantly. Under basal conditions, the mRNA expressions of both the insulin 1 and insulin 2 tended to be higher in large islets but not statistically significant (Figure 21A & B).

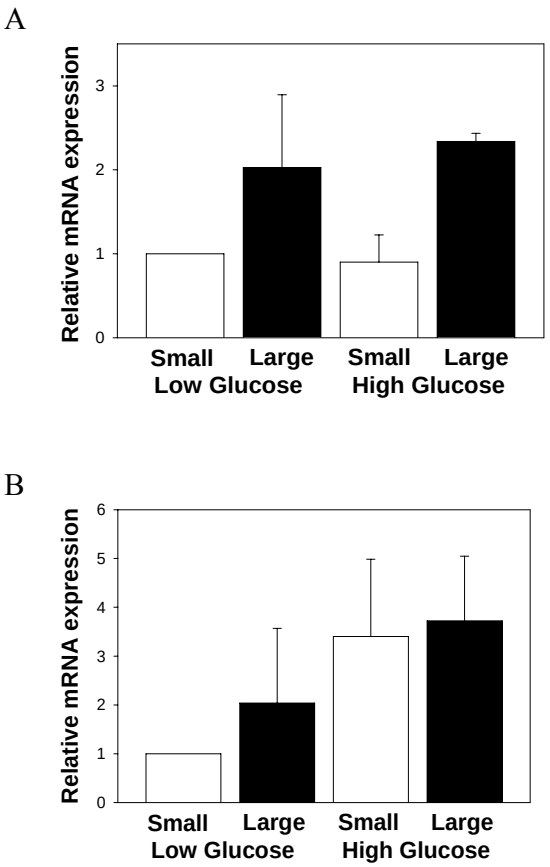

Figure 21. Preproinsulin mRNA levels. There are two insulin genes, insulin1 (A) and insulin2 (B), in rat islets. After 30 minutes glucose stimulation, the mRNA levels of insulin 1 and insulin 2 in either small or large islets did not increase significantly. N = 3 experiments in each group. Each experiment contained at least 3,000 small islets or 600 large islets from 6 rats. The expressions in each group were presented as relative fold difference to small islets under low glucose.

The gene expressions of three transcription factors (MafA, NeuroD/Beta2 and PDX-1) involved in the upregulation of insulin gene expression were assayed at both the mRNA and protein levels. After 30 minutes of high glucose, the gene expressions of MafA and NeuroD/Beta2 in both mRNA and protein levels did not significantly change in either population of islets (Figure 22A toD). The PDX-1 protein levels decreased significantly in both small and large islets after 30 minutes high glucose stimulation (Figure 22F). However, the decreases were not seen in the mRNA levels (Figure 22E).

After reanalyzing the data from the low glucose group by using unpaired t-test, the gene expressions of MafA and NeuroD/Beta2 in both mRNA and protein levels were showing significantly higher in large islets under basal conditions (Figure 22A toD). However, the PDX-1 protein levels were significantly lower in large islets, but the decrease was not seen in the mRNA levels (Figure 22E and F).

Glucose-stimulated Insulin Gene Translation

After 30 minutes high glucose stimulation, proinsulin levels increased significantly in both the small and large islets. Furthermore, in high glucose condition, the large islets had more proinsulin, when normalized to cell numbers, than small islets (Figure 23A). When measuring the downstream product, insulin, there was not a significant glucose-stimulated increase in insulin content in either the large or small islets (Figure 23B). After reanalyzing the data from the low glucose group by using unpaired t-test, proinsulin levels were significantly higher in the large islets (Figure 23A). However, there was no difference in insulin content between small and large islets, when normalized to cell number (Figure 23B).

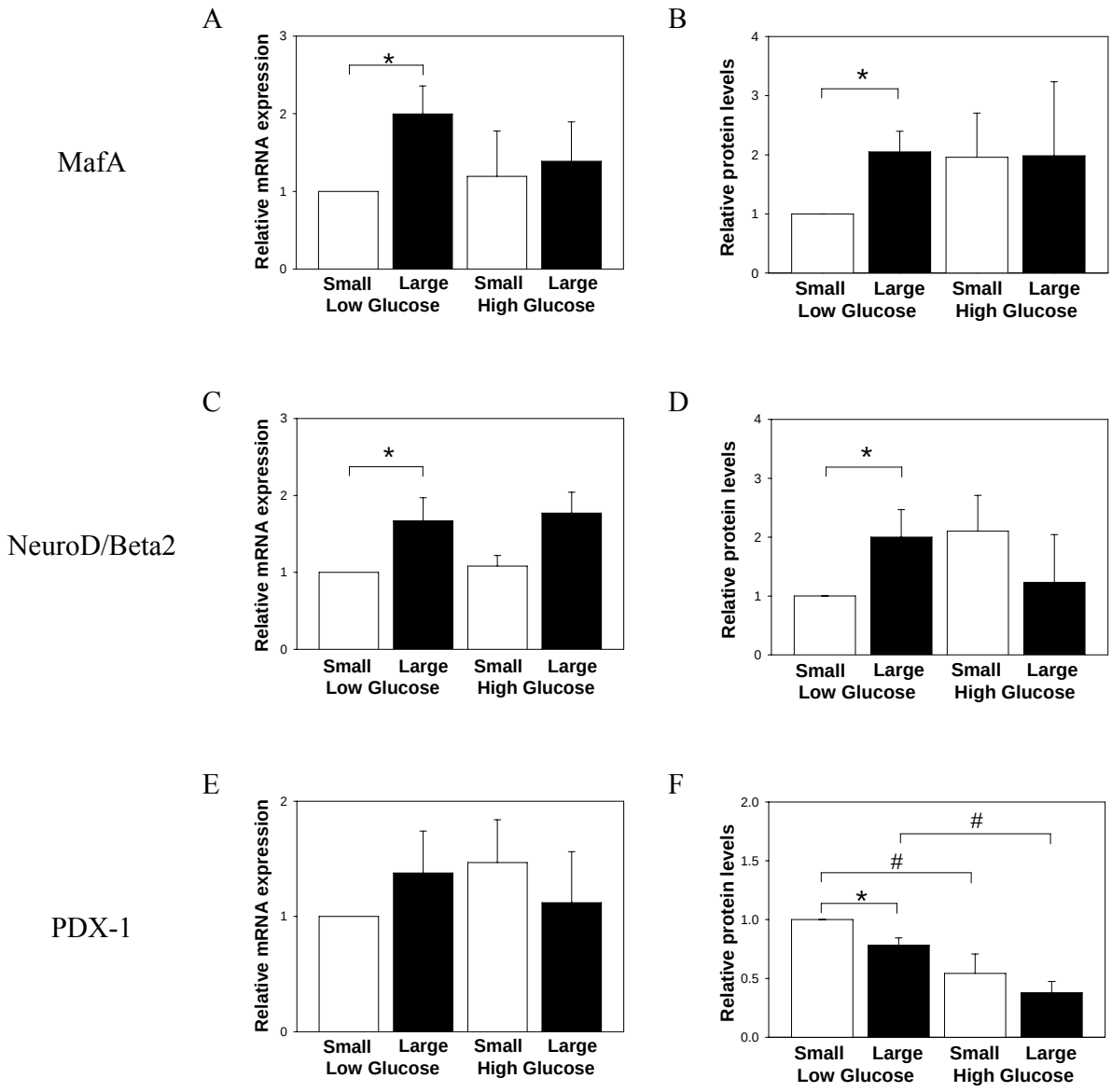

Figure 22. Gene expressions of insulin gene transcription factors. (A) MafA mRNA levels; (B) MafA protein levels; (C) NeuroD/Beta2 mRNA levels; (D) NeuroD/Beta2 protein levels; (E) PDX-1 mRNA levels; (F) PDX-1 protein levels. MafA and NeuroD/Beta2 in both mRNA and protein levels did not significantly change after 30 minutes high glucose in either small or large islets, but PDX-1 protein levels decreased significantly in both small and large islets. After reanalyzing the data by using unpaired t-test, MafA and NeuroD/Beta2 in both mRNA and protein levels showed significantly higher levels in large islets under basal conditions. However, the PDX-1 protein levels were significantly lower in large islets. N = 3 experiments in each group. Each experiment contained at least 3,000 small islets or 600 large islets from 6 rats. The expressions in each group were presented as relative fold difference to small islets under low glucose. (#: $p < 0.05$ according to two-way ANOVA with Fisher's LSD test; *: $p < 0.05$ according to unparied t-test)

A

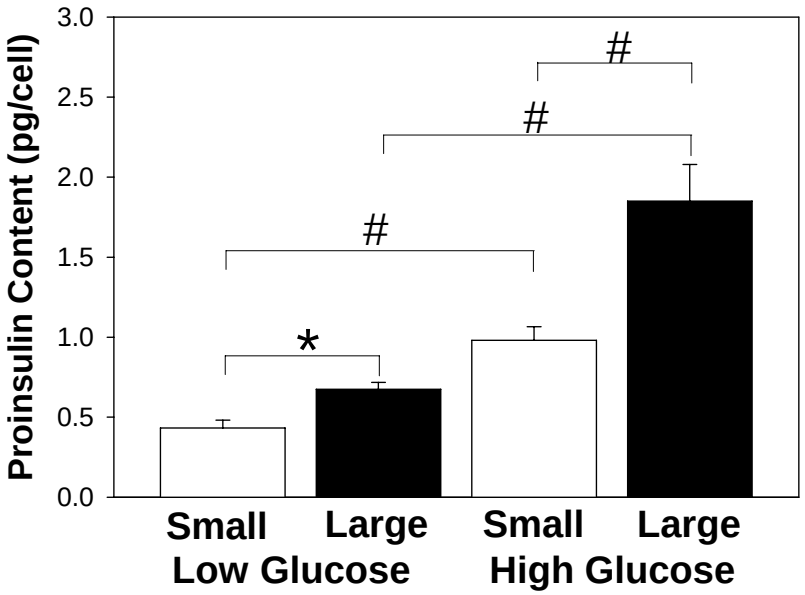

B

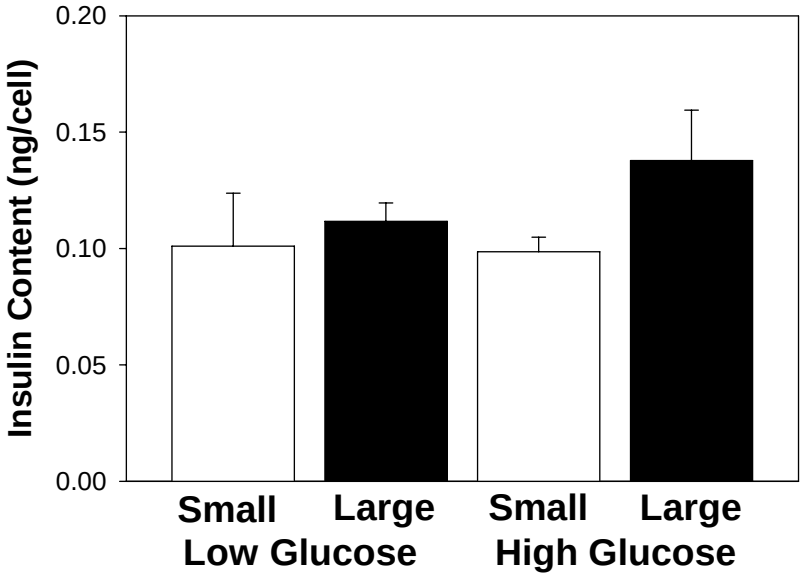

Figure 23. Proinsulin and insulin content per cell. (A) When normalized to cell, total proinsulin content from small and large isolated islets (measured by ELISA) showed that large islets contained more proinsulin per cell in high glucose. In addition, both small and large islets contained higher proisnulin levels in high glucose when compared to basal conditions. Large islets contained more proinsulin per cell under basal conditions when compared using t-test. (B) When normalized to cell, total insulin content showed no significant difference in both small and large islet under basal conditions or high glucose. N = 6 experiments in each group. Each experiment contained at least 40 small islets or 10 large islets from 2 rats. (#: $p < 0.05$ according to two-way ANOVA with Fisher's LSD test; *: $p < 0.05$ according to unparied t-test)

Glucose-stimulated Insulin Secretion

Figure 24A illustrated the results of insulin secretion in the glucose perifusion experiments. Under high glucose stimulation, the typical biphasic responses (between 0 and 20 minute) were recognized in both small and large islets indicating that both islet populations had normal glucose-stimulated secretion patterns (Figure 24A). When normalized to cell number, there was no statistical difference in the level of the insulin secretion between small and large islets. At the end of experiment, the total insulin content per cell was no different between small and large islets (0.12 ± 0.02 vs. 0.11 ± 0.02 ng per cell, $p = 0.74$) under basal conditions. While there were some time-dependent differences in the responses between the two groups, the calculated area under curve showed no difference ($p = 0.98$) between two groups which indicated that the total amount of secreted insulin over the experiments was not different in small and large islets (Figure 24B). Interestingly, the stimulation index (SI), which calculates the percent increase in insulin secretion compared to basal rates, was higher in the large islets than in smalls (3.16 ± 0.40 vs. 1.95 ± 0.31, $p < 0.05$) indicating that large islets might have higher responsiveness to glucose for insulin secretion.

A

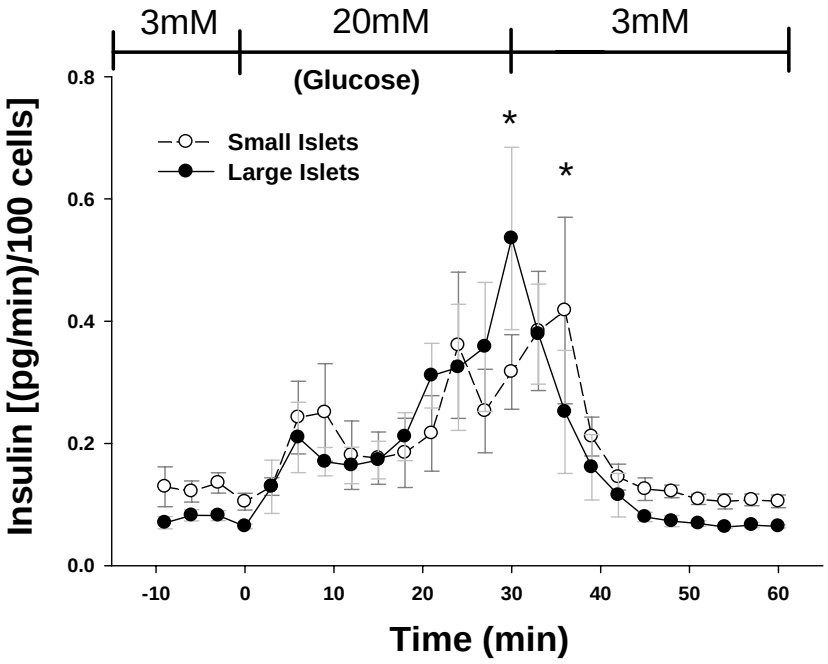

B

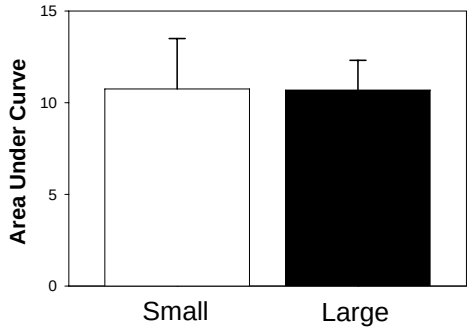

Figure 24. Glucose-stimulated insulin secretion. (A) When normalized to cell, there was no statistical difference in the level or timing of the insulin secretion rate between small and large islets except at 30 and 36 minutes. (B) The area under the curve (between 0 to 45 minute) was not different between small and large islets ($p = 0.98$). N = 3 experiments in each group. Each experiment contained at least 850 small islets or 120 large islets from 2 rats. (*: $p < 0.05$ according to two-way ANOVA with Fisher's LSD test)

4.5. Discussion

Our group has been engaged in determining whether small and large islets have different mechanisms in the insulin production that lead to inferior insulin secretion per volume (islet equivalent, IE) in large islets. We hypothesized that the diffusion barrier in large islets may play a role. However, elimination of the diffusion in the large islets improved the viability but did not improve the insulin secretion, which indicated diffusion barrier can not account for the inferior insulin secretion per IE in large islets (Williams et al., 2010). Next, we questioned the accuracy of using IE as a normalization method. We identified an overestimation in tissue volume quantification when using IE, which may underestimate the actual islet function especially in large islets. In addition, islet tissue is cluster of cells and there was no difference in the percentage of insulin-producing β cells between small and large islet in vitro or in situ (H. H. Huang et al., 2011). Therefore, at present work, we used total cell number in islets to normalize insulin secretion between groups. Surprisingly, when normalized to cell number, there was no difference in insulin secretion between small and large islets. Therefore, we suggested the previous conclusion of different insulin secretion between small and large islets when normalized by IE needs to be reconsidered.

Glucose is the main regulator of insulin biosynthesis including insulin gene transcription and translation in β cell. It was commonly believed that over a short period, glucose regulates the insulin biosynthesis mainly by increasing the translation of preproinsulin mRNA rather than insulin gene transcription. The effect of glucose in insulin gene transcription was commonly accepted as a long-term effect. Thus, the previous reports for the mechanisms of glucose-stimulated insulin gene transcription were mainly designed in the high glucose static incubation over several hours or even days (Khoo et al., 2003; Ling, Heimberg, Foriers, Schuit, & Pipeleers, 1998; Ritz-Laser et al., 1999). However, there were two groups reporting that a

short time period of glucose stimulation elevated the preproinsulin mRNA levels in β cells. Efrat et al. suggested that 10 minutes high glucose (16.7 mM) stimulates insulin gene transcription about 3-fold, and the transcriptional activity is maximal at 30 minutes (Efrat et al., 1991). In addition, Leibiger et al. reported that incubating isolated rat islets in high glucose (16.7 mM) for only 15 minutes, results in a 5-fold elevation in preproinsulin mRNA levels within 60 minutes after stimulation (Leibiger et al., 1998). Moreover, from the physiological perspective, β cells in the pancreatic islets are exposed to the elevated glucose for minutes after food-uptake. Therefore, we chose 30 minutes high glucose stimulation to investigate the mechanisms of insulin gene transcription and translation. The results showed that both small and large showed a significant increase in proinsulin content, the product after preproinsulin mRNA translation, after 30 minutes high glucose challenge. This result was in agreement with the well-accepted argument described above. However, in insulin gene transcription, there was no significant increase in preproinsulin mRNA between basal conditions and 30 minutes high glucose stimulation in both groups of islets. The different experimental design could explain the inconsistency between my results and the previous reports by Efrat and Leibiger. First, Efrat et al. used β tumor cell lines and here, we used isolated rat islets here. Second, Leibiger et al. extracted the RNA from isolated rat islets 60 minutes after the start of 15 minutes high glucose stimulation. Whereas, we extracted the RNA from islets right after the 30 minute glucose stimulation. Therefore, we suggest that how acute glucose stimulation affects insulin gene transcription remains unclear.

In addition, we determined whether insulin gene transcription factors play role in early phase of glucose-stimulated insulin biosynthesis. After 30 minutes of high glucose, there were no significant changes in the gene expressions of MafA and NeuroD/Beta2 compared to the basal conditions. Interestingly, 30 minutes of high glucose stimulation significantly decreased the PDX-1 protein levels in both groups of islets. However, one study using MIN6 cells (β cell line)

showed that PDX-1 protein levels were increased after 30 minutes high glucose (16mM)(Macfarlane et al., 1999). Another study showed an increased PDX-1 gene expression in mRNA levels in rat islets after one hour high glucose (16mM) stimulation (Vilches-Flores, Delgado-Buenrostro, Navarrete-Vazquez, & Villalobos-Molina, 2010). To our best understanding, our finding is the first showing that acute glucose stimulation suppressed PDX-1 protein levels in isolated rat islets. Therefore, we suggested the detailed mechanisms about how PDX-1 gene expressions are regulated in early phase of glucose-stimulated insulin gene transcription remains to be elucidated.

After 30 minutes of high glucose stimulation, there was higher proinsulin biosynthesis in large islets. However, the difference was not seen in the downstream product, insulin content. The reason might be due to the relative fold difference is huge between insulin and proinsulin in the cell. On average, the proinsulin content is approximately 0.43~1.85 pg per cell while the insulin content is approximately 99~138 pg per cell, which is about 110 times higher than proinsulin. Therefore, the changes in insulin levels in early response to glucose might not be identified as significantly as the proinsulin. In addition, it has been suggested that insulin content was not associated with the insulin secretory capacity (Uchizono, Alarcon, Wicksteed, Marsh, & Rhodes, 2007). The reason might be due to the large in the intracellular insulin storage pool in comparison to the releasable pool (Rorsman & Renstrom, 2003). Moreover, it has been also suggested that young newly formed insulin granules are preferentially secreted (Howell & Taylor, 1967; Rhodes & Halban, 1987) while the majority of stored insulin granules are old, and if they do not undergo exocytosis, are retired by intracellular degradation with a 3 to 5 days half-life (Halban, 1991; Halban & Wollheim, 1980; Schnell, Swenne, & Borg, 1988). In our perifusion study, the total amount of insulin secreted under high glucose stimulation was only less than 0.05% of total insulin content in both small and large islets. Therefore, it seems likely

that the superior proinsulin biosynthesis in large islets did not correspond to insulin secretion in early response to glucose, and therefore is not a good predictor of functional islet secretion.

In chapter 3, we reported that there was no significant difference in total protein per cell between small and large islets. Similar results were also found when normalized by total DNA. In this chapter, after reanalyzing the protein levels in small and large islets under basal conditions by using t-test, higher MafA and Beta2/NeuroD protein levels were seen in large islets. The same trends were also shown in mRNA levels. In addition, PDX-1 protein levels were lower in large islets. All these findings implied that small and large islets may possess some inherent differences in gene expressions of these transcription factors.

In summary, the difference in the mechanisms of insulin gene transcription between small and large islets can not be concluded when the islets were challenged by 30 minutes of high glucose stimulation. However, we identified a higher glucose-stimulated proinsulin content in large islets, while there was no significant difference in insulin content and secretion between small and large islets when normalized by cell. These findings implied that the superior glucose-stimulated proinsulin biosynthesis in large islets may not correspond to insulin secretion in early phase of glucose stimulation.

Chapter 5

Summary of findings, discussion and future direction

5.1. Summary of findings

Solid understanding for islet biology is believed to be crucial to optimize the success of curing diabetes. However, the previous conclusions in the literature about isolated islets have been based on the conventional IE measurement for tissue volume normalization, and may need to be reconsidered. In this dissertation, I have proven that the IE measurement overestimated the tissue amount being used, leading to some erroneous conclusions being drawn from the experiments. Accordingly, I proposed a more accurate method to normalize islet tissue volume by using the total cell number. Based on this new measurement, the different characteristics in the insulin production and secretion pathway between small and large islets were identified.

Compared to small islets, large islets have superior glucose-stimulated proinsulin biosynthesis after 30 minutes glucose stimulation. However, no significant changes could be identified at the transcriptional levels except the decrease in PDX-1, even though this short time period of high glucose mimics a physiological-like challenge in vivo. Surprisingly, when normalized to cell number, insulin secretion was not different between small and large islets, unlike the results published previously in the literatures when normalized to IE. In addition, small and large islets have the same percentage of β cells, but small islets have higher density both in vitro and in situ. While small and large islets might contain the same amount of protein per cell, large islets showed higher protein levels of prosinulin, NeuroD/Beta2 and MafA with a lower PDX-1 under basal conditions. Therefore, it seems like that the different characteristics between small and large islets in the insulin production pathway did not correspond to measured insulin secretion.

5.2. Discussion

5.2.1. The implications to islet transplantation

A consistent and accurate method to quantify the yield of isolated islet is of critical importance to the transplantation in the clinic. The findings in this dissertation may have direct and significant implications to current islets transplantation. To date, islet transplantation is an experimental procedure for type 1 diabetic patients. From 1999 to 2008, approximately 828 islet transplantation perfusions have been performed on 412 patients in more than 40 institutions worldwide (Alejandro, Barton, Hering, & Wease, 2008). By placing healthy insulin-producing islets into the recipients, the islet transplantation procedure is capable of producing a stable blood glucose level, especially reducing the incidence of hypoglycemia for severely ill patients with type 1 diabetes. However, the outcome of normal glycemic control for diabetics has only been a clinical reality for a short period of time.

In the clinic, IE is highly relied on to quantify the dosage of the islets transplanted. However, in this dissertation, one of my conclusions was that IE is not an accurate measurement for islet volume. Thus, all the previous reports about islet tissue yield from the donors and the dosage of transplantation for the recipients may need to be reconsidered. I believe the inaccuracy in the tissue volume estimation might be directly or indirectly related to the transplantation outcome. Therefore, it will be very significant to perform another retrospective study on the correlation between the transplantation outcome and the actual tissue volume received by the patients by recalculating the previous data of islet volume from IE to total cell number. It is my expectation that the total cell number being transplanted will be a more reliable and valid predictor for islet transplantation outcome.

Transplanting small islets has been suggested as having a better outcome in humans (Lehmann et al., 2007) and in rodents (MacGregor et al., 2006; Su et al., 2010). One of the

assumptions was that the better transplantation outcome was due to greater insulin secretion in small islets. Here, I showed small and large islets have the same insulin secretion rate no matter when normalized to cell or normalized to total insulin content. Therefore, these results basically have ruled out this assumption. While there are some other factors that may affect the results of transplantation such as the quality of islet graft after isolation (Lakey, Tsujimura, Shapiro, & Kuroda, 2002; Lakey et al., 1996; Ricordi et al., 2003; R. M. Smith & Gale, 2005) and the revascularization rate of islets after transplantation (Menger et al., 1989), our research group suggested the superior transplantation outcome when using small islets might be mainly due to diffusion barriers in large islets. In the pancreas, islets are nourished by adequate blood supply (Ballian & Brunicardi, 2007; Zanone et al., 2008). Whereas, in culture or after transplantation, the nutrition and oxygen supply solely rely on diffusion. The long diffusion distance in large islets has been shown related to poor cell viability with a more dead cells in the core area (Lehmann et al., 2007; MacGregor et al., 2006; Williams et al., 2010; S. J. Williams et al., 2009). Even though small and large islets have same insulin secreting rate, I suggest that the potency small islets with their greater viability cannot be overlooked for transplantation.

When normalizing total cell number in one islet to its relative IE value, I identified an inverse correlation between total cell number per IE and islet size, which indicated that more cells per IE in small islets than in large islets. Since the two reports in rodents described above (MacGregor et al., 2006; Su et al., 2010) were transplanting same IE of small and large islets in to diabetic animals, there might be a possibility that the better outcome in small islets was due to more islet cells were transplanted. However, without further reanalyzing the original data of IE measurement by using our new method, this assumption could not be tested. Therefore, it will be a very significant future study to transplant the same number of cells from small or large islets into the diabetic animals and compare the results.

5.2.2. The implications to islet biology research

The findings of different characteristics existing in small and large islets strengthened the justification for normalizing islet tissue amount being used when comparing results between preparations in islet research. In early days, normalizing to islet number was one of the common methods. Yet, islet size has been suggested a major determinant for functional heterogeneity among islets (Reaven, Gold, Walker, & Reaven, 1981). For example, when compared side-by-side, one large islet can produce more insulin than one small islet (T. Aizawa et al., 2001). Thus, the variability between different sizes of islets in each preparation must be considered in the experiments. In other words, the results might not be correct, if the data were simply normalized to islet number. Therefore, to avoid the variability due to islet size, several other normalization methods including islet dry weight (Wolters & Konijnendijk, 1980), total protein content (Hayek & Woodside, 1979), insulin content (Schatz, Maier, Hinz, Nierle, & Pfeiffer, 1973), total DNA content (Colella, Bonner-Weir, Braunstein, Schwalke, & Weir, 1985), islet area seen under the stereomicroscope (Jahr, Gottschling, & Zuhlke, 1978) and islet volume (Hayek & Woodside, 1979; Reaven et al., 1981) have been used in the literature. Among all, normalizing to islet volume is suggested as the simpler and more convenient method (Reaven et al., 1981). As I described previously, IE currently is a popular measurement based on the concept of islet volume for the islet research for transplantation in laboratories. However, I showed IE is not accurate to estimate islet volume. Therefore, I suggested total cell number is the best estimate for islet volume. To our best understanding, the only other group that also suggesting this method is Pisania et al.. They also concluded normalizing to total cell number can avoid the overestimation when using IE measurement (Pisania, Weir et al., 2010). Therefore, I suggested that the functional heterogeneity between various sizes of islets must be considered and

normalizing islet volume by total cell number is highly recommended when comparing the results of each preparation in the islet biology researches.

One may raise the questions about the relationship between small and large islets and whether these two populations play different roles in glucose homeostasis in the pancreas. One of the assumptions is that large islets might be born from small islets to functionally compensate the metabolic demand in body. It has been suggested that the β cells in adult pancreatic islets exhibited a plasticity in increasing their population to adapt natural changes in metabolic load such as obesity or pregnancy (Bouwens & Rooman, 2005; Dhawan, Georgia, & Bhushan, 2007). In our lab, we have seen cell proliferation (both in α and β cells) in 100% of large islets, but only in 42% of small islets in the rat pancreas (data not shown). In addition, it has been shown that there are more small islets in the pancreas, even though the small islets accounted for only a very small percentage of the total islet volume (Hellman, 1959a; Kaihoh et al., 1986; MacGregor et al., 2006). Therefore, it seems likely that most small islets in the pancreas were silent until they are triggered to proliferate by some external stimuli when necessary. Small islets may hold the capacity to become large islets to compensate the body demand. Thus, large islets may take more responsibility of glucose homeostasis if they developed because of the extra body demand. The higher stimulation index in large islets I have shown here, which is in agreement with a previous report (T Aizawa et al., 2001), might be able to support this argument. In addition, under low glucose conditions (static incubation), small islets secreted more insulin per cell than large islets (data not shown). Whereas, when facing high glucose, we have seen insulin secretion in large islets was comparable to small islets when normalized to cell. Therefore, I suggested large islets might develop from small islets to compensate for metabolic demand, while small islets are the main insulin secretors under basal conditions. Although the hypothesis maybe over simplistic, it is based on my insulin secretion results, a common method to study islets.

5.2.3. Inconsistent results in insulin content in vitro and in situ

There was an inconsistency in the results of insulin content between chapter 2 and chapter 4. In chapter 2, large islets showed a lower insulin content in vitro and in situ. However, in chapter 4, there was no difference in insulin content between small and large islets when normalized by cell in vitro. There are at least four possibilities that can account for this conflict.

First, the techniques used and normalization methods were different. In chapter 2, two different methods were used to measure the insulin content in vitro. The first approach was to detect the insulin levels from the protein extract of whole islet tissue by ELISA and normalized the results by IE. However, as I suggested, the method of data normalization may affected the in vitro results. Therefore, I believe the results in chapter 4 could be more representative to the truth. The second method was using the TEM histological approach to estimate the number of insulin granules per β cell area on the tissue section of isolated islets. The result showed that β cell from isolated large islets had less insulin granules per area of cell. There are certainly inherent limitations in image analysis when applying two-dimensional histological techniques to study the three-dimensional isolated islet. In other words, the insulin granules density measured under a two-dimensional plane may not be representative enough to the total amount of insulin granules in a three-dimensional islet. Therefore, increasing the sample size being measured on the serial sections of the same cell and average the data might be able to minimize this limitation.

Second, the isolation procedure removes islets from the surrounding exocrine tissue using an enzymatic process. It is well known that the isolation process is more detrimental to some cells compared to others. Potentially, this process could change the insulin content of islets (Brandhorst, Brandhorst, Brendel, Hering, & Bretzel, 1998) and especially affect cells at the periphery (el-Naggar et al., 1993; Morini et al., 2006). Therefore, in vivo islets have a different level than in vitro. One assumption is that higher surface area per volume in small islets may

have greater chance in losing insulin granules at the periphery of islets than the large islets during the isolation process. To avoid the limitation due to isolation procedure, laser capture microdissection (LCM) technique can be applied to harvest the islets directly from the pancreas. Therefore, the insulin content from the LCM-collected islets could be measured and compared to the isolated islets.

Third, there may not be a correlation between in the number of insulin granules and the total insulin content. In addition, the variability due to the size of the granules also needs to be considered. Therefore, to test this assumption, it will be significant to re-estimate the granule density by measuring the ratio of total area of insulin granules to total β cell area and analysis the correlation with total insulin content in small and large islets.

Last but not least, the results of insulin content per cell in chapter 4 might be underestimated, because the data were normalized by total islet cells including β cells and non-β cells. To examine this hypothesis, the β cells from small or large isolated islets could be sorted out by flow cytometer after dissociating the islets into single cells and measured for the insulin content after homogenizing the cells.

5.3. Future Directions

5.3.1. Estimating islet volume by cell number in humans

I have created and tested a new method to better estimate islet volume by cell number in rat. It is of crucial to apply the same concept and techniques to establish a new model in human islets. In addition, I will consider the variations of islets from donors between age, gender, body weight, and race etc. I believe all the efforts will have a direct and immediate implication on human islet research and transplantation.

5.3.2. Performing retrospective studies for transplantation outcome

Our lab will cooperate with human islet transplantation institutes to perform a series of retrospective studies. We will reanalyze the dosage of islets that patients received based on our cell number model and investigate the correlation between the transplantation outcome and the actual tissue volume received by the patients.

5.3.3. Transplant same amount of cells from small and large islets

To better understand how the characteristic differences between small and large islets affect transplantation outcomes, it will be necessary to transplant islets based on an accurate standardization of the tissue amount. Therefore, it will be a very significant to transplant the same amount of cells from small or large islets into diabetic animals and compare the results.

5.3.4. Integrating our volume estimation model with the digital image analysis method

It has been suggested that the digital image analysis (DIA) method offers the advantages of minimizing operator-dependant variations and shortening the evaluation time when estimating the volume of islets especially with low purity or irregular shapes (Friberg et al., 2011). The typical procedure utilizing the DIA method estimates the islet size by computer and calculates the IE accordingly. The new method I proposed here is based on the standard clinical procedure

to measure the islet size manually under the microscope. Thus, a future approach will be to blend my cell number procedure with the DIA method. In other words, another new regression model could be established based on total cell number per islet and the islet size measured by the DIA method. Therefore, my goal is to create a patentable computer system with a solid data base according to different categories of tissue source as described above, and distribute the system to ensure the most accurate estimation on islet tissue volume will always be used in islet research and transplantation.

5.4. Overall Summary

This dissertation is innovative because it is the first investigation of insulin production and secretion properties between islet subpopulations at the cellular and molecular level. We have obtained greater understanding of the biological foundation of islets as well as a better method to quantify islets for research and clinical use. It is my expectation that all the efforts will not only elucidate new intricacies concerning islet biology that will guide other researchers working in related fields such as converting stem cells to insulin-producing β cells or regenerating β cells, but also will have a significant positive impact on the current islet transplantation research to optimize the success for curing type 1 diabetes.

REFERENCES

Aguayo-Mazzucator, C., Sanchez-Soto, C., Godinez-Puig, V., Gutie'rrez-Ospina, G., & Hiriart, M. (2006). Restructuring of pancreatic islets and insulin secretion in a postnatal critial window [Electronic Version]. *PLoS ONE*, e35. Retrieved doi:10.1371/journal.pone.0000035.

Ahlgren, U., Jonsson, J., Jonsson, L., Simu, K., & Edlund, H. (1998). beta-cell-specific inactivation of the mouse Ipf1/Pdx1 gene results in loss of the beta-cell phenotype and maturity onset diabetes. *Genes Dev, 12*(12), 1763-1768.

Ahren, B. (1999). Regulation of insulin secretion by nerves and neuropeptides. *Ann Acad Med Singapore, 28*(1), 99-104.

Aizawa, T., Kaneko, T., Yamauchi, K., Yajima, H., Nishizawa, T., Yada, T., et al. (2001). Size-related and size-unrelated functional heterogeneity among pancreatic islets. *Life Sci., 69*, 2627-2639.

Aizawa, T., Kaneko, T., Yamauchi, K., Yajima, H., Nishizawa, T., Yada, T., et al. (2001). Size-related and size-unrelated functional heterogeneity among pancreatic islets. *Life Sci, 69*(22), 2627-2639.

Alejandro, R., Barton, F. B., Hering, B. J., & Wease, S. (2008). 2008 Update from the Collaborative Islet Transplant Registry. *Transplantation, 86*(12), 1783-1788.

Avgoustiniatos, E. (2002). *Oxygen diffusion limitations in pancreatic islet culture and immunoisolation.* Massachusetts Institute of Technology, Cambridge.

Baetens, D., Malaisse, F., Perrelet, A., & Orci, L. (1979). Endocrine pancreas: three-dimensional reconstruction shows two types of islets of Langerhans. *Science, 206*, 1323-1325.

Balamurugan, A. N., Breite, A. G., Anazawa, T., Loganathan, G., Wilhelm, J. J., Papas, K. K., et al. (2010). Successful human islet isolation and transplantation indicating the importance of class 1 collagenase and collagen degradation activity assay. *Transplantation, 89*(8), 954-961.

Ballian, N., & Brunicardi, F. C. (2007). Islet vasculature as a regulator of endocrine pancreas function. *World J Surg, 31*(4), 705-714.

Bellin, M. D., Sutherland, D. E., Beilman, G. J., Hong-McAtee, I., Balamurugan, A. N., Hering, B. J., et al. (2011). Similar islet function in islet allotransplant and autotransplant recipients, despite lower islet mass in autotransplants. *Transplantation, 91*(3), 367-372.

Bloomfield, A. L. (1958). A bibliography of internal medicine; diabetes mellitus-from Rollo (1798) to Banting (1921). *AMA Arch Intern Med, 101*(6), 1159-1171.

Bonnevie-Nielsen, V., & Skovgaard, L. (1984). Pancreatic islet volume distribution: direct measurement in preparations stained by perfusion in situ. *Acta Endocrinol (Copenh), 105*(3), 379-384.

Bosco, D., Armanet, M., Morel, P., Niclauss, N., Sgroi, A., Muller, Y., et al. (2010). Unique Arrangement of a- and b-Cells in Human Islets of Langerhans. *Diabetes, 59*, 1202-1210.

Bouwens, L., & Rooman, I. (2005). Regulation of pancreatic beta-cell mass. *Physiol Rev, 85*(4), 1255-1270.

Brandhorst, H., Brandhorst, D., Brendel, M. D., Hering, B. J., & Bretzel, R. G. (1998). Assessment of intracellular insulin content during all steps of human islet isolation procedure. *Cell Transplant, 7*(5), 489-495.

Bratanova-Tochkova, T. K., Cheng, H., Daniel, S., Gunawardana, S., Liu, Y. J., Mulvaney-Musa, J., et al. (2002). Triggering and augmentation mechanisms, granule pools, and biphasic insulin secretion. *Diabetes, 51 Suppl 1*, S83-90.

Buchwald, P., Wang, X., Khan, A., Bernal, A., Fraker, C., Inverardi, L., et al. (2009). Quantitative assessment of islet cell products: estimating the accuracy of the existing protocol and accounting for islet size distribution. *Cell Transplant, 18*(10), 1223-1235.

Cabrera, O., Berman, D., Kenyon, N., Ricordi, C., Berggren, P.-O., & Caicedo, A. (2006). The unique cytoarchitecture of human pancreatic islets has implications for islet cell function. *PNAS, 103*(7), 2334–2339.

Cerasi, E. (1975). Mechanisms of glucose stimulated insulin secretion in health and in diabetes: some re-evaluations and proposals. *Diabetologia, 11*(1), 1-13.

Chan, C., Saleh, M., Purje, A., & MacPhail, R. (2002). Glucose-inducible hypertrophy and suppression of anion efflux in rat beta cells. *J Endo, 173*, 45-52.

Chan, C. B., & Surette, J. J. (1999). Glucose refractoriness of beta-cells from fed fa/fa rats is ameliorated by nonesterified fatty acids. *Can J Physiol Pharmacol, 77*(12), 934-942.

Chan, C. B., Wright, G. M., Wadowska, D. W., MacPhail, R. M., Ireland, W. P., & Sulston, K. W. (1998). Ultrastructural and secretory heterogeneity of fa/fa (Zucker) rat islets. *Mol Cell Endocrinol, 136*(2), 119-129.

Chang, K. (2002, Mar 12). Oldest Bacteria Fossils? Or Are They Merely Tiny Rock Flaws? *New York Times,* p. F4.

Clayton, H., Turner, J., Swift, S., James, R., & Bell, P. (2001). Supplementation of islet culture medium with insulin may have a beneficial effect on islet secretory function. *Pancreas, 22*(1), 72-74.

Coffey, L. C., Berman, D. M., Willman, M. A., & Kenyon, N. S. (2009). Immune cell populations in nonhuman primate islets. *Cell Transplant, 18*(10), 1213-1222.

Colella, R. M., Bonner-Weir, S., Braunstein, L. P., Schwalke, M., & Weir, G. C. (1985). Pancreatic islets of variable size--insulin secretion and glucose utilization. *Life Sci, 37*(11), 1059-1065.

Cummings, B. P., Digitale, E. K., Stanhope, K. L., Graham, J. L., Baskin, D. G., Reed, B. J., et al. (2008). Development and characterization of a novel rat model of type 2 diabetes mellitus: the UC Davis type 2 diabetes mellitus UCD-T2DM rat. *Am J Physiol Regul Integr Comp Physiol, 295*(6), R1782-1793.

Curry, D. L., Bennett, L. L., & Grodsky, G. M. (1968). Dynamics of insulin secretion by the perfused rat pancreas. *Endocrinology, 83*(3), 572-584.

D'Aleo, V., Del Guerra, S., Gualtierotti, G., Filipponi, F., Boggi, U., De Simone, P., et al. (2010). Functional and survival analysis of isolated human islets. *Transplant Proc, 42*(6), 2250-2251.

Daniel, S., Noda, M., Straub, S. G., & Sharp, G. W. (1999). Identification of the docked granule pool responsible for the first phase of glucose-stimulated insulin secretion. *Diabetes, 48*(9), 1686-1690.

de Koning, E. J., van den Brand, J. J., Mott, V. L., Charge, S. B., Hansen, B. C., Bodkin, N. L., et al. (1998). Macrophages and pancreatic islet amyloidosis. *Amyloid, 5*(4), 247-254.

Dean, P. (1973). Ultrastructural morphometry of the pancreatic β-cell *Diabetologia, 9*(2), 115-119.

Dhawan, S., Georgia, S., & Bhushan, A. (2007). Formation and regeneration of the endocrine pancreas. *Curr Opin Cell Biol, 19*(6), 634-645.

Dutta, S., Bonner-Weir, S., Montminy, M., & Wright, C. (1998). Regulatory factor linked to late-onset diabetes? *Nature, 392*(6676), 560.

Efrat, S., Surana, M., & Fleischer, N. (1991). Glucose induces insulin gene transcription in a murine pancreatic beta-cell line. *J Biol Chem, 266*(17), 11141-11143.

el-Naggar, M. M., Elayat, A. A., Ardawi, M. S., & Tahir, M. (1993). Isolated pancreatic islets of the rat: an immunohistochemical and morphometric study. *Anat Rec, 237*(4), 489-497.
Elayat, A., el-Naggar, M., & Tahir, M. (1995). An immunocytochemical and morphometric study of the rat pancreatic islets. *J. Anat, 186*(3), 629-637.
Elayat, A. A., el-Naggar, M. M., & Tahir, M. (1995). An immunocytochemical and morphometric study of the rat pancreatic islets. *J Anat, 186 (Pt 3)*, 629-637.
Elrick, L. J., & Docherty, K. (2001). Phosphorylation-dependent nucleocytoplasmic shuttling of pancreatic duodenal homeobox-1. *Diabetes, 50*(10), 2244-2252.
Fetterhoff, T. J., Wile, K. J., Coffing, D., Cavanagh, T., & Wright, M. J. (1994). Quantitation of isolated pancreatic islets using imaging technology. *Transplant Proc, 26*(6), 3351.
Friberg, A. S., Brandhorst, H., Buchwald, P., Goto, M., Ricordi, C., Brandhorst, D., et al. (2011). Quantification of the islet product: presentation of a standardized current good manufacturing practices compliant system with minimal variability. *Transplantation, 91*(6), 677-683.
Fujita, Y., Takita, M., Shimoda, M., Itoh, T., Sugimoto, K., Noguchi, H., et al. (2011). Large human islets secrete less insulin per islet equivalent than smaller islets in vitro. *Islets, 3*(1), 1-5.
Furuzawa, Y., Ohmori, Y., & Watanabe, T. (1992). Immunohistochemical morphometry of pancreatic islets in the cat. *J. Vet. Med. Sci., 54*(6), 1165-1173.
Girman, P., Berkova, Z., Dobolilova, E., & Saudek, F. (2008). How to use image analysis for islet counting. *Rev Diabet Stud, 5*(1), 38-46.
Girman, P., Kriz, J., Friedmansky, J., & Saudek, F. (2003). Digital imaging as a possible approach in evaluation of islet yield. *Cell Transplant, 12*(2), 129-133.
Goldstein, M. B., & Davis, E. A., Jr. (1968). The three dimensional architecture of the islets of Langerhans. *Acta Anat (Basel), 71*(2), 161-171.
Goodge, K. A., & Hutton, J. C. (2000). Translational regulation of proinsulin biosynthesis and proinsulin conversion in the pancreatic beta-cell. *Semin Cell Dev Biol, 11*(4), 235-242.
Guest, P. C., Rhodes, C. J., & Hutton, J. C. (1989). Regulation of the biosynthesis of insulin-secretory-granule proteins. Co-ordinate translational control is exerted on some, but not all, granule matrix constituents. *Biochem J, 257*(2), 431-437.
Hagman, D. K., Hays, L. B., Parazzoli, S. D., & Poitout, V. (2005). Palmitate inhibits insulin gene expression by altering PDX-1 nuclear localization and reducing MafA expression in isolated rat islets of Langerhans. *J Biol Chem, 280*(37), 32413-32418.
Haist, R., & Pugh, E. (1947). Volume measurements of the Islets of Langerhans and the effects of age and fasting *Am. J. Physiol., 152*(1), 36-41.
Halban, P. A. (1991). Structural domains and molecular lifestyles of insulin and its precursors in the pancreatic beta cell. *Diabetologia, 34*(11), 767-778.
Halban, P. A., & Wollheim, C. B. (1980). Intracellular degradation of insulin stores by rat pancreatic islets in vitro. An alternative pathway for homeostasis of pancreatic insulin content. *J Biol Chem, 255*(13), 6003-6006.
Harper, M. E., Ullrich, A., & Saunders, G. F. (1981). Localization of the human insulin gene to the distal end of the short arm of chromosome 11. *Proc Natl Acad Sci U S A, 78*(7), 4458-4460.
Hayek, A., & Woodside, W. (1979). Correlation between morphology and function in isolated islets of the Zucker rat. *Diabetes, 28*(6), 565-569.
Hellman, B. (1959a). Actual distribution of the number and volume of the islets of Langerhans in different size classes in non-diabetic humans of varying ages. *Nature, 184(Suppl 19)*, 1498-1499.

Hellman, B. (1959b). The volumetric distribution of the pancreatic islet tissue in young and old rats. *Acta Endocrinol (Copenh), 31*(1), 91-106.
Howell, S. L., & Taylor, K. W. (1967). The secretion of newly synthesized insulin in vitro. *Biochem J, 102*(3), 922-927.
Huang, H.-H., Novikova, L., Williams, S., Smirnova, I., & Stehno-Bittel, L. (2011). Low insulin content of large islet population is present in situ and in isolated islets. *Islets, 3*(1).
Huang, H. H., Novikova, L., Williams, S. J., Smirnova, I. V., & Stehno-Bittel, L. (2011). Low insulin content of large islet population is present in situ and in isolated islets. *Islets, 3*(1), 6-13.
Hughes, S. J., Clark, A., McShane, P., Contractor, H. H., Gray, D. W., & Johnson, P. R. (2006). Characterisation of collagen VI within the islet-exocrine interface of the human pancreas: implications for clinical islet isolation? *Transplantation, 81*(3), 423-426.
Imai, J., Katagiri, H., Yamada, T., Ishigaki, Y., Ogihara, T., Uno, K., et al. (2005). Constitutively active PDX1 induced efficient insulin production in adult murine liver. *Biochem Biophys Res Commun, 326*(2), 402-409.
Islam, S. (2010). *The Islets of Langerhans*: Springer-Verlag.
Itoh, N., & Okamoto, H. (1980). Translational control of proinsulin synthesis by glucose. *Nature, 283*(5742), 100-102.
Jörns, A., Barklage, E., & Grube, D. (1988). Heterogeneities of the islets in the rabbit pancreas and the problem of "paracrine" regulation of islet cells. *Anat Embryol (Berl), 178*(4), 297-307.
Jahr, H., Gottschling, D., & Zuhlke, H. (1978). Correlation of islet size and biochemical parameters of isolated islets of Langerhans of rats. *Acta Biol Med Ger, 37*(4), 659-662.
Jonsson, J., Carlsson, L., Edlund, T., & Edlund, H. (1994). Insulin-promoter-factor 1 is required for pancreas development in mice. *Nature, 371*(6498), 606-609.
Kaddis, J. S., Danobeitia, J. S., Niland, J. C., Stiller, T., & Fernandez, L. A. (2010). Multicenter analysis of novel and established variables associated with successful human islet isolation outcomes. *Am J Transplant, 10*(3), 646-656.
Kaihoh, T., Masuda, T., Sasano, N., & Takahashi, T. (1986). The size and number of Langerhans islets correlated with their endocrine function: a morphometry on immunostained serial sections of adult human pancreases. *Tohoku J Exp Med, 149*(1), 1-10.
Kataoka, K., Han, S. I., Shioda, S., Hirai, M., Nishizawa, M., & Handa, H. (2002). MafA is a glucose-regulated and pancreatic beta-cell-specific transcriptional activator for the insulin gene. *J Biol Chem, 277*(51), 49903-49910.
Kessler, L., Bakopoulou, S., Kessler, R., Massard, G., Santelmo, N., Greget, M., et al. (2010). Combined pancreatic islet-lung transplantation: a novel approach to the treatment of end-stage cystic fibrosis. *Am J Transplant, 10*(7), 1707-1712.
Kessler, L., Greget, M., Metivier, A. C., Moreau, F., Armanet, M., Santelmo, N., et al. (2010). Combined pancreatic islets-lung transplantation in cystic fibrosis-related diabetes: case reports. *Transplant Proc, 42*(10), 4338-4340.
Khoo, S., Griffen, S. C., Xia, Y., Baer, R. J., German, M. S., & Cobb, M. H. (2003). Regulation of insulin gene transcription by ERK1 and ERK2 in pancreatic beta cells. *J Biol Chem, 278*(35), 32969-32977.
Kissler, H. J., Niland, J. C., Olack, B., Ricordi, C., Hering, B. J., Naji, A., et al. (2010). Validation of methodologies for quantifying isolated human islets: an Islet Cell Resources study. *Clin Transplant, 24*(2), 236-242.
Korsgren, O., Nilsson, B., Berne, C., Felldin, M., Foss, A., Kallen, R., et al. (2005). Current status of clinical islet transplantation. *Transplantation, 79*(10), 1289-1293.

Lacy, P. E., Walker, M. M., & Fink, C. J. (1972). Perifusion of isolated rat islets in vitro. Participation of the microtubular system in the biphasic release of insulin. *Diabetes, 21*(10), 987-998.

Lakey, J. R., Tsujimura, T., Shapiro, A. M., & Kuroda, Y. (2002). Preservation of the human pancreas before islet isolation using a two-layer (UW solution-perfluorochemical) cold storage method. *Transplantation, 74*(12), 1809-1811.

Lakey, J. R., Warnock, G. L., Rajotte, R. V., Suarez-Alamazor, M. E., Ao, Z., Shapiro, A. M., et al. (1996). Variables in organ donors that affect the recovery of human islets of Langerhans. *Transplantation, 61*(7), 1047-1053.

Lawrence, M. C., McGlynn, K., Park, B. H., & Cobb, M. H. (2005). ERK1/2-dependent activation of transcription factors required for acute and chronic effects of glucose on the insulin gene promoter. *J Biol Chem, 280*(29), 26751-26759.

Lehmann, R., Fernandez, L. A., Bottino, R., Szabo, S., Ricordi, C., Alejandro, R., et al. (1998). Evaluation of islet isolation by a new automated method (Coulter Multisizer Ile) and manual counting. *Transplant Proc, 30*(2), 373-374.

Lehmann, R., Zuellig, R. A., Kugelmeier, P., Baenninger, P. B., Moritz, W., Perren, A., et al. (2007). Superiority of small islets in human islet transplantation. *Diabetes, 56*(3), 594-603.

Leibiger, B., Moede, T., Schwarz, T., Brown, G. R., Kohler, M., Leibiger, I. B., et al. (1998). Short-term regulation of insulin gene transcription by glucose. *Proc Natl Acad Sci U S A, 95*(16), 9307-9312.

Lembert, N., Wesche, J., Petersen, P., Doser, M., Becker, H. D., & Ammon, H. P. (2003). Areal density measurement is a convenient method for the determination of porcine islet equivalents without counting and sizing individual islets. *Cell Transplant, 12*(1), 33-41.

Lernmark, A. (1974). The preparation of, and studies on, free cell suspensions from mouse pancreatic islets. *Diabetologia, 10*(5), 431-438.

Ling, Z., Heimberg, H., Foriers, A., Schuit, F., & Pipeleers, D. (1998). Differential expression of rat insulin I and II messenger ribonucleic acid after prolonged exposure of islet beta-cells to elevated glucose levels. *Endocrinology, 139*(2), 491-495.

Luzi, L., & DeFronzo, R. A. (1989). Effect of loss of first-phase insulin secretion on hepatic glucose production and tissue glucose disposal in humans. *Am J Physiol, 257*(2 Pt 1), E241-246.

Macfarlane, W. M., McKinnon, C. M., Felton-Edkins, Z. A., Cragg, H., James, R. F., & Docherty, K. (1999). Glucose stimulates translocation of the homeodomain transcription factor PDX1 from the cytoplasm to the nucleus in pancreatic beta-cells. *J Biol Chem, 274*(2), 1011-1016.

MacFarlane, W. M., Read, M. L., Gilligan, M., Bujalska, I., & Docherty, K. (1994). Glucose modulates the binding activity of the beta-cell transcription factor IUF1 in a phosphorylation-dependent manner. *Biochem J, 303 (Pt 2)*, 625-631.

Macfarlane, W. M., Shepherd, R. M., Cosgrove, K. E., James, R. F., Dunne, M. J., & Docherty, K. (2000). Glucose modulation of insulin mRNA levels is dependent on transcription factor PDX-1 and occurs independently of changes in intracellular Ca2+. *Diabetes, 49*(3), 418-423.

MacGregor, R. R., Williams, S. J., Tong, P. Y., Kover, K., Moore, W. V., & Stehno-Bittel, L. (2006). Small rat islets are superior to large islets in in vitro function and in transplantation outcomes. *Am J Physiol Endocrinol Metab, 290*(5), E771-779.

Malecki, M. T., Jhala, U. S., Antonellis, A., Fields, L., Doria, A., Orban, T., et al. (1999). Mutations in NEUROD1 are associated with the development of type 2 diabetes mellitus. *Nat Genet, 23*(3), 323-328.

Matsumoto, S., Noguchi, H., Takita, M., Shimoda, M., Tamura, Y., Olsen, G., et al. (2010). Super-high-dose islet transplantation is associated with high SUITO index and prolonged insulin independence: a case report. *Transplant Proc, 42*(6), 2156-2158.

Matsuoka, T. A., Artner, I., Henderson, E., Means, A., Sander, M., & Stein, R. (2004). The MafA transcription factor appears to be responsible for tissue-specific expression of insulin. *Proc Natl Acad Sci U S A, 101*(9), 2930-2933.

Menger, M. D., Jaeger, S., Walter, P., Feifel, G., Hammersen, F., & Messmer, K. (1989). Angiogenesis and hemodynamics of microvasculature of transplanted islets of Langerhans. *Diabetes, 38 Suppl 1*, 199-201.

Morini, S., Braun, M., Onori, P., Cicalese, L., Elias, G., Gaudio, E., et al. (2006). Morphological changes of isolated rat pancreatic islets: a structural, ultrastructural and morphometric study. *J Anat, 209*(3), 381-392.

Mythili, D. M., Patra, S. S., & Gunasekaran, S. (2003). Culture prior to transplantation preserves the ultrastructural integrity of monkey pancreatic islets. *J Electron Microsc (Tokyo), 52*(4), 399-405.

Naya, F. J., Huang, H. P., Qiu, Y., Mutoh, H., DeMayo, F. J., Leiter, A. B., et al. (1997). Diabetes, defective pancreatic morphogenesis, and abnormal enteroendocrine differentiation in BETA2/neuroD-deficient mice. *Genes Dev, 11*(18), 2323-2334.

Naya, F. J., Stellrecht, C. M., & Tsai, M. J. (1995). Tissue-specific regulation of the insulin gene by a novel basic helix-loop-helix transcription factor. *Genes Dev, 9*(8), 1009-1019.

Niclauss, N., Bosco, D., Morel, P., Demuylder-Mischler, S., Brault, C., Milliat-Guittard, L., et al. (2011). Influence of donor age on islet isolation and transplantation outcome. *Transplantation, 91*(3), 360-366.

Niclauss, N., Sgroi, A., Morel, P., Baertschiger, R., Armanet, M., Wojtusciszyn, A., et al. (2008). Computer-assisted digital image analysis to quantify the mass and purity of isolated human islets before transplantation. *Transplantation, 86*(11), 1603-1609.

O'Gorman, D., Kin, T., Imes, S., Pawlick, R., Senior, P., & Shapiro, A. M. (2010). Comparison of human islet isolation outcomes using a new mammalian tissue-free enzyme versus collagenase NB-1. *Transplantation, 90*(3), 255-259.

Obermuller, S., Calegari, F., King, A., Lindqvist, A., Lundquist, I., Salehi, A., et al. (2010). Defective secretion of islet hormones in chromogranin-B deficient mice. *PLoS One, 5*(1), e8936.

Offield, M. F., Jetton, T. L., Labosky, P. A., Ray, M., Stein, R. W., Magnuson, M. A., et al. (1996). PDX-1 is required for pancreatic outgrowth and differentiation of the rostral duodenum. *Development, 122*(3), 983-995.

Olbrot, M., Rud, J., Moss, L. G., & Sharma, A. (2002). Identification of beta-cell-specific insulin gene transcription factor RIPE3b1 as mammalian MafA. *Proc Natl Acad Sci U S A, 99*(10), 6737-6742.

Orci, L., Ravazzola, M., Storch, M. J., Anderson, R. G., Vassalli, J. D., & Perrelet, A. (1987). Proteolytic maturation of insulin is a post-Golgi event which occurs in acidifying clathrin-coated secretory vesicles. *Cell, 49*(6), 865-868.

Perez-Armendariz, E., Atwater, I., & Rojas, E. (1985). Glucose-induced oscillatory changes in extracellular ionized potassium concentration in mouse islets of Langerhans. *Biophys J, 48*(5), 741-749.

Pipeleers, D. G., in't Veld, P. A., Van de Winkel, M., Maes, E., Schuit, F. C., & Gepts, W. (1985). A new in vitro model for the study of pancreatic A and B cells. *Endocrinology, 117*(3), 806-816.

Pisania, A., Papas, K. K., Powers, D. E., Rappel, M. J., Omer, A., Bonner-Weir, S., et al. (2010). Enumeration of islets by nuclei counting and light microscopic analysis. *Lab Invest, 90*(11), 1676-1686.

Pisania, A., Weir, G. C., O'Neil, J. J., Omer, A., Tchipashvili, V., Lei, J., et al. (2010). Quantitative analysis of cell composition and purity of human pancreatic islet preparations. *Lab Invest, 90*(11), 1661-1675.

Rafiq, I., da Silva Xavier, G., Hooper, S., & Rutter, G. A. (2000). Glucose-stimulated preproinsulin gene expression and nuclear trans-location of pancreatic duodenum homeobox-1 require activation of phosphatidylinositol 3-kinase but not p38 MAPK/SAPK2. *J Biol Chem, 275*(21), 15977-15984.

Rafiq, I., Kennedy, H. J., & Rutter, G. A. (1998). Glucose-dependent translocation of insulin promoter factor-1 (IPF-1) between the nuclear periphery and the nucleoplasm of single MIN6 beta-cells. *J Biol Chem, 273*(36), 23241-23247.

Reaven, E. P., Gold, G., Walker, W., & Reaven, G. M. (1981). Effect of variations in islet size and shape on glucose-stimulated insulin secretion. *Horm Metab Res, 13*(12), 673-674.

Rhodes, C. J., & Halban, P. A. (1987). Newly synthesized proinsulin/insulin and stored insulin are released from pancreatic B cells predominantly via a regulated, rather than a constitutive, pathway. *J Cell Biol, 105*(1), 145-153.

Ricordi, C. (1991). Quantitative and qualitative standards for islet isolation assessment in humans and large mammals. *Pancreas, 6*(2), 242-244.

Ricordi, C., Fraker, C., Szust, J., Al-Abdullah, I., Poggioli, R., Kirlew, T., et al. (2003). Improved human islet isolation outcome from marginal donors following addition of oxygenated perfluorocarbon to the cold-storage solution. *Transplantation, 75*(9), 1524-1527.

Ricordi, C., Gray, D. W., Hering, B. J., Kaufman, D. B., Warnock, G. L., Kneteman, N. M., et al. (1990). Islet isolation assessment in man and large animals. *Acta Diabetol Lat, 27*(3), 185-195.

Ricordi, C., Socci, C., Davalli, A. M., Staudacher, C., Baro, P., Vertova, A., et al. (1990). Isolation of the elusive pig islet. *Surgery, 107*(6), 688-694.

Ris, F., Niclauss, N., Morel, P., Demuylder-Mischler, S., Muller, Y., Meier, R., et al. (2011). Islet autotransplantation after extended pancreatectomy for focal benign disease of the pancreas. *Transplantation, 91*(8), 895-901.

Ritz-Laser, B., Meda, P., Constant, I., Klages, N., Charollais, A., Morales, A., et al. (1999). Glucose-induced preproinsulin gene expression is inhibited by the free fatty acid palmitate. *Endocrinology, 140*(9), 4005-4014.

Robitaille, R., Dusseault, J., Henley, N., Rosenberg, L., & Halle, J. P. (2003). Insulin-like growth factor II allows prolonged blood glucose normalization with a reduced islet cell mass transplantation. *Endocrinology, 144*(7), 3037-3045.

Rorsman, P., & Renstrom, E. (2003). Insulin granule dynamics in pancreatic beta cells. *Diabetologia, 46*(8), 1029-1045.

Saito, K., Iwama, N., & Takahashi, T. (1978). Morphometrical analysis on topographical difference in size distribution, number and volume of islets in the human pancreas. *Tohoku J Exp Med, 124*(2), 177-186.

Saito, K., Takahashi, T., Yaginuma, N., & Iwama, N. (1978). Islet morphometry in the diabetic pancreas of man. *J. Exp. Med, 125*, 185-197.

Saito, T., Gotoh, M., Satomi, S., Uemoto, S., Kenmochi, T., Itoh, T., et al. (2010). Islet transplantation using donors after cardiac death: report of the Japan Islet Transplantation Registry. *Transplantation, 90*(7), 740-747.

Salomon, D., & Meda, P. (1986). Heterogeneity and contact-dependent regulation of hormone secretion by individual B cells. *Exp Cell Res, 162*(2), 507-520.

Schatz, H., Maier, V., Hinz, M., Nierle, C., & Pfeiffer, E. F. (1973). Stimulation of H-3-leucine incorporation into the proinsulin and insulin fraction of isolated pancreatic mouse islets in the presence of glucagon, theophylline and cyclic AMP. *Diabetes, 22*(6), 433-441.

Schnell, A. H., Swenne, I., & Borg, L. A. (1988). Lysosomes and pancreatic islet function. A quantitative estimation of crinophagy in the mouse pancreatic B-cell. *Cell Tissue Res, 252*(1), 9-15.

Schuit, F. C., In't Veld, P. A., & Pipeleers, D. G. (1988). Glucose stimulates proinsulin biosynthesis by a dose-dependent recruitment of pancreatic beta cells. *Proc Natl Acad Sci U S A, 85*(11), 3865-3869.

Searls, Y., Smirnova, I., Fegley, B., & Stehno-Bittel, L. (2004). Exercise attenuates diabetes-induced ultrastructural changes in rat cardiac tissue. *Med Sci Sports Exerc, 36*(11), 1863-1870.

Searls, Y. M., Smirnova, I. V., Fegley, B. R., & Stehno-Bittel, L. (2004). Exercise attenuates diabetes-induced ultrastructural changes in rat cardiac tissue. *Med Sci Sports Exerc, 36*(11), 1863-1870.

Shapiro, A., Lakey, J., Ryan, E., Korbutt, G., Toth, E., Warnock, G., et al. (2000). Islet transplantation in seven patients with type 1 diabetes mellitus using a glucocorticoid-free immunosuppressive regimen. *N Engl J Med, 343*(4), 230-238.

Shimoda, M., Noguchi, H., Naziruddin, B., Fujita, Y., Chujo, D., Takita, M., et al. (2010a). Assessment of human islet isolation with four different collagenases. *Transplant Proc, 42*(6), 2049-2051.

Shimoda, M., Noguchi, H., Naziruddin, B., Fujita, Y., Chujo, D., Takita, M., et al. (2010b). Improved method of human islet isolation for young donors. *Transplant Proc, 42*(6), 2024-2026.

Smith, P. H. (1975). Structural modification of Schwann cells in the pancreatic islets of the dog. *Am J Anat, 144*(4), 513-517.

Smith, R. M., & Gale, E. A. (2005). Survival of the fittest? Natural selection in islet transplantation. *Transplantation, 79*(10), 1301-1303.

Stefan, Y., Meda, P., Neufeld, M., & Orci, L. (1987). Stimulation of insulin secretion reveals heterogeneity of pancreatic B cells in vivo. *J Clin Invest, 80*(1), 175-183.

Stegemann, J. P., O'Neil, J. J., Nicholson, D. T., & Mullon, C. J. (1998). Improved assessment of isolated islet tissue volume using digital image analysis. *Cell Transplant, 7*(5), 469-478.

Stegemann, J. P., O'Neil, J. J., Nicholson, D. T., Mullon, C. J., & Solomon, B. A. (1997). Automated counting and sizing of isolated porcine islets using digital image analysis. *Transplant Proc, 29*(4), 2272-2273.

Stoffers, D. A., Ferrer, J., Clarke, W. L., & Habener, J. F. (1997). Early-onset type-II diabetes mellitus (MODY4) linked to IPF1. *Nat Genet, 17*(2), 138-139.

Stoffers, D. A., Zinkin, N. T., Stanojevic, V., Clarke, W. L., & Habener, J. F. (1997). Pancreatic agenesis attributable to a single nucleotide deletion in the human IPF1 gene coding sequence. *Nat Genet, 15*(1), 106-110.

Su, Z., Xia, J., Shao, W., Cui, Y., Tai, S., Ekberg, H., et al. (2010). Small islets are essential for successful intraportal transplantation in a diabetes mouse model. *Scand J Immunol, 72*(6), 504-510.

Sudhof, T. C. (1995). The synaptic vesicle cycle: a cascade of protein-protein interactions. *Nature, 375*(6533), 645-653.

Sutton, J. M., Schmulewitz, N., Sussman, J. J., Smith, M., Kurland, J. E., Brunner, J. E., et al. (2010). Total pancreatectomy and islet cell autotransplantation as a means of treating patients with genetically linked pancreatitis. *Surgery, 148*(4), 676-685; discussion 685-676.

Takita, M., Naziruddin, B., Matsumoto, S., Noguchi, H., Shimoda, M., Chujo, D., et al. (2011). Implication of pancreatic image findings in total pancreatectomy with islet autotransplantation for chronic pancreatitis. *Pancreas, 40*(1), 103-108.

Tasaka, Y., Matsumoto, H., Inoue, Y., & Hirata, Y. (1989). Contents and secretion of glucagon and insulin in rat pancreatic islets from the viewpoint of the localization in the pancreas. *Tohoku J. Exp. Med.,, 159*, 123-130.

Uchizono, Y., Alarcon, C., Wicksteed, B. L., Marsh, B. J., & Rhodes, C. J. (2007). The balance between proinsulin biosynthesis and insulin secretion: where can imbalance lead? *Diabetes Obes Metab, 9 Suppl 2*, 56-66.

van der Burg, M. P., Scheringa, M., Basir, I., & Bouwman, E. (1997). Assessment of isolated islet equivalents. *Transplant Proc, 29*(4), 1971-1973.

Vilches-Flores, A., Delgado-Buenrostro, N. L., Navarrete-Vazquez, G., & Villalobos-Molina, R. (2010). CB1 cannabinoid receptor expression is regulated by glucose and feeding in rat pancreatic islets. *Regul Pept, 163*(1-3), 81-87.

Wang, H., Brun, T., Kataoka, K., Sharma, A. J., & Wollheim, C. B. (2007). MAFA controls genes implicated in insulin biosynthesis and secretion. *Diabetologia, 50*(2), 348-358.

Watanabe, T., Yaegashi, H., Koizumi, M., Toyota, T., & Takahashi, T. (1999). Changing distribution of islets in the developing human pancreas: a computer-assisted three-dimensional reconstruction study. *Pancreas, 18*(4), 349-354.

Welsh, M., Scherberg, N., Gilmore, R., & Steiner, D. F. (1986). Translational control of insulin biosynthesis. Evidence for regulation of elongation, initiation and signal-recognition-particle-mediated translational arrest by glucose. *Biochem J, 235*(2), 459-467.

White, S., Hughes, D., Contractor, H., & London, N. (1999). A comparison of cross sectional surface area densities between adult and juvenile porcine islets of Langerhans. *Horm Metab Res, 31*(9), 519-524.

Wicksteed, B., Alarcon, C., Briaud, I., Lingohr, M. K., & Rhodes, C. J. (2003). Glucose-induced translational control of proinsulin biosynthesis is proportional to preproinsulin mRNA levels in islet beta-cells but not regulated via a positive feedback of secreted insulin. *J Biol Chem, 278*(43), 42080-42090.

Williams, S., Huang, H.-H., Kover, K., Moore, W., Berkland, C., Singh, M., et al. (2010). Reduction of Diffusion Barriers in Isolated Islets Improves Survival, But Not Insulin Secretion. *Organogenesis, 6*(2), 115-124.

Williams, S., Wang, Q., MacGregor, R., Siahaan, T., Stehno-Bitel, L., & Berkland, C. (2009). Adhesion of pancreatic beta cells to biopolymer films. *Biopolymers, 91*(8), 676-685.

Williams, S. J., Wang, Q., Macgregor, R. R., Siahaan, T. J., Stehno-Bittel, L., & Berkland, C. (2009). Adhesion of pancreatic beta cells to biopolymer films. *Biopolymers, 91*(8), 676-685.

Wittingen, J., & Frey, C. F. (1974). Islet concentration in the head, body, tail and uncinate process of the pancreas. *Ann Surg, 179*(4), 412-414.

Wolters, G. H., & Konijnendijk, W. (1980). Relationship between insulin secretion, insulin content and dry weight of single rat pancreatic islets. *Acta Endocrinol (Copenh), 94*(3), 365-370.

Yasutaka Fujita, M. T., Masayuki Shimoda, Takeshi Itoh, Koji Sugimoto, Hirofumi Noguchi, Bashoo Naziruddin, Marlon F. Levy and Shinichi Matsumoto. (2011). Large human islets secrete less insulin per islet equivalent than smaller islets in vitro. *Islets, 3*(1).

Yoon, K. H., Ko, S. H., Cho, J. H., Lee, J. M., Ahn, Y. B., Song, K. H., et al. (2003). Selective beta-cell loss and alpha-cell expansion in patients with type 2 diabetes mellitus in Korea. *J Clin Endocrinol Metab, 88*(5), 2300-2308.

Yorde, D. E., & Kalkhoff, R. K. (1986). Quantitative morphometric studies of pancreatic islets obtained from tolbutamide-treated rats. *J Histochem Cytochem, 34*(9), 1195-1200.

Yoshida, S., Kajimoto, Y., Yasuda, T., Watada, H., Fujitani, Y., Kosaka, H., et al. (2002). PDX-1 induces differentiation of intestinal epithelioid IEC-6 into insulin-producing cells. *Diabetes, 51*(8), 2505-2513.

Zanone, M. M., Favaro, E., & Camussi, G. (2008). From endothelial to beta cells: insights into pancreatic islet microendothelium. *Curr Diabetes Rev, 4*(1), 1-9.

Zhang, C., Moriguchi, T., Kajihara, M., Esaki, R., Harada, A., Shimohata, H., et al. (2005). MafA is a key regulator of glucose-stimulated insulin secretion. *Mol Cell Biol, 25*(12), 4969-4976.